

Review

Not peer-reviewed version

Electrochemical Detection of Heavy Metal Ions Based on Nanocomposite Materials

[Mahendra D. Shirsat](#)^{*} and [Tibor Hianik](#)^{*}

Posted Date: 7 July 2023

doi: 10.20944/preprints202307.0064.v1

Keywords: Electrochemical Sensor; Nanocomposite; Detection of Heavy Metal Ions; Metal-Organic Framework; Conducting Polymer; Carbon nanotube; Graphene; Graphitic carbon nitride



Preprints.org is a free multidiscipline platform providing preprint service that is dedicated to making early versions of research outputs permanently available and citable. Preprints posted at Preprints.org appear in Web of Science, Crossref, Google Scholar, Scilit, Europe PMC.

Copyright: This is an open access article distributed under the Creative Commons Attribution License which permits unrestricted use, distribution, and reproduction in any medium, provided the original work is properly cited.

Review

Electrochemical Detection of Heavy Metal Ions Based on Nanocomposite Materials

Mahendra D. Shirsat ^{1,2,*} and Tibor Hianik ^{1,*}

¹ Department of Nuclear Physics and Biophysics, Faculty of Mathematics, Physics, and Informatics, Comenius University, Bratislava, 842 48, Slovak Republic; tibor.hianik@fmph.uniba.sk

² RUSA Centre for Advanced Sensor Technology, Department of Physics, Dr Babasaheb Ambedkar Marathwada University, Aurangabad- 431001, MS, India; mdshirsat.phy@bamu.ac.in

* Correspondence: Authors: mdshirsat.phy@bamu.ac.in (M.D.S.); tibor.hianik@fmph.uniba.sk (T.H.)

Abstract: Heavy metal ions (HMIs) have acute toxic effects on the health and are dangerous for human existence and the ecosystem. Therefore, its sensitive and selective detection is of great importance. In recent years various nanocomposite materials have been used by researchers for the detection of HMIs by using various modalities of electrochemical techniques. This review article summarizes the recent advances in developing electrochemical sensors based on numerous nanocomposite materials for detecting heavy metal ions. Nanocomposites materials, such as Metal-Organic Framework (MOF), organic conducting polymers (OCP), carbon nanotubes, graphene/reduced graphene oxide, graphitic carbon nitride, metal oxide, chitosan, mxenes, metal nanoparticle-based nanocomposites, etc. have been explored by various researchers to improve the sensing properties of electrochemical sensors. This review emphasized the synthesis and characterization techniques of nanocomposite materials, modalities for HMI detection by electrochemical technique and the electrochemical sensors. Moreover, this review highlights the development of portable biosensors for detecting HMIs in real-world scenarios, such as environmental monitoring, food safety, and clinical diagnosis. This review also demonstrates the importance of electrochemical sensors-based on nanocomposite materials as a reliable, sensitive, and selective tool for detecting HMIs.

Keywords: electrochemical sensor; nanocomposite; detection of heavy metal ions; metal-organic framework; conducting polymer; carbon nanotube; graphene; graphitic carbon nitride

1. Introduction

Heavy metal ions (HMIs) in various water bodies on the earth's surface are almost unavoidable due to industrialization. Moreover, their composition differs among different localities, depending on the extent of industrialization in that particular locality [1].

Heavy metals have relatively high atomic weight and density, between 3.5 to 7 g/cm³ [2]. The most known heavy metals are iron (Fe), zinc (Zn), arsenic (As), copper (Cu), nickel (Ni), cadmium (Cd), mercury (Hg), lead (Pb), tin (Sn), etc. These metals are available naturally and cannot be degraded or destroyed. Though some HMIs are needed for the human body's functioning, such as iron (Fe²⁺), zinc (Zn²⁺), manganese (Mn²⁺), and cobalt (Co²⁺) but can be toxic in large amounts [3]. Whereas HMIs like lead (Pb²⁺), mercury (Hg²⁺), arsenic (As²⁺), and cadmium (Cd²⁺) are toxic in nature and contaminants even in small amounts [4].

Some heavy metals such as copper, selenium, and zinc are required as trace elements to keep the human body's metabolism running smoothly. However, at higher concentrations, they can lead to poisoning. The primary sources of daily-purpose water (drinking water) are surface and groundwater. According to United States Environmental Protection Agency (USEPA), the urban regions depend on the surface water source, and the rural regions depend on the groundwater source. The surface water includes streams, lakes, ponds, rivers, and oceans. Drilling wells obtain the groundwater, which is located under the ground's surface and between the rocks. The treated water is mainly from surface water, and various physical filters are used to purify it from dust and other

particles. Also, various chemicals – chlorine and fluorine compounds- are added to kill microorganisms [5].

Heavy metals can be found in the groundwater compared to the surface water. However, the possibility of finding heavy metals in the groundwater increases when ore mines or rich minerals are deposited in the vicinity [6]. The permissible maximum contamination level (MCL) recommended by the USEPA for heavy metals is mentioned in Table 1.

Table 1. The maximum contamination level (MCL) of some heavy metals in drinking water [7, 8].

Heavy metal		MCL (µg/L)
Antimony	Sb	6
Arsenic	As	10
Cadmium	Cd	5
Chromium	Cr	100
Copper	Cu	1.3
Lead	Pb	15
Mercury	Hg	2
Nickel	Ni	100
Selenium	Se	50

Because some heavy metals are very hazardous and can be ingested via drinking water, the MCL of these heavy metals has been recommended in the least amounts by USEPA and by European Environment Agency (EEA).

The leading causes of water pollution are anthropogenic activities where contaminants are dumped into water bodies (rivers, lakes, oceans), resulting in the degradation of the aquatic ecosystem. There are three types of water pollution. First, surface water pollution is the contamination of rivers and lakes, mainly caused by petroleum spills, industrial chemical wastes, wastes with high content of heavy metals, and acid rain. Second, marine pollution is caused by surface water pollution, which kills marine life, disturbing the aquatic ecosystem. Third, groundwater pollution is caused by water movement under the ground, sewage dumping, on-site sanitization plants, hydraulic fracturing, landfills, and chemical fertilizers and pesticides in agriculture [9]. Modern urbanization, industrialization, overpopulation, deforestation, and other factors contribute to environmental deterioration. The degradation of the quality of natural resources and their quantity is meant to as environmental pollution. Heavy metal pollution in the water can lead to serious environmental and health issues. Heavy metals such as lead, mercury, cadmium, arsenic, and chromium are toxic to humans and aquatic life and can accumulate in the food chain over time. HMIs enter water bodies through various sources, such as industrial discharges, agricultural runoff, and domestic sewage. These pollutants can persist in the water environment long and are difficult to remove. The effects of heavy metal pollution in the water can range from acute toxicity to chronic toxicity, carcinogenicity, and mutagenicity. Exposure to HMIs can lead to various health problems, such as neurological disorders, kidney damage, liver damage, and cancer.

Various treatment methods, such as coagulation-flocculation, adsorption, ion exchange, and membrane filtration, have been developed to combat heavy metal pollution. Additionally, regulations and policies have been established by government authorities to limit the discharge of heavy metals into water bodies.

HMIs are toxic substances; therefore, it is imperative to establish relevant techniques for detecting and monitoring them. One practical approach is using sensors to detect and measure the

concentration of specific heavy metal ions in a sample. The sensors provide a fast, accurate, and cost-effective way to monitor the presence of HMIs. Furthermore, sensors can be designed to work in various environments, making them ideal for use in laboratory and field settings. Overall, the development and use of sensors for heavy metal ion detection are crucial for protecting public health and the environment from the harmful effects of these toxic substances.

Nanocomposite-based sensors have gained significant attention in recent years because of their synergistic effect on detecting HMIs with improved sensing properties [10-12]. Researchers worldwide are actively investigating the development and optimization of nanocomposite materials for sensors for heavy metal ion detection. Researchers are exploring various nanocomposite materials, which include graphene oxide, Metal-Organic Framework (MOF), carbon nanotube, organic conducting polymer (OCP), mxenes-based nanocomposites, and metal oxide-based nanocomposites for the detection of a range of HMIs [13-18]. These studies highlight the potential of nanocomposite-based sensors for detecting HMIs and demonstrate the importance of continued research and development in this field. Our research group has also explored various nanocomposite materials based on MOF, OCPs, and carbon nanotubes to detect HMIs [19-29].

Many review papers on the electrochemical detection of HMIs are available in the literature. Malik et al. [30] have comprehensively reviewed various methods to detect and remove HMIs from different sources, including water and soil. The authors discussed the negative impact of heavy metal pollution on the environment and human health, emphasizing the need for efficient and cost-effective techniques to control it. This review covers various detection methods for HMIs, including atomic absorption spectroscopy (AAS), inductively coupled plasma atomic emission spectroscopy (ICP-AES), and X-ray fluorescence (XRF). Additionally, the authors discussed different types of adsorbents and their efficiency in removing heavy metal ions, including activated carbon, clay minerals, and natural and synthetic polymers. Furthermore, they highlighted the importance of considering the factors that affect the efficiency of the removal process, such as the type and concentration of heavy metals, pH, temperature, and contact time. They also discussed the advantages and limitations of different techniques, including biosorption, coagulation/flocculation, electrochemical treatment, and membrane filtration. Overall, the paper provides a valuable resource for researchers and professionals in environmental chemistry, offering a comprehensive overview of the latest methods and techniques for detecting and removing heavy metal ions, but does not provide a quantitative analysis or comparison of their efficiency or effectiveness.

Rubino et al. [31] have extensively reviewed electrochemical methods for detecting HMIs in environmental samples, specifically in water. The authors focused on using screen-printed electrodes (SPEs) as a promising technique for HMIs detection due to their low cost, high sensitivity, and ability to be miniaturized for portable analysis. This review discussed the advantages and limitations of different types of SPEs and the different techniques used to prepare them. The authors also review the different electrochemical detection methods, including cyclic voltammetry, differential pulse voltammetry, square wave voltammetry, and anodic stripping voltammetry, and their exploration for the detection of various HMIs. This review provides a broad overview of the different types of SPEs and electrochemical detection methods but does not provide a detailed comparison of their sensitivity, selectivity, and detection limits, which would be helpful for researchers in this field.

Kajal et al. [32] have provided a comprehensive overview of the potential applications of MOFs for electrochemical sensors for environmental analysis. The authors discussed the unique properties of MOFs, including their high porosity, surface area, and tunable properties, which make them attractive candidates for sensor applications. The paper reviews the recent advancement in electrochemical sensors based on MOF to detect various environmental pollutants, including heavy metals, organic pollutants, and gases. The authors also highlight the challenges and limitations of MOF-based sensors, including stability, reproducibility, and selectivity issues. Overall, the paper provides a valuable reference for researchers and practitioners interested in applying MOFs in electrochemical sensor development for environmental analysis. While the paper briefly mentions the challenges and limitations of MOF-based sensors, such as stability, reproducibility, and selectivity

issues, it does not provide a detailed discussion on how these challenges can be addressed or mitigated, which may limit the practicality and applicability of MOF-based sensors.

Nemiwal et al. [33] have provided an overview of the recent progress in developing electrochemical sensing strategies for point-of-care (POC) applications. The authors discuss the advantages of electrochemical sensing techniques, which make them attractive candidates for POC applications. The paper reviews the recent advances in electrochemical sensing strategies for detecting various analytes, including biomolecules, gases, and heavy metals. The authors also discuss the challenges and limitations of electrochemical sensing techniques, such as the need for precise calibration, reproducibility, and sensor robustness. The paper provides a valuable reference for researchers and practitioners interested in applying electrochemical sensing strategies for POC analysis. However, it does not critically analyze the strengths and weaknesses of the various electrochemical sensing techniques discussed. This may make it difficult for readers to assess the relative merits of each technique for their specific application.

Munonde et al. [34] discuss application of nanocomposites for electrochemical sensors to detect HMIs in environmental water samples. The authors emphasize the importance of detecting trace metals in water as they can cause harmful effects on human health and the environment. The paper describes nanocomposites' development using materials such as carbon nanotubes, graphene, and metal nanoparticles. The authors also discuss the fabrication and characterization of these nanocomposites. The nanocomposites were tested for their effectiveness in detecting trace metals such as lead, cadmium, and mercury in water samples. The results showed that the nanocomposites had high sensitivity and selectivity towards these metals. The paper also highlights the potential applications of these nanocomposites in environmental monitoring and water treatment. The authors suggest that using these nanocomposites as sensors can lead to the development more efficient and cost-effective methods for detecting trace metals in water. Overall, the research paper provides valuable insights into using nanocomposites as electrochemical sensors for detecting trace metals in environmental water samples and demonstrates their potential for future water monitoring and treatment applications. While the authors provide promising results for detecting trace metals in water samples using nanocomposites, the research was conducted under laboratory conditions. Further research is needed to evaluate the effectiveness of nanocomposites in real-world scenarios.

Buledi et al. [35] have provided a comprehensive overview of the recent developments in using nanocomposite-based sensors to detect HMIs from aqueous media. The paper discusses the properties and synthesis of various nanomaterials such as carbon nanotubes, graphene, and metal oxide nanoparticles and their application in developing sensors for heavy metal detection. The authors review the recent advances in the design and fabrication of nanomaterial-based sensors and their applications for detecting heavy metals in aqueous solutions. They discuss the various sensing mechanisms employed in these sensors, such as electrochemical, optical, and piezoelectric sensing mechanisms. The paper also highlights the advantages and limitations of each sensing mechanism and the challenges in developing efficient and selective sensors for detecting HMIs.

Furthermore, the authors provide a detailed analysis of the HMIs detected using nanomaterial-based sensors, including lead, cadmium, mercury, and arsenic. They discuss the sources of these heavy metals in the environment and the potential health risks associated with their exposure. In conclusion, the paper emphasizes the importance of developing efficient and selective sensors for detecting heavy metals in aqueous media. The use of nanomaterial-based sensors is shown to be a promising approach due to their high sensitivity, selectivity, and rapid response time. The paper highlights the need for further research to address the challenges faced in developing nanomaterial-based sensors and their application in detecting heavy metals in real-world scenarios. Although the paper provides a detailed analysis of various types of nanomaterials and their application in detecting heavy metals, it does not cover all the available nanomaterials or sensing mechanisms for heavy metal detection.

Other researchers also have attempted to write a review of the electrochemical detection of HMIs based on various nanomaterials [36-46]. However, a comprehensive approach for the review of nanocomposite materials for the detection of heavy metal ions highlighting their beneficial aspects

and limitations in terms of lower detection limit (at par with the level suggested by USEPA), sensitivity, selectivity, stability, and use of real-time detection of heavy metal ions have been missing in or another way.

To put our findings in the perspective state of the art, it should be remembered that several prior review publications have examined the many operational principles of HMIs sensors. In contrast, others have focused on the impact of one particular class of materials used to detect HMIs.

However, present review will provide a comprehensive overview of the wide range of nanocomposite materials, their synthesis techniques, detection techniques for HMIs, and performance evaluation of electrochemical sensors. Moreover, we have found some research gaps in nanocomposite materials for detecting HMIs and identified some challenging issues of using single nanostructured materials (carbon nanotubes, graphene, organic conducting polymers, and MOFs) and suggested beneficial aspects of using nanocomposites of these materials for electrochemical sensors. This review summarizes the recent advancements in a wide range of nanocomposites for electrochemical sensor applications and is expected to enhance the comprehension of the factors that affect electrochemical sensor performance and aid readers and researchers in selecting appropriate nanocomposites for their intended electrochemical sensing investigations. In addition, this review emphasizes the analysis of the sensors based on various nanocomposite materials, specifically in the aspects of sensitivity, selectivity, the limit of detection (LOD), stability, repeatability, reproducibility, and linearity, in which the studied results help in selecting a particular nanocomposite to specific heavy metal ions detection. Finally, we have provided challenges and futuristic aspects in developing portable devices using nanocomposites for the electrochemical detection of HMIs.

2. Heavy Metal Ion Sensors Modalities: Recent Trends

Various techniques have been developed and utilized to detect HMIs in aqueous solutions, including but not limited to spectroscopic, chromatographic, and electrochemical methods. Some of the spectroscopic detection techniques commonly employed for the detection of HMIs in aqueous media are atomic absorption spectroscopy (AAS), atomic emission spectrometry (AES), atomic fluorescence spectrometry (AFS), X-ray absorption spectrometry (XAS), inductively coupled plasma-mass spectrometry (ICP-MS), and electron spin resonance (ESR) spectroscopy, etc. [28, 47, 48]. Chromatographic methods are also widely employed for the detection of HMIs in aqueous solutions, with high-performance liquid chromatography (HPLC), ion chromatography (IC), and gas chromatography (GC) being some of the most commonly used techniques. [49]. While these advanced methods provide accurate and sensitive detection of HMIs in laboratory settings, their practical application can be challenging due to their complex operating procedures, high costs, the requirement for skilled personnel, sophisticated equipment, and lengthy response times. In contrast to spectroscopy and chromatography techniques, some detection methods offer rapid results, such as electrochemistry-based sensors [50], surface plasmon resonance (SPR) sensors [51], chemo-sensors [52], biosensors [53], and electronic sensors [54]. On the other hand, specific sensors, such as biosensors, may necessitate continuous monitoring by an individual to ensure the complete and accurate detection of HMIs. Of all the available sensors for detecting heavy metal ions, recent developments in electrochemical detection techniques and field-effect transistor (FET)-based sensors have shown promising results for sensing HMIs in aqueous environments, primarily due to their exceptional benefits such as ease of handling, real-time detection, rapid response, low cost, and portability [55, 56].

The typical experimental arrangement for electrochemical detection of HMIs involves an electrolytic cell that contains an ionic conductor (an electrolyte) and an electronic conductor (an electrode). In this instance, the electrolyte is an aqueous solution containing heavy metal ions. The potential of the cell is determined at the interface between the electrode and the solution containing the electrolyte. Several half-reactions occur within the electrolytic cell, with one of the relevant half-reactions typically occurring at the working electrode (WE). The reference electrode (RE) is the other electrode with respect to which the potential of the cell is measured. In a typical electrochemical experiment, an external power supply is utilized to generate an excitation signal and determine the

response function in the chemical solution while ensuring that various system variables are maintained constant. This can be represented as follows:

Excitation signal -> Electrode -> Response function

The current is usually transferred between the working electrode (WE) and the counter electrode (CE) in a three-electrode cell setup, where the CE is referred to as the third electrode. Figure 1 illustrates a standard three-electrode cell configuration employed for the electrochemical sensing of heavy metal ions in aqueous solutions.

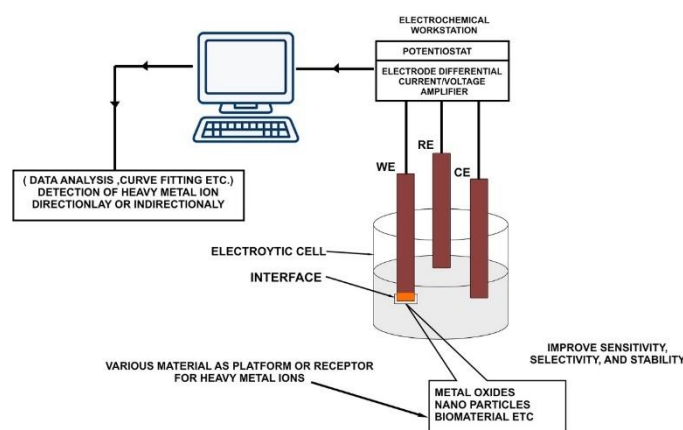


Figure 1. The general setup for electrochemical detection of heavy metal ions. Reproduced from [57] with permission of Elsevier.

The configuration above comprises three electrodes situated within an electrolytic cell, with the WE modified with various interface materials to serve as a platform for HMIs. In this electrochemical setup, the current is usually transmitted between the WE and CE. The CE is positioned in a separate section from the WE by means of glass separators, and its material is selected such that it does not interfere with the WE. The potential is typically determined between the WE and RE using a high input impedance device to avoid any current drawn from the RE. An electrochemical workstation, either a portable in-field device or laboratory equipment, electrically links these electrodes. It contains a built-in power source that supplies excitation signals to the electrode configuration and measurement units to receive and measure the response signals. The electrochemical workstation is linked to a computer equipped with the necessary software platforms for interpreting and analyzing the data obtained from the experiment.

In the case of solutions with low resistance, a two-electrode cell setup featuring the WE and RE is utilized to measure the electrode potential. Various electrochemical techniques are available for detecting HMIs in an aqueous solution, categorized by the different electrical signals produced in the solution due to the presence of these ions [58]. Electrochemical techniques for detecting HMIs in an aqueous solution can generate different electrical signals including changes in current, voltage, electrochemical impedance, charge, and electroluminescence. Based on the specific electrical signal generated, electrochemical techniques are classified into several categories: amperometry, voltammetry, potentiometry, electrochemical impedance spectroscopy, coulometry, and electrochemiluminescence. These techniques have different working principles, advantages, and limitations and can be used in various applications to detect and analyze HMIs in aqueous solutions [59]. An electrochemical measurement can either control the current and measure the resulting potential or control the potential and measure the resulting current. Thus, the measurement techniques are divided into potentiostatic or galvanostatic methods. Most electrochemical techniques for detecting heavy metal ions in an aqueous solution involve controlling one of these parameters to measure the change in the other parameter. Some electrochemical techniques rely on controlling either the current or potential to measure changes in the other parameter, while others, such as potentiometric and impedance measurement techniques, do not require a control signal.

Potentiometric methods are used to determine the type of HMIs present by measuring the potential across the electrodes. In contrast, impedance measurement techniques identify changes in double-layer capacitance, solution resistance, and charge transfer resistance caused by HMIs. The detection of HMIs is frequently accomplished using electrochemiluminescence, which measures the light emission generated during the electrochemical reaction. The intensity of this light emission is directly proportional to the concentration of the target analyte [60]. Various electrochemical techniques are employed to detect HMIs in an electrolytic solution based on different measurement signals to determine the analyte concentration and type. These techniques require using various electroanalytical instruments such as high input impedance potentiometers, galvanostats, and impedance measuring devices. Figure 2 provides a detailed classification of these electrochemical techniques.

Apart from the above-mentioned modalities, field effect transistor (FET) based devices have grabbed wide attention due to their superior characteristics [61]. A FET sensor typically includes three terminals, namely the source, drain and gate terminals. The source and drain terminals are connected through a sensing channel material, while the back or top gate terminal is used to achieve transistor-like properties. FET sensors work through two main sensing mechanisms: charge modulation and dielectric modulation. In charge-modulated FET sensors, the surface interactions between the sensing channel material and the target analyte cause changes in the channel properties through direct charge transfer or charge induction effect. Dielectric-modulated FET sensing platforms rely on changes in gate dielectric constant that result from the binding of the target analyte and sensing probe to perform transduction. As a result, variations in the threshold voltage of the FET sensor occur and can be detected through analysis of the transfer curves. For HMIs detection with FET sensors, various sensing channel materials (e.g., graphene [62], MoS₂ [63], BPs, MOF, and MXenes [64]) have been reported, and multiple chemical or biological probes (such as thioglycolic acid (TGA), L-glutathione reduced (GSH), dithiothreitol (DTT), and single-stranded DNA (ssDNA)) have been utilized. The FET sensors utilize the changes in the electrical properties of the sensing channel material caused by the interactions with HMIs. These changes in electrical characteristics are then detected and recorded as response signals which can be further analyzed for HMIs. By establishing a correlation between the electrical signals generated by the sensing channel material and the concentration of the target analytes, FET sensing platforms can be utilized for the quantitative detection of a wide range of HMIs.

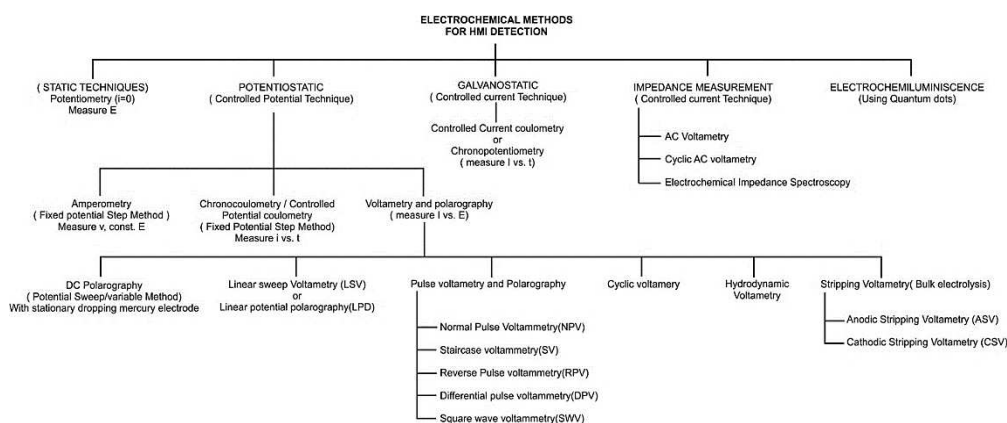


Figure 2. Classification tree for various electrochemical methods for heavy metal ions (HMIs) detection. Reproduced from [57] with permission of Elsevier.

3. Portable Electrochemical Sensor

Recent developments in the field of portable electrochemical sensors have focused on the detection of HMIs. Electrochemical sensors provide a rapid, sensitive, and selective method for detecting these toxic pollutants.

These portable electrochemical sensors are designed to be small, lightweight, and easy to use. Recent developments in this field have focused on improving the sensitivity and selectivity of these electrochemical sensors. For example, researchers have developed novel electrode materials, like graphene and carbon nanotubes, that can enhance the sensitivity of the sensors. They have also used different types of functional groups to modify the electrode surface, improving the selectivity of the sensors.

Portable, handheld sensing devices for the electrochemical detection of HMIs have gained significant attention in recent years due to their ease of use, cost-effectiveness, and portability. These devices are typically designed to be compact, battery-powered, and integrated with a smartphone or other mobile devices, enabling real-time monitoring of heavy metal ions in the field.

Several commercial portable and handheld electrochemical sensors for HMIs are available. These devices typically use ion-selective electrodes (ISEs) or screen-printed electrodes (SPEs) to measure the concentration of HMIs in a sample.

Despite the availability of commercial devices, there is still a need for more sensitive, accurate, and reliable portable sensing devices for the electrochemical detection of HMIs. Ongoing research efforts are focused on developing new sensing platforms that can overcome the limitations of current devices, such as poor selectivity, sensitivity, and stability.

Recent developments in this field have focused on improving the portability and user-friendliness of these sensors. Researchers have developed smartphone apps that can control the sensors and analyze the data collected [65-71]. Researchers have also developed miniaturized sensors that can be easily carried in a pocket or attached to a keychain [71-74].

Jiang et al. [65] have reported a novel smartphone-based electrochemical cell sensor for evaluating the toxicity of HMIs Cd^{2+} , Hg^{2+} , and Pb^{2+} . The objective of the research is to create a sensor for assessing the toxicity of these HMIs in rice using a smartphone-based electrochemical cell. The authors used a 3D printing technique to fabricate a low-cost, disposable electrochemical cell sensor. The sensor was then coupled with a smartphone to measure the electrochemical signals of HMIs. The results exhibited that the sensor was highly sensitive and could detect HMIs at low concentrations. The authors also compared the performance of the developed sensor with that of a traditional electrochemical sensor and found that their sensor was more sensitive and had a lower LOD. Overall, the study suggests that the smartphone-based electrochemical cell sensor can be a promising tool for evaluating the toxicity of heavy metal ions in rice samples.

Recent developments in portable electrochemical cell sensors have improved their ability to detect HMIs, making them valuable tool for environmental monitoring and public health. However, existing portable devices for detecting HMIs ions have several shortcomings that can limit their accuracy, reliability, and usability. Some of these shortcomings are:

- Limited sensitivity: Existing portable devices may not be sensitive enough to detect low concentrations of HMIs accurately.
- Poor selectivity: Portable devices can suffer from poor selectivity, leading to false-positive or false-negative results, particularly in complex samples.
- Limited stability: Some portable devices may have a limited operational lifespan due to the degradation of electrodes or instability of the sensing materials, leading to reduced accuracy and reliability.
- Limited sample handling: Some portable devices may require complex sample preparation steps or may not be suitable for use in the field.

To address these shortcomings, researchers must focus on developing new sensing platforms offering higher sensitivity, selectivity, and stability. These platforms include:

- Advanced electrode materials: For example, nanomaterials can improve the sensitivity and selectivity of portable sensing devices.
- Advanced sensing techniques: Researchers are exploring relevant sensing techniques, such as electrochemical impedance spectroscopy (EIS), to enhance the selectivity and sensitivity of portable sensing devices.
- Microfluidic systems: Integrating microfluidic systems into portable devices can enable better control of sample handling and reduce the need for complex sample preparation.

- Machine learning algorithms: Integrating machine learning algorithms can improve the accuracy and reliability of portable sensing devices by enabling real-time data analysis and pattern recognition.

Overall, addressing the shortcomings of existing portable devices for detecting HMIs will require integrating advanced materials, techniques, and algorithms to enhance the sensitivity, selectivity, stability, and usability of these devices.

4. Nanocomposites for the Detection of HMIs

4.1. Metal-Organic Framework (MOF) Based Nanocomposites

Metal-organic frameworks (MOFs) are a class of hybrid crystalline porous materials consisting of metal ions and organic 'linker' molecules with an extraordinarily large internal surface area. MOFs have gained attention as a material for detecting HMIs due to their unique structural and chemical properties. Some advantages of using MOFs for HMIs detection include the following:

- High selectivity: MOFs can be designed with specific ligands to selectively capture certain HMIs, enabling the detection of individual or multiple metal ions in complex samples.
- High sensitivity: MOFs have high surface area and porosity, allowing for efficient adsorption of HMIs and resulting in highly sensitive detection with low detection limits.
- Tunable properties: MOFs have tunable properties, including pore size, surface area, and functionality, which can be tailored to enhance their performance for specific HMIs.
- Fast response time: MOF-based sensors have a fast response time due to the efficient electron transfer properties of MOFs, allowing for real-time detection of HMIs.
- Stability: MOFs are stable in a wide range of chemical and physical conditions, making them suitable for use in harsh environments.

Overall, MOFs have the potential to be highly effective and efficient materials for HMIs detection with applications in environmental monitoring, food safety, and industrial processes. Despite their promising advantages, MOFs also have some limitations that include:

- Cost: The production of MOFs can be costly, particularly for large-scale applications. This can limit their use in some industries.
- Stability: While MOFs are generally stable, some can degrade over time or in certain conditions, which can affect their performance and lifespan as sensors.
- Reproducibility: MOFs can be difficult to synthesize with high reproducibility, making it challenging to ensure consistent performance between different batches of sensors.
- Interference: Other ions or molecules in the sample matrix can compete for adsorption sites on the MOF, leading to false positives or reduced sensitivity for detecting the target HMIs.
- Detection range: MOF-based sensors may have limited detection ranges for specific HMIs, making them less suitable for detecting trace levels of those ions.
- Poor electronics conductance: MOFs have poor electronics conductance, which limits their use for sensor applications.

These limitations highlight the need for continued research and development to optimize MOF-based nanocomposites for HMIs detection and to overcome these challenges. Therefore, to address these limitations, researchers have explored other active materials like carbon nanostructure, metal oxide, metal nanoparticles, graphene, etc. Among the different materials, significantly reduced graphene oxide (rGO) has gained substantial attention from researchers and has been widely used as a nanocomposite with MOF for detecting HMIs [75-85]. Researchers have also explored other materials to have nanocomposite of MOF to detect HMIs [83, 84, 86-88].

Fang et al. [75] have reported the development of an electrochemical sensor for detecting ciprofloxacin in water samples using nanocomposites of Zr(IV)-based MOFs and rGO. They have synthesized the Zr(IV)-based MOFs and rGO separately and then combined them to create the nanocomposites. They found that the addition of rGO to the MOFs improved the electrochemical properties of the nanocomposites, making them more sensitive to ciprofloxacin. Then they tested the nanocomposites for electrochemical detection ciprofloxacin in water. They found that the sensor had a linear range of detection between 0.02 and 1 μM and a LOD of 6.67 nM, which is much lower than

the maximum contaminant level set by the USEPA for ciprofloxacin in drinking water. Overall, this research demonstrates the potential of using these nanocomposites as a highly sensitive and selective electrochemical sensor for detecting ciprofloxacin in water samples.

Cui et al. [81] have reported the development of an electrochemical sensor for the detection of nickel (II) using a zeolitic imidazolate framework-8@dimethylglyoxime/ β -cyclodextrin/reduced graphene oxide (ZIF-8@DMG/ β -CD/rGO). In this work, they combined DMG with ZIF-8 and obtained the enrichment unit of ZIF8@DMG. It was then loaded on conductive reduced graphene oxide (RGO), modified with β -cyclodextrin (β -CD). The finally synthesized composite ZIF-8@DMG/ β -CD/rGO was used to develop a sensor for detecting Ni (II). The coordination bonding and hydrogen bonding were explored to link DMG onto ZIF-8. Moreover, DMG acted as ligand molecules of Ni (II) (Figure 3). Based on SEM and TEM images, they have claimed that ZIF-8@DMG exhibited a disordered structure with a non-uniform size of less than 300 nm, which suggest the presence of DMG affected the growth process and final structure of ZIF-8 to some extent. Moreover, typical nanosheet structure and wrinkles of β -CD/rGO can be observed from of ZIF- 8@DMG/ β -CD/rGO. This confirms the successful combination of ZIF-8@DMG and β -CD/rGO. The sensor shows good sensitivity and selectivity towards nickel (II) ions, with a wide linear range of 0.01–1.0 μ M and a low LOD of 0.005 μ M. The sensor also shows excellent stability and reproducibility, making it a promising tool for the detection of Ni²⁺ ions in environmental and industrial settings.

Wang et al. [89] have presented the development of a sensitive and selective electrochemical sensor for detecting lead (Pb) and copper (Cu) ions. The sensor was based on a MOF/polypyrrole (MOF/PPy) nanocomposite functionalized electrode. Initially, they prepared. Employing a chemical polymerization process, PPy nanowires were synthesized, and subsequently, an in-situ electrochemical technique was employed to deposit the MOF (NH₂-MIL-53(Al)) onto the PPy nano substrates.

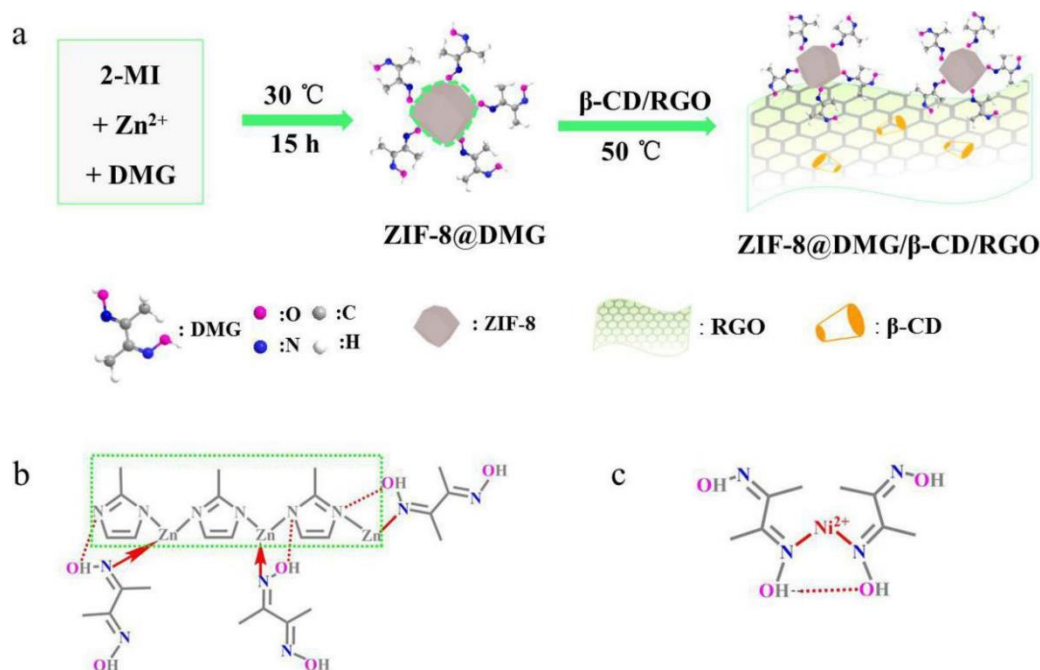


Figure 3. Schematic illustrations for (a) fabrication of ZIF-8@DMG/ β -CD/rGO; (b) possible interaction mechanism between ZIF-8 and DMG (Red arrows represent coordination bond; Red dotted lines represent hydrogen bond); (c) possible interaction mechanism between DMG and Ni (II) (Red arrows represent coordination bond; Red solid lines represent hydrogen bond). Reproduced from [81] with permission of Elsevier. .

Differential pulse voltammetry (DPV) techniques were employed to assess the electrochemical performance of the sensor. A distinct peak was observed for various concentrations of Pb(II) and Cu(II) during the DPV analysis. Nonlinear enhancement in peak currents was observed in the

concentration range of 1 to 400 $\mu\text{g/L}$ (Figure 4), whereas a linear increase in peak currents was observed in the low concentration range of 1 to 20 $\mu\text{g/L}$. High sensitivity and selectivity towards Pb and Cu ions were observed in the sensor, with LOD of 0.315 $\mu\text{g/L}$ and 0.244 $\mu\text{g/L}$, respectively. The sensor was also highly stable and reproducible, even after multiple testing cycles.

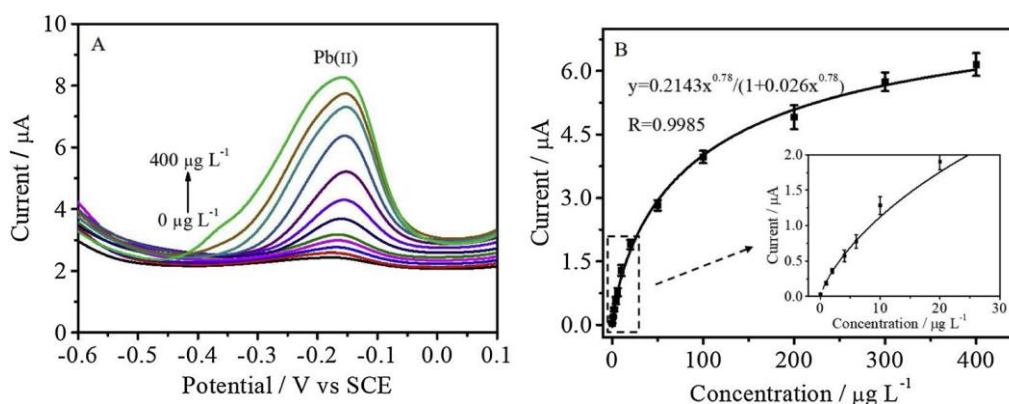


Figure 4. DPV response (A) and calibration curve (B) toward Pb (II) in the concentration range of 1–400 $\mu\text{g/L}$. Reproduced from [89] with permission of Elsevier.

The researchers further tested the sensor's performance in natural water samples collected from tap water. The sensor accurately and precisely detected Pb and Cu ions in these samples. Overall, the study demonstrates the potential of MOF/PPy nanocomposite functionalized electrodes as highly sensitive and selective electrochemical sensors for detecting HMIs in water samples.

Ru et al. [90] have presented a new method for detecting arsenic in water using a combination of a UiO-67 MOF, GO, and platinum nanoparticles (PtNPs). The UiO-67 MOF has a porous structure that can adsorb and concentrate arsenic, while GO and PtNPs improve the electrochemical properties of the sensor. The sensor was highly sensitive and selective for detecting arsenic in water, with a lower LOD than the safety standard set by the World Health Organization (WHO), as shown in Figure 5. The work concludes that this new sensing platform could be helpful for environmental monitoring and toxicological evaluation. Moreover, their investigation includes the development of a quick, simple, eco-friendly, and sensitive detection method for arsenic in water. Finally, the investigation includes that it has only been tested on a limited range of environmental samples, and further testing is needed to determine its applicability in different contexts.

Zhao Yang et al. [91] have described a new method for detecting HMIs in water samples. The sensing platform comprises cobalt/nitrogen-doped carbon (NC) composite polyhedrons linked with multi-walled carbon nanotubes (MWCNTs). Moreover, the sensing platform also was fabricated by growing nanoporous ZIF-67 on MWCNTs, followed by carbonization. Due to its large specific surface area and excellent electrical conductivity, the resulting platform offers numerous active sites for metal ion attachment. Figure 6 shows the schematic diagram of the construction process of the Co@NC/MWCNT-modified electrode and the simultaneous detection of Cd^{2+} and Pb^{2+} . The platform was tested for detecting Cd^{2+} and Pb^{2+} ions in water and showed a relatively wide linear range and low LOD.

Additionally, the platform also demonstrated good anti-interference performance in actual water samples. Moreover, this work concludes that the platform can be used in trace HMIs monitoring in natural water environments. The investigations in this work include the development of a fast and sensitive platform for HMIs detection and demonstrating exemplary performance in actual water samples. However, their investigation focuses on only two types of HMIs and the need for further testing in a wider range of water samples.

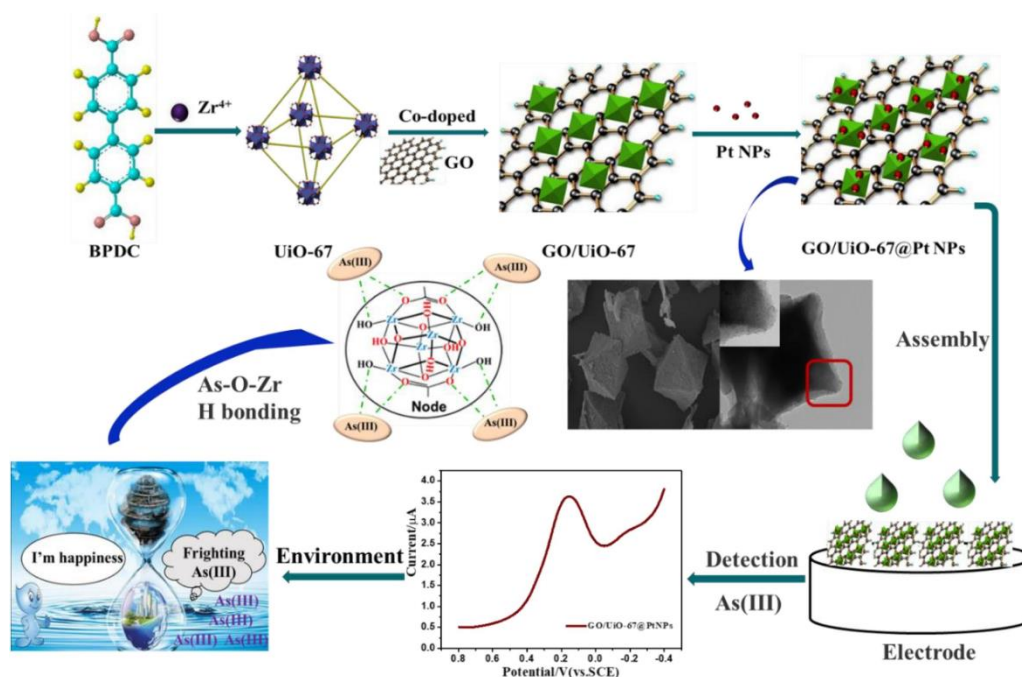


Figure 5. Schematic illustration of the fabrication process of GO/Uio-67@PtNPs for the electrochemical detection of As(III) in water samples. Reproduced from [90] with permission of Elsevier.

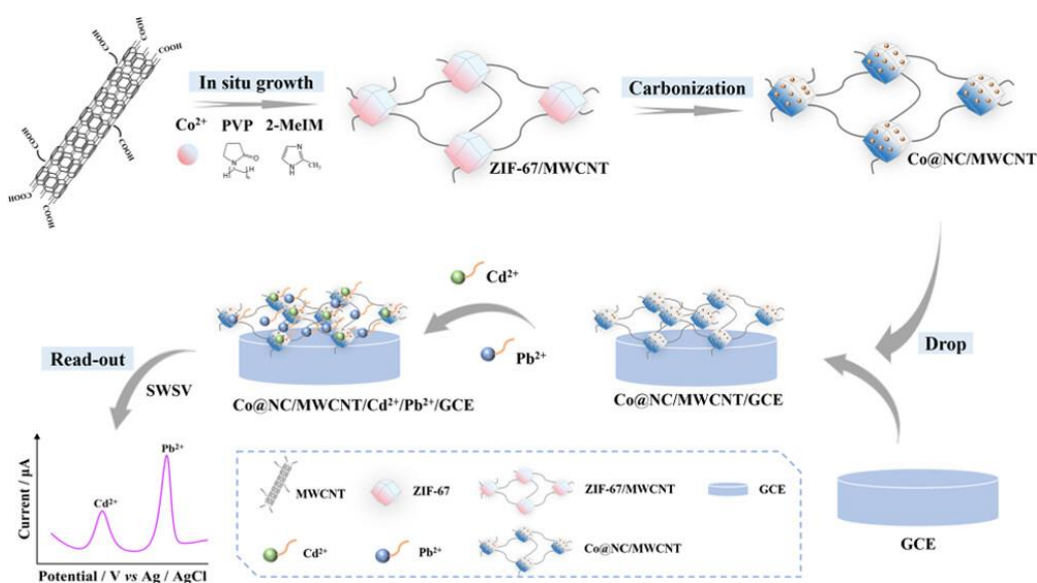


Figure 6. Schematic diagram of the construction process of the Co@NC/MWCNT-modified electrode and the simultaneous detection of Cd²⁺ and Pb²⁺. Reproduced from [91] with permission of American Chemical Society.

Yang et al. [86] have also prepared a new nanocomposite material by attaching mercaptan functionalized MOFs to three-dimensional kenaf stem-derived carbon (3D-KSC) for the removal and electrochemical detection of mercury ion (Hg(II)). The researchers used coordination between Zr (IV) and 2,5-dimercaptoterephthalic acid to prepare the Zr-DMBD MOFs, which were then attached to the 3D-KSC. They also conducted electrochemical measurements and tested the material's ability to remove Hg(II) from natural wastewater. The nanocomposite material showed high sensitivity ($324.58 \mu\text{A} \cdot \mu\text{M}^{-1} \cdot \text{cm}^{-2}$), a linear detection range of $0.25 \mu\text{M}$ - $3.5 \mu\text{M}$, and a low LOD of $0.05 \mu\text{M}$. It also effectively removed Hg(II) from natural wastewater.

Moreover, the researchers concluded that the Zr-DMBD MOFs/3D-KSC nanocomposite material was effective for both the removal and detection of Hg(II). This composite has exhibited high

sensitivity, selectivity, stability, and reproducibility. This shows great potential as a practical solution for real-world applications. The investigation resulted in the developing of a new nanocomposite material that can effectively remove and detect Hg(II) from wastewater. The material has several positive aspects, including high sensitivity, selectivity, stability, and reproducibility. The investigation did not explore the potential for scaling up the production of the nanocomposite material or the cost-effectiveness of using it for practical applications. Additionally, the investigation did not explore the potential for the material to remove or detect other HMIs.

4.2. Organic Conducting Polymer (OCP) Based Nanocomposite

Organic conducting polymers (OCP) are one of the ideal materials for electrochemical sensors due to their distinctive chemical and electrical properties. Some reasons why OCP are suitable for electrochemical sensors include the following:

- Electrical conductivity: Organic conducting polymers are highly conductive, which enables the detection of HMIs through changes in the electrical properties of the polymer upon interaction with the metal ions.
- Electroactive nature: Organic conducting polymers are electroactive and can undergo reversible redox reactions at their surface. This property makes them well-suited for electrochemical sensors, which rely on redox reactions to detect and quantify analytes.
- Sensitivity: Organic conducting polymers have high sensitivity to HMIs, allowing for detection at low concentrations.
- Selectivity: The selectivity of organic conducting polymers for HMIs can be tailored by modifying the polymer structure or incorporating specific ligands or functional groups, enabling the detection of specific metal ions in complex samples.
- Overall, the unique properties of conducting polymers make them well-suited for electrochemical sensors to detect HMIs, with applications in environmental monitoring, food safety, and industrial processes.

Despite their advantages, conducting polymers also have some limitations for use in electrochemical sensors for the detection of HMIs, including:

- Reproducibility: Organic conducting polymers can be difficult to synthesize with high reproducibility, making it challenging to ensure consistent performance between different batches of sensors.
- Long-term stability: Some organic conducting polymers can undergo degradation over time, affecting their performance and lifespan as sensors.
- Interference: Other ions or molecules in the sample matrix can compete for adsorption sites on the conducting polymer, leading to false positives or reduced sensitivity for detecting the target heavy metal ions.
- Detection range: Organic conducting polymer-based sensors may have limited detection ranges for specific HMIs, making them less suitable for detecting trace levels of those ions.
- Environmental impact: Organic conducting polymers may have environmental impacts due to their non-biodegradable nature, although efforts are being made to develop more sustainable alternatives.

Therefore, to address these limitations, researchers have explored other materials, such as graphene, carbon nanotubes, metal nanoparticles, etc., to form nanocomposites with organic conducting polymers [92-107]. These composites offer several advantages, such as high sensitivity, selectivity, stability, and reproducibility, making them suitable for detecting HMIs in various applications.

The organic conducting polymer-based nanocomposites are designed to adsorb and capture HMIs from aqueous solutions, and the captured ions are then detected using electrochemical techniques. Incorporating materials such as graphene, carbon nanotubes, and metal nanoparticles into the polymer matrix can enhance the sensor's performance by improving the electron transfer rate and increasing the active surface area of the sensor.

The choice of the composite material, its synthesis method, and the electrochemical detection method used can significantly influence the performance of the sensor. The composite-based sensors

have been successfully applied for the detection of HMIs in various matrices such as water, soil, and food samples. These sensors have potential applications in environmental monitoring, industrial process control, and medical diagnostics.

Fall et al. [108] have reported rGO@CNT@Fe₂O₃/PPy nanocomposite for the electrochemical detection of Pb²⁺. The authors started by synthesizing a nanocomposite material comprising reduced graphene oxide (rGO), carbon nanotubes (CNTs), iron oxide nanoparticles (Fe₂O₃), and PPy. This nanocomposite was then used as a sensing material to detect Pb²⁺ ions in water samples. The study showed that the rGO@CNT@Fe₂O₃/PPy nanocomposite had excellent electrochemical properties, such as a high surface area, good conductivity, excellent stability, and strong adsorption ability towards Pb²⁺ ions. A linear calibration curve was obtained for the sensor utilizing rGO@CNT@Fe₂O₃/PPy nanocomposite, with a range of 0.02 to 0.26 μM (R² = 0.992), a sensitivity of 162.8 μA·μM⁻¹, and a LOD of 0.1 nM. The nanocomposite showed a broad linear range and a low LOD for Pb²⁺ ions, indicating its high sensitivity for the detection of this heavy metal in water. Several experiments were carried out by the authors to assess the rGO@CNT@Fe₂O₃/PPy nanocomposite's performance in detecting Pb²⁺ ions. The findings demonstrated that the nanocomposite was highly sensitive and selective towards Pb²⁺ ions, even in the presence of other interfering ions. The synthesis process of rGO@CNT@Fe₂O₃/PPy onto GCE and the electrochemical detection of Pb²⁺ are depicted in Figure 7.

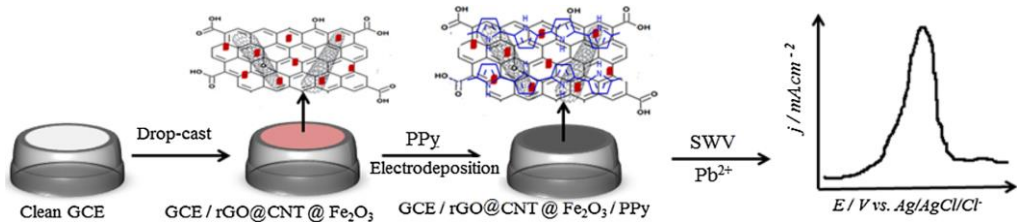


Figure 7. A comprehensive schematic illustrating synthesis of rGO@CNT@Fe₂O₃/PPy on the GCE and electrochemical detection of Pb²⁺. Reproduced from [108] with permission of Elsevier.

Authors have compared their work with other PPy-based electrochemical sensors for the detection of Pb²⁺ in terms of sensitivity and LOD. The details of the comparison are illustrated in Table 2. As per Table 2, the performance of the rGO@CNT@Fe₂O₃/PPy is better than similar to the earlier reported work. This is because of the substantial active surface area and remarkable adsorption capacity of CNT and Fe₂O₃, along with PPy's nitrogen affinity towards Pb²⁺. Overall, the study demonstrated that the rGO@CNT@Fe₂O₃/PPy nanocomposite is a promising material for the electrochemical detection of Pb²⁺ ions in water samples. The development of such materials is essential for environmental monitoring and protection, as lead contamination in water sources can pose serious health risks to humans and the environment.

Table 2. Comparison of different modified electrodes for the determination of Pb²⁺. According to [108] with permission of Elsevier.

Electrode	Method	Deposition potential	Deposition time (s)	Linear range (μM)	LOD (μM)	Ref.
PPy/CNFs/CPE	SWASV	-1.2 V vs. SCE	600	0.2–130	0.05	[109]
Fe ₂ O ₃ /G/Bi-GCE	DPASV	-1.2 V vs. Ag/AgCl	300	1–100	0.07	[17]
rGO/PPy-SPE	DPASV	-1.2 V vs. Ag/AgCl	600	1.4–28; 28–280;	0.07	[110]

				280– 14,000		
PPy/CNT/NH ₂ -ITO	DPV		600	0.01 – 2.9 × 10 ⁻³	[111]	
Bi/PPy/MWCNT/CPE	SWASV	1.2 V vs. SCE	240	0.11– 0.099	[93]	
GO@Fe ₃ O ₄ @2-CBT	SWASV	1.2 V vs. Ag/AgCl	180	3×10 ⁻⁴ – 0.072; 0.072– 0.43	[112]	
PA/PPy/ZIF-8@ZIF-67	DPV	–	–	0.02– 2.9 × 10 ⁻⁴	[113]	
ITO/AP/PPy	DPASV	-1.2 V vs. SCE	200	0.01– 0.25	[114]	
rGO@CNT@Fe ₂ O ₃ /PPy/GCE	SWASV	-1.3 V vs. Ag/AgCl	300	0.02– 1 × 10 ⁻⁴	[108]	

DPASV: differential pulse anodic stripping voltammetry, SWASV: square wave anodic stripping voltammetry, GCE: glassy carbon electrode, SPE: screen printed electrode, CPE: carbon paste electrode, G: graphene, GO: graphene oxide, rGO: reduced graphene oxide, CNFs: carbon nanofibers, MWCNT: multi-walled carbon nanotubes, PPy: polypyrrole, Bi: bismuth, ITO: indium tin oxide. PA: phytic acid; AP: aminophenyl. 2-CBT: benzothiazole-2-carboxaldehyde, Fe₃O₄: magnetite, CNT: carbon nanotube.

A novel electrochemical sensor for the detection of mercury ions (Hg²⁺) has been developed using a Pt/g-C₃N₄/polyaniline nanocomposite, as reported by Mahmoudian et al. [96] A nanocomposite consisting of platinum (Pt), graphitic carbon nitride (g-C₃N₄), and polyaniline (PANI) was used for fabrication of sensor. A simple and cost-effective method was used to synthesize Pt/g-C₃N₄/PANI nanocomposite and was characterized using various techniques.

The electrochemical properties of the Pt/g-C₃N₄/PANI nanocomposite were evaluated, and it was found that the nanocomposite exhibited excellent electrocatalytic activity towards the reduction of Hg²⁺ ions. The fabricated sensor demonstrated a wide linear range of 1-500 nM, with a low LOD of 0.014 nM. The sensor also exhibited good selectivity towards Hg²⁺ ions, even in the presence of other interfering ions.

The FESEM image of Pt/g-C₃N₄/PANI nanocomposite confirms a significant increase in surface area due to the presence of g-C₃N₄. Moreover, the authors have reduced Pt²⁺ ions in the presence of L-cysteine, confirmed in the EDX spectrum. Overall, the results suggest that the Pt/g-C₃N₄/PANI nanocomposite is a promising material for developing high-performance electrochemical sensors to detect Hg²⁺ ions in environmental and industrial applications. The study highlights the potential of using nanocomposites for the development of advanced sensing technologies.

In a publication by Deshmukh et al. [115], they documented an electrochemical method for sensing Pb(II) ions utilizing a nanocomposite platform comprising EDTA-modified PPy/SWNTs. The study aimed to develop a nanocomposite platform for the sensitive and selective detection of Pb ions using an electrochemical method. The researchers utilized a nanocomposite platform consisting of ethylenediaminetetraacetic acid (EDTA) modified PPy and SWNTs to detect Pb(II) ions. The modified PPy/SWNTs nanocomposite was characterized using various analytical techniques, including SEM, TEM, FTIR. The study found that the nanocomposite platform exhibited excellent electrocatalytic activity towards the oxidation of Pb(II) ions and high selectivity and sensitivity towards Pb(II) ions. The LOD was found to be as low as 0.07 μM, which is much lower than the permissible limit set by

the WHO. Overall, the study concluded that the EDTA-modified PPy/SWNTs nanocomposite platform shows excellent potential for the sensitive and selective detection of Pb(II) ions, which can have critical applications in environmental monitoring and public health.

SEM images of unmodified PPy, PPy/SWNTs, and EDTA-PPy/SWNTs nanocomposite confirms the uniform deposition of PPy on the surface of SWNTs, where SWNTs act as the backbone of the nanocomposite structure. The accumulation of EDTA molecules on the surface of PPy/SWNTs have resulted in a more granular structure. This kind of surface morphology will be suitable for HMIs sensing because surface roughness will help to enhance the possibilities of accumulation or trapping of an analyte. The authors have investigated the performance of three different electrodes, viz. bare PPy/SSE, PPy/SWNTs/SSE, and EDTA-PPy/SWNTs/SSE, for the detection of Pb(II) ions. The highest Pb(II) sensing peak was observed in response to EDTA-PPy/SWNTs/SSE nanocomposite (Figure 8).

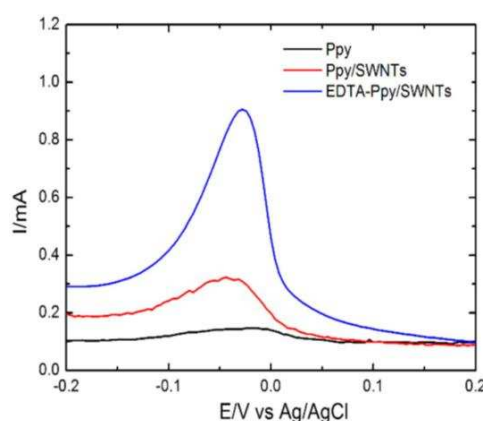


Figure 8. DPV-based response of electrodes covered by unmodified PPy, PPy/SWNTs, and EDTA-PPy/SWNTs toward $8 \times 10^2 \mu\text{M}$ Pb(II) ions dissolved in 0.2 M ABS pH 4.9, by the accumulation of metal ions by dip coating technique followed by stripping with DPV technique. The applied DPV parameters viz. increment of 5 mV, the step amplitude of 50 mV and a pulse period of 0.2 s in 0.5M H_2SO_4 [115].

The performance of the sensor based on EDTA-PPy/SWNTs composite exhibited excellent over the concentration range from $8 \times 10^2 \mu\text{M}$ to $0.15 \mu\text{M}$ in 0.5 M H_2SO_4 for Pb(II) metal ions. However, the linearity of the sensor was not very appreciating.

4.3. Carbon Nanotubes Based Nanocomposites

Carbon nanotubes are promising materials for detecting HMIs due to their unique structural and chemical properties. Some of the advantages of using carbon nanotube-based nanocomposites for HMIs detection include:

- **High sensitivity:** Carbon nanotubes have a large surface area and high aspect ratio, allowing efficient HMIs adsorption. This results in highly sensitive detection with low detection limits.
- **Selectivity:** The surface chemistry of carbon nanotubes can be modified to selectively capture specific HMIs, enabling the detection of individual or multiple metal ions in complex samples.
- **Rapid response time:** Carbon nanotube-based sensors have a fast response time due to carbon nanotubes' efficient electron transfer properties. This allows for real-time detection of HMIs.
- **Durability:** Carbon nanotubes are highly durable and can withstand harsh chemical and physical conditions, making them suitable for use in various environmental and industrial settings.
- **Low cost:** Carbon nanotube-based sensors are relatively inexpensive to produce compared to traditional HMIs detection methods, making them a cost-effective alternative.

Overall, carbon nanotubes have the potential to be effective and efficient materials for HMIs detection with applications in environmental monitoring, food safety, and industrial processes.

Therefore, carbon nanotubes and their composites have been comprehensively explored for electrochemical detection of HMIs. In addition, various research groups have also explored other

allotropes of carbon along various nanostructured materials for the detection of HMIs. Various methodologies have been adopted to enhance the synergy of these materials by doping process, functionalization process, and developing hybrid system [19, 91, 116-124].

Wu et al. [116] have reported the development of a low-cost sensor based on Fe_3O_4 nanoparticles/fluorinated multi-walled carbon nanotubes for the simultaneous electrochemical detection of multiple heavy metals in the environment and food, which exhibits high sensitivity and selectivity. The hydrothermal method was adopted by the group for Fe_3O_4 nanoparticles/fluorinated multi-walled carbon nanotubes (F-MWCNT) composite formation ($\text{Fe}_3\text{O}_4/\text{F-MWCNTs}$). The developed electrochemical sensor showed elevated results of detection for Cd^{2+} , Pb^{2+} , Cu^{2+} , and Hg^{2+} by square wave anodic stripping voltammetry (SWASV).

The sensitivity observed was 108.79, 125.91, 160.85, and 312.65 $\mu\text{A}\cdot\text{mM}^{-1}\cdot\text{cm}^{-2}$ toward Cd^{2+} , Pb^{2+} , Cu^{2+} , and Hg^{2+} , respectively, which was obviously higher than that of $\text{Fe}_3\text{O}_4/\text{MWCNTs}$ and Fe_3O_4 based sensor. The $\text{Fe}_3\text{O}_4/\text{F-MWCNTs}$ sensor demonstrated excellent performance in terms of detection range and sensitivity. Specifically, the sensor exhibited linear detection ranges of 0.5–30.0 μM for Cd^{2+} , Pb^{2+} , Cu^{2+} , and 0.5–20.0 μM for Hg^{2+} with a LOD of 0.05, 0.08, 0.02, and 0.05 nM for Cd^{2+} , Pb^{2+} , Cu^{2+} , and Hg^{2+} respectively. Furthermore, the sensor's performance was in good agreement with conventional detection methods (ICP-MS or AFS) when tested with soybean and river water samples. Moreover, the sensor demonstrated outstanding selectivity, recovery, reproducibility, and stability. Although Fe_3O_4 possesses wide applications, its use hinders due to its aggregation issues due to high surface energy, leading to less catalytic activities. Hence, the composite with F-MWCNT leads to a synergetic effect in the detection limit of Fe_2O_3 . MWCNT was intentionally fluorinated to raise the electro-conductivity of MWCNT. One possible explanation for the improved heavy metal detection performance of F-MWCNTs is the strong electronegativity of fluorine. This property is believed to impart negative charges to the F-MWCNTs, enhancing the adsorption of HMIs and ultimately resulting in better detection performance.

The representative TEM images show the size of Fe_3O_4 nanoparticles around 5 nm, and Fe_3O_4 nanoparticles were uniformly grown on the surface of MWCNTs or F-MWCNTs. The surface of F-MWCNTs was rougher than that of MWCNTs, further indicating the successful fluorination of MWCNTs. However, the system has indicated superiority over other sensors, still lacks low detection limits, and is selective to particular HMIs.

Bodkhe et al. [19] have reported Au-modified SWCNT incorporated in MOF-199 for the detection of Pb^{2+} ions. In this work, the solvothermal route was adopted for the synthesis of the composite. They observed a significant decrease in the surface area of MOF 199 (1374.98 m^2/g) by modification by Au-SWCNT, i.e., 856.11 m^2/g . The DPV method is used for the detection of Pb^{2+} ions. A calibration plot was generated for the electrochemical response of Au/SWNTs@MOF-199 to Pb^{2+} ions over a range of 0.1 mM–1 pM ($R^2 = 99.58$), demonstrating the sensor's high sensitivity. Additionally, the sensor exhibited a low LOD of 25 pM and a rapid response time of just a few seconds. The proposed system shows the lowest possible detection limit compared to earlier reported work. However, scalability towards actual/real samples is missing in the manuscript. Also, the feasibility of proposed materials towards flexible substrates is missing in the manuscript. The DPV depicted in Figure 9 demonstrates the selective detection of Pb^{2+} ions amidst other metal ions. The DPV response indicated the presence of distinctive, well-defined, and separated reduction peaks located at approximately -0.45 V and -0.01 V, solely for Pb^{2+} ions. The peak shift observed may be attributed to the buffer solution pH, resulting in a rapid stripping response of the electrode. Additionally, the formation of lead oxide during the accumulation stage with the sensing material (Au/SWNTs@MOF-199) was concluded. Current peaks for other metal ions were not significant as Pb^{2+} ion peaks. This confirms that Au/SWNTs@MOF-199 is selective only for Pb^{2+} ions.

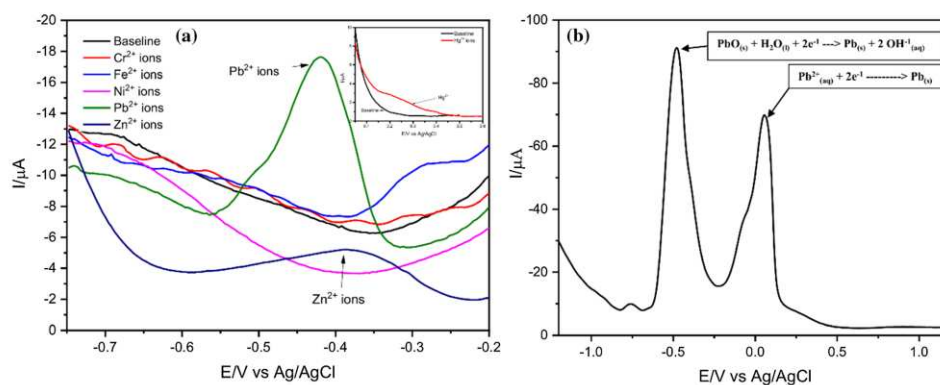


Figure 9. a) Individual sensing response of metal ions, viz. Zn^{2+} , Cr^{2+} , Ni^{2+} , Fe^{2+} , Pb^{2+} and Hg^{2+} (inset); b) interference study of Zn^{2+} . Reproduced from [19] with permission of Springer.

Xu et al. [117] have created a cost-effective, highly sensitive, and active electrochemical sensor, the $\text{Fe}_3\text{O}_4/\text{MWCNTs}/\text{LSG}/\text{CS}/\text{GCE}$, by functionalizing $\text{Fe}_3\text{O}_4/\text{MWCNTs}$ /laser scribed graphene composites with chitosan-modified GCE. This sensor was designed to detect Cd^{2+} and Pb^{2+} simultaneously using SWASV. Through in situ plating of a bismuth film, they observed favorable electrochemical responses with a broad linear range between 1 and 200 $\mu\text{g}/\text{L}$ and an ultralow LOD of 0.1 and 0.07 $\mu\text{g}/\text{L}$ for Cd^{2+} and Pb^{2+} , respectively. The sensor demonstrated excellent reproducibility, repeatability, stability, and practical applicability, making it highly reliable.

A reliable and sensitive anodic stripping voltammetry (ASV) technique was reported by Le et al. [118], utilizing a series of MWCNTs modified with antimony oxide ($\text{Sb}_2\text{O}_3/\text{MWCNTs}$) paste electrode. This technique was successfully utilized for the simultaneous electrochemical detection of Cd^{2+} and Pb^{2+} ions. Initially, a paste electrode was prepared using a composite of MWCNTs. The MWCNTs bulk electrode was subsequently modified using different concentrations (1%, 3%, and 4% wt. %) of Sb_2O_3 , thereby enhancing the detection capability of cadmium ions (Cd^{2+}) and lead ions (Pb^{2+}). The 3 wt.% $\text{Sb}_2\text{O}_3/\text{MWCNTs}$ electrode displayed outstanding analytical detection capabilities for Cd^{2+} and Pb^{2+} using the linear sweep anodic stripping voltammetry (LSASV) technique. The current response exhibited proper linear curves in relation to the concentration of Cd^{2+} (80–150 ppb) and Pb^{2+} (5–35 ppb). Interestingly, the analytical sensitivity of the Cd^{2+} and Pb^{2+} was 1.93 and 2.69 $\mu\text{A}\cdot\text{L}\cdot\mu\text{g}^{-1}$, respectively, higher than 1.5 and 1.3 times the individual ion's sensitivity.

Mariyappan et al. [119] developed a Sr-doped FeNi-S nanoparticle by a simple one-step pyrolysis process and successfully integrated it with SWCNTs ($\text{Sr@FeNi-S}/\text{SWCNTs}$) using an ultrasonication method. Electrochemical impedance analysis of the $\text{Sr@FeNi-S}/\text{SWCNTs}$ electrode shows favorable kinetic charges for transport compared to those of Sr@FeNi-S and SWCNTs. A glassy carbon electrode modified with $\text{Sr@FeNi-S}/\text{SWCNTs}$ was constructed and used for the selective and sensitive electrochemical determination of trace amounts of mercury (Hg(II)) using DPV. The results showed a wide linear range (0.05–279 μM), with low LOD of 0.52 nM of Hg(II) and a sensitivity of 1.84 $\mu\text{A}\cdot\mu\text{M}^{-1}\cdot\text{cm}^{-2}$.

Katowah et al. [120] have fabricated a unique network core-shell structure based on poly(Pyrrole-co-O-Toluidine) (PPCOT) - NiFe_2O_4 (NF) nanoparticles (NPs). It was decorated with cross-linked SWCNTs (C-SWCNTs). This nanocomposite was used for the detection of Fe^{3+} ions. The improved properties were attributed to the 3D structure of C-SWCNTs, which offers a large specific surface area that improves the electrical conductivity of the ternary PPCOT/NF/C-SWCNT nanocomposite. The fabricated sensor exhibited good sensitivity and a lower LOD of 11.02 $\text{mA}\cdot\text{mM}^{-1}\cdot\text{cm}^{-2}$ and 97.08 ± 4.85 pM, respectively. They exhibited excellent linearity for concentrations ranging from 0.1 nM to 0.01 mM with excellent reproducibility and response time.

A research team by Yıldız et al. [121] has recently published a study detailing their development and use of an electrochemical sensor utilizing a pencil graphite electrode (PGE) that has been coated with a combination of MWCNT and nano-sized sodium montmorillonite (NNA_M). The team also collected bismuth nanoparticles (BiNP) on the electrode surface during the analyte deposition process

to enhance the sensor's capabilities, leading to improved electrochemical analysis. The heavy metal cations, zinc (II), cadmium (II), lead (II), and copper (II) were qualified at the potentials of about -1.0 , -0.70 , -0.47 , and 0.00 V, respectively, and they quantified within the linear concentration ranges of 2.36 – 40.0 ; 40.0 – 180.0 μM , 0.32 – 2.0 ; 2.0 – 240.0 μM , 0.03 – 5.0 ; 5.0 – 80.0 μM and 0.52 – 10.0 ; 10.0 – 40.0 μM , respectively. The results of the electrochemical quantification reveal that the newly developed electrode is a cost-effective solution with a highly conductive surface area. The electrode can produce a significantly higher SWAS signal, making it a more efficient tool for electrochemical analysis than an unmodified PGE. Repeatability and reproducibility for BiNP/MWCNT-NNaM/PGE electrodes were found to be $\text{RSD} < 9.5\%$ and $\text{RSD} < 8.0\%$, respectively. The interference effects of the cations Mn^{2+} , Al^{3+} , Ni^{2+} , Sb^{3+} , Co^{2+} , Fe^{3+} , Cr^{3+} , Ca^{2+} , Mg^{2+} and Na_3PO_4 at concentrations ten-fold lower than the analytes are tolerable ($<4.5\%$). Detection limits as low as 0.707 μM , 0.097 μM , 0.008 μM , and 0.157 μM were observed for Zn (II), Cd (II), Pb (II), and Cu (II), respectively.

A recent study (Zhao et al. 2023 [91]) introduces a novel sensing platform, Co@NC/MWCNT, for the simultaneous monitoring of Cd^{2+} and Pb^{2+} . This platform is based on ZIF-67-derived cobalt/nitrogen-doped carbon (NC) composite polyhedrons linked with MWCNTs. The MWCNTs are first grown in situ with nanoporous ZIF-67, followed by carbonization to endow the composite with good electrical conductivity and a large specific surface area. This provides more active sites for subsequent metal ion attachment. The proposed sensing platform showed a relatively more comprehensive linear range of 0.12 – 2.5 μM , with lower LOD of 4.5 nM (Cd^{2+}) and 4.9 nM (Pb^{2+}) under optimal parameters.

Yu et al. [122] have developed a simple and efficient method for synthesizing a nanocomposite comprising carbon nanotubes (CNTs) and MOFs, and demonstrated its utility in constructing an electrochemical sensor for the detection of Cd^{2+} in aqueous solutions. The sensing surface of the sensor was created by casting a drop of the CNTs-MOFs nanocomposite onto the electrode, which was then dried at room temperature before being immersed in a Cd^{2+} -containing acetate buffer solution for electrochemical measurements. The electrochemical characterizations validated the good conductivity and excellent Cd^{2+} -responsive properties of CNTs-MOFs. As expected, the analytical performance for Cd^{2+} determination was satisfactory, with a broad linear detection range of 0.3 μM – 150 μM , a LOD of 0.2 μM , and good selectivity.

A recent study (Tan et al. [123]) reports the synthesis of a novel hybrid material, $\text{NH}_2\text{-UiO-66@ZIF-8}$ (NU66@Z8), by integrating amino functionalized zirconium-based metal-organic framework ($\text{NH}_2\text{-UiO-66}$) and zinc-based zeolitic imidazolate framework (ZIF-8). This core-shell architecture hybrid material was combined with carboxylated multi-walled carbon nanotubes (CMWCNT) to fabricate an electrochemical platform for detecting Pb^{2+} and Cu^{2+} . The platform was created by depositing the NU66@Z8-CMWCNT composite onto a GCE. The sensor developed under optimal conditions demonstrated exceptional sensing capability, with a low LOD (1 nM for Pb^{2+} and 10 nM for Cu^{2+}) and a broad determination range (0.003 – 70 μM for Pb^{2+} and 0.03 – 50 μM for Cu^{2+}). The sensor also exhibited high selectivity towards common interfering ions and good repeatability. The real sample recoveries of the proposed sensor were in the range of 95.0 – 103% for Pb^{2+} ($\text{RSD} \leq 5.3\%$) and 94.2 – 106% for Cu^{2+} ($\text{RSD} \leq 5.9\%$), suggesting that the NU66@Z8/CMWCNT is suitable for examining trace heavy metals in the natural environment.

4.4. Graphene, Graphene Oxide and Reduced Graphene Oxide-Based Nanocomposites

Graphene has emerged as a promising material for detecting heavy metal ions due to its unique structural and chemical properties. Some of the advantages of using graphene for HMIs detection include:

- High sensitivity: Graphene has an exceptionally high surface area-to-volume ratio, allowing for efficient HMIs adsorption. This results in highly sensitive detection with low detection limits.
- Selectivity: The surface chemistry of graphene can be modified to selectively capture specific HMIs, enabling the detection of individual or multiple metal ions in complex samples.
- Rapid response time: Graphene-based sensors have a fast response time due to graphene's efficient electron transfer properties. This allows for real-time detection of HMIs.

- **Stability:** Graphene is highly stable and can withstand harsh chemical and physical conditions, making it suitable for use in various environmental and industrial settings.
- **Low cost:** Graphene-based sensors are relatively inexpensive to produce compared to traditional HMIs detection methods, making them a cost-effective alternative.

Overall, graphene's unique properties make it an attractive material for HMIs detection with potential applications in environmental monitoring, food safety, and industrial processes. Therefore, graphene/graphene oxide and reduced graphene oxide nanocomposites have been explored by various researchers to detect HMIs [125-139].

Cheng et al. [128] have reported the synthesis of reduced graphene oxide (rGO) and silver nanoparticle (AgNPs) nanocomposites for the detection of HMIs. The hydrothermal reduction method has been used for preparation of the rGO/Ag NPs composites in this work. The synthesized rGO/AgNPs composites were labelled as FxG where x was the volume of added AgNO₃ solution (2 mL, 4 mL, 6 mL, 8 mL, respectively) accordingly four different combinations viz. F2G, F4G, F6G, and F8G have been investigated. The schematic graphic of the synthesis of AgNPs and rGO/AgNPs composite is shown in Figure 10. The authors reported extremely low LOD below 0.1 pM, however, the lowest concentration of heavy metals examined was only 1 nM.

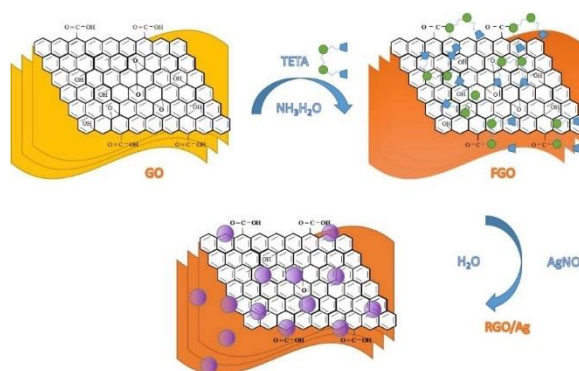


Figure 10. The scheme of the formation of Ag NPs and rGO/AgNPs composites. Reproduced from [128] with permission of Elsevier.

4.5. Graphitic Carbon Nitride (g-C₃N₄) - Based Nanocomposites

Graphitic carbon nitride (g-C₃N₄) has several advantages for the detection of HMIs:

- **High sensitivity:** g-C₃N₄ has a high surface area and strong adsorption ability, allowing it to capture and detect trace amounts of HMIs in the solution.
- **Selectivity:** g-C₃N₄ has a high selectivity towards HMIs due to its surface's unique electronic and chemical properties. This means it can distinguish between HMIs and detect only the specific metal ion(s) of interest.
- **Low cost:** g-C₃N₄ is a relatively low-cost material, making it an attractive option for practical applications.
- **Stability:** g-C₃N₄ is stable under a wide range of conditions, including high temperatures and harsh chemical environments, making it suitable for real-world applications.
- **Environmental friendliness:** Unlike many other HMIs detection methods, g-C₃N₄ does not rely on toxic reagents or generate harmful waste products, making it an environmentally friendly option.

These advantages make g-C₃N₄ a promising material for detecting HMIs in various settings, from industrial wastewater treatment to environmental monitoring. While graphitic carbon nitride (g-C₃N₄) has several advantages for sensor applications, there are also some challenges that researchers have to face:

- **Poor conductivity:** g-C₃N₄ is an insulating material, which means it has poor electrical conductivity. This limits its usefulness in specific sensor applications that require high conductivity.

- Limited response time: g-C₃N₄ sensors can have a relatively slow response time compared to other sensing materials, which may limit their use in specific applications that require fast response times.
- Limited stability: While g-C₃N₄ is generally stable under a wide range of conditions, it can be prone to degradation over time, particularly under certain environmental conditions. This can impact the sensor's performance and longevity.
- Lack of standardization: There is currently a lack of standardized protocols for synthesizing and characterizing g-C₃N₄, making comparing results between different studies difficult.
- Sensitivity to environmental conditions: g-C₃N₄ sensors can be sensitive to changes in environmental conditions, such as temperature and humidity, affecting their performance.

To address these challenges, researchers have explored the advantageous aspects of g-C₃N₄ by having nanocomposite with other materials for the detection of HMIs [140-149].

Zheng et al. [140] reported disposable electrochemical sensors fabricated onto photo paper using screen printing techniques. Bismuth-modified graphitic carbon nitride (Bi/g-C₃N₄) was used for the electrochemical detection of Pb(II) and Cd(II). The Bi/g-C₃N₄ composite was characterized by structural, spectroscopic, morphological, and electrochemical techniques.

The electrode based on Bi/g-C₃N₄ composite was investigated for detecting Cd(II) in the concentration range from 30 µg/L to 120 µg/L with a LOD of 17.5 µg/L. Similarly, the electrode based on Bi/g-C₃N₄ composite was investigated for the detection of Pb(II) in the concentration range of 30 to 110 µg/L. The authors have used a novel composite for determining HMIs using electrochemical modality. The LOD was below the maximum concentration level suggested by USEPA. The sensor exhibited excellent sensitivity with the capability of doing real sample analysis. However, the sensor's repeatability, reproducibility, and stability aspects have been discussed.

Eswaran et al. [148] have developed a simple, cost-effective, and efficient method for fabricating a nano-engineered poly(melamine)/graphitic-carbon nitride nano-network (PM/g-C₃N₄) modified screen-printed carbon electrode (SPE) for the simultaneous electrochemical monitoring of toxic HMIs in environmental water. The team used a single-step in-situ electrochemical polymerization deposition technique to deposit g-C₃N₄ and melamine monomer on pre-anodized SPE (ASPE) through cyclic voltammetry. The resulting modified electrode showed high sensitivity and selectivity toward HMIs detection. The performance of the PM/g-C₃N₄/ASPE sensor was investigated by DPV for the detection of Pb²⁺ and Cd²⁺ ions. The PM/g-C₃N₄/ASPE sensor exhibited stable, repeatable, anti-interference behavior with the capability of detecting Pb²⁺ and Cd²⁺ ions in natural water samples.

The DPV response of PM/g-C₃N₄ for the detection of Cd²⁺ and Pb²⁺ is shown in Figure 11 (a) and (b), respectively. The sensor exhibited excellent linear response in the concentrations range from 0.1 to 1.0 µM, and the LOD for Pb²⁺ and Cd²⁺ was 0.008 µM and 0.02 µM, respectively. The performance of this sensor was also investigated for actual water samples, which is an advantageous aspect of this article. However, the repeatability and reproducibility aspects of the sensors have not been discussed.

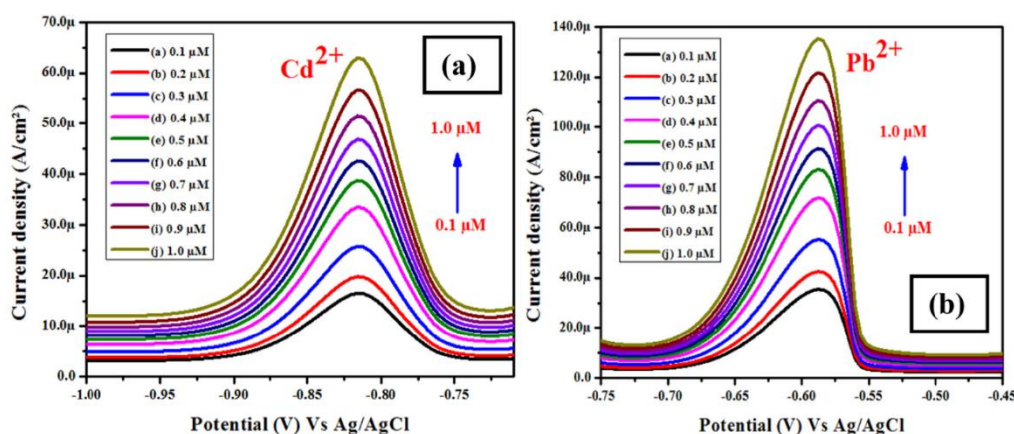


Figure 11. The DPV response of the ASPE-PM/g-C₃N₄ composite-modified electrode of (a) Pb²⁺ and (b) Cd²⁺ over a concentration range of 0.1–1.0 µM. Reproduced from [148] with permission of Elsevier.

Hexavalent chromium (Chromium (VI) (Cr^{6+})) is a toxic element that is most threatening the human cycle as well as the environment. Karthika et al. [144] have reported a novel electrochemical sensor for the detection of this highly toxic element, chromium (VI), in actual samples. A graphene carbon nitride-doped silver molybdate immobilized Nafion ($\text{g-C}_3\text{N}_4/\text{AgM}/\text{Nf}$) modified glassy carbon electrode (GCE) was developed using a straightforward sonochemical approach for the sensor's construction. The sensor showed excellent selectivity and sensitivity towards the detection of chromium (VI) with a LOD of 1.6 nM and sensitivity of $65.8 \mu\text{A} \cdot \mu\text{M}^{-1} \cdot \text{cm}^{-2}$. The sensor also demonstrated good stability and reproducibility with a linear range of 0.1 to $0.7 \mu\text{M}$. The proposed sensor can be used as a reliable and effective tool for the detection of chromium (VI) in environmental and industrial samples. The stepwise fabrication of the $\text{g-C}_3\text{N}_4/\text{AgM}/\text{Nf}$ modified glassy carbon electrode for the Cr^{6+} sensor is shown in Figure 12.

The SEM image of AgM confirms the formation of AgM nanorods with an average size of 100 nm. A sheet-like structure having a normal size of 100 nm is confirmed for $\text{g-C}_3\text{N}_4$. The adsorption of $\text{g-C}_3\text{N}_4$ onto the surface of AGM by electrostatic communication is confirmed by nanorod-shaped structures. The presence of an element viz. O, Mo, C, N, and Ag without any other significant impurities are confirmed by the EDAX spectrum of ($\text{g-C}_3\text{N}_4/\text{AgM}$). The sensing response for $\text{g-C}_3\text{N}_4/\text{AgM}/\text{Nf}$ modified GC electrode exhibited a linear response for a range of concentrations of Cr^{6+} (10 to $100 \mu\text{M}$).

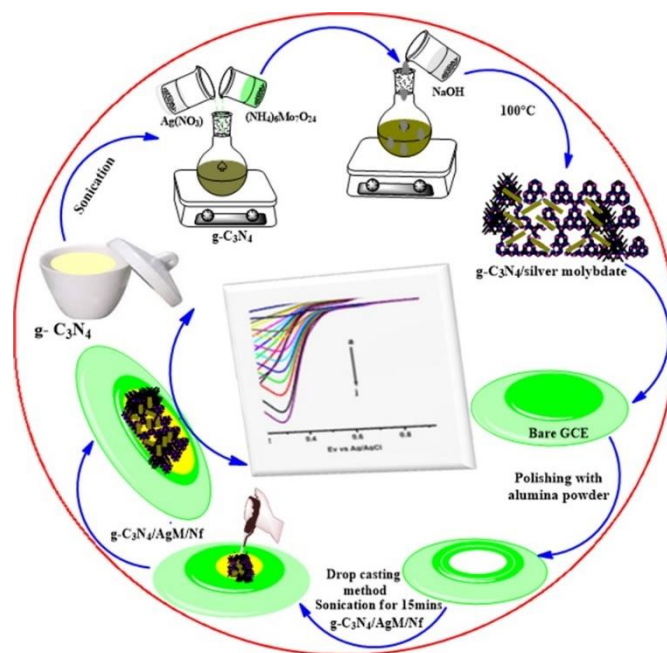


Figure 12. The scheme of the stepwise fabrication of $\text{g-C}_3\text{N}_4/\text{AgM}/\text{Nf}$ modified glassy carbon electrode for Cr^{6+} sensor. Reproduced from [144] with permission of Elsevier.

4.6. Metal Oxide-Based Nanocomposite

Metal oxide-based nanocomposites have emerged as a promising solution for detecting HMIs due to their properties to achieve high sensitivity and selectivity of the sensor. These nanocomposites typically comprise a metal oxide nanoparticle and a functional organic or inorganic material. The metal oxide nanoparticles serve as the sensing element, and the functional material enhances the selectivity and sensitivity of the nanocomposite.

Several metal oxide nanoparticles, such as zinc oxide, titanium dioxide, and iron oxide, have been incorporated into nanocomposites for HMIs detection. Additionally, various functional materials, such as graphene, carbon nanotubes, and molecularly imprinted polymers, have been used to enhance the selectivity and sensitivity of the nanocomposites.

Metal oxide-based nanocomposites offer several advantages for HMIs detection, including high sensitivity, selectivity, and stability. Moreover, they can be easily integrated into portable devices for the on-site detection of HMIs in environmental samples.

While metal oxide-based nanocomposites offer great potential for detecting HMIs, there are several challenges that researchers will face in their development and use. Some of the key challenges include:

- Sensitivity and selectivity optimization: Metal oxide-based nanocomposites require their sensitivity and selectivity optimization for detecting specific HMIs in complex samples. This requires the development of new functional materials and improved sensing mechanisms.
- Interference from other ions: HMIs detection in complex samples can be complicated by interference from other ions, resulting in false positives or negatives. Researchers will need to develop methods to eliminate or reduce these interferences.
- Stability and reproducibility: The stability and reproducibility of metal oxide-based nanocomposites can be affected by environmental factors, such as pH and temperature, impacting their sensing performance. Researchers will need to develop strategies to enhance the stability and reproducibility of these nanocomposites.
- Environmental impact: The potential environmental impact of metal oxide-based nanocomposites, including their potential release into the environment, is an important consideration that requires careful evaluation.

Therefore, to address these challenges, researchers have explored various nanostructured materials to form nanocomposites with metal oxide for HMIs detection and for the development of practical applications of these nanocomposites [106, 124, 150-166].

A new electrochemical sensing interface utilizing a composite of CeO₂ nanomaterials supported on expanded graphite as the sensitive material was reported by Huang et al. [153]. They have synthesized CeO₂ nanomaterials through a hydrothermal method. Three kinds of CeO₂ nanostructures have been proposed in the present investigation, and their morphologies are tuned from nanorods (r-CeO₂) and nanocubes (c-CeO₂) to nanopolyhedras (p-CeO₂). Moreover, expanded graphite (EG) has been selected as a support to load these CeO₂ nanomaterials. It has been claimed that the interface using nanorod-shape CeO₂ nanomaterials supported on expanded graphite exhibits superior electrochemical activity, namely remarkable signal enhancement for monitoring Cd²⁺ and Pb²⁺ ions. The CeO₂ nanorods (r-CeO₂) exhibited excellent electrochemical sensing performance due to the high surface area and the low charge transfer resistance. Simultaneous determination of Cd²⁺ and Pb²⁺ ions was also performed on r-CeO₂/EG/GCE. The DPV responses for different concentrations of Cd²⁺ and Pb²⁺ ions are shown in Figure 13. The sensor based on the r-CeO₂/EG/GCE composite showed detection limits of 0.39 and 0.21 µg/L for Cd²⁺ and Pb²⁺ ions, respectively, with good repeatability and reproducibility. However, the stability of the sensor has not been investigated.

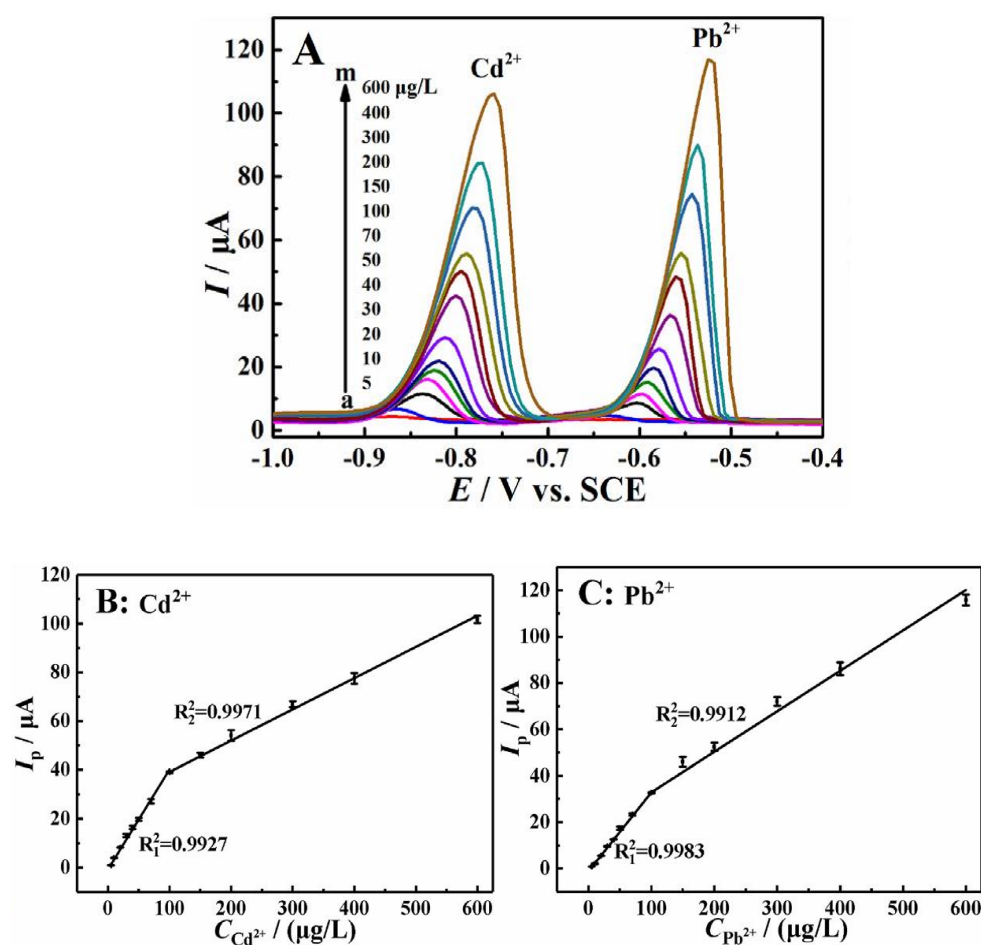


Figure 13. (A) DPVs of Cd²⁺ and Pb²⁺ with different concentrations; Calibration curve for the detection of Cd²⁺ (B) and Pb²⁺ (C). The pulse amplitude, pulse width, and scan rate are 50 mV, 40 ms, and 40 mV s⁻¹, respectively. Reproduced from [153] with permission of Elsevier.

Singh et al. [163] have reported selective and sensitive electrochemical detection of Pb (II) and Cu (II) ions by using Cerium oxide-catalyzed chemical vapour deposition-grown carbon nanofibers. Acetylene and cerium oxide was used for growing the Ce-CNFs. As synthesized, Ce-CNFs were multi-parametrically tested for their structural, functional, morphological, and surface area information via X-Ray diffraction (XRD), Raman, SEM, and Brunauer-Emmett-Telle (BET) respectively. Electrochemical studies of bare GCE and CeCNFs/GCE electrodes were done in 0.1 M ABS using CV and DPV methods at optimal experimental conditions. A schematic representation of the steps involved in making a Ce-CNFs-based electrochemical sensor for real-time detection of Pb (II) and Cu (II) is shown in Figure 14.

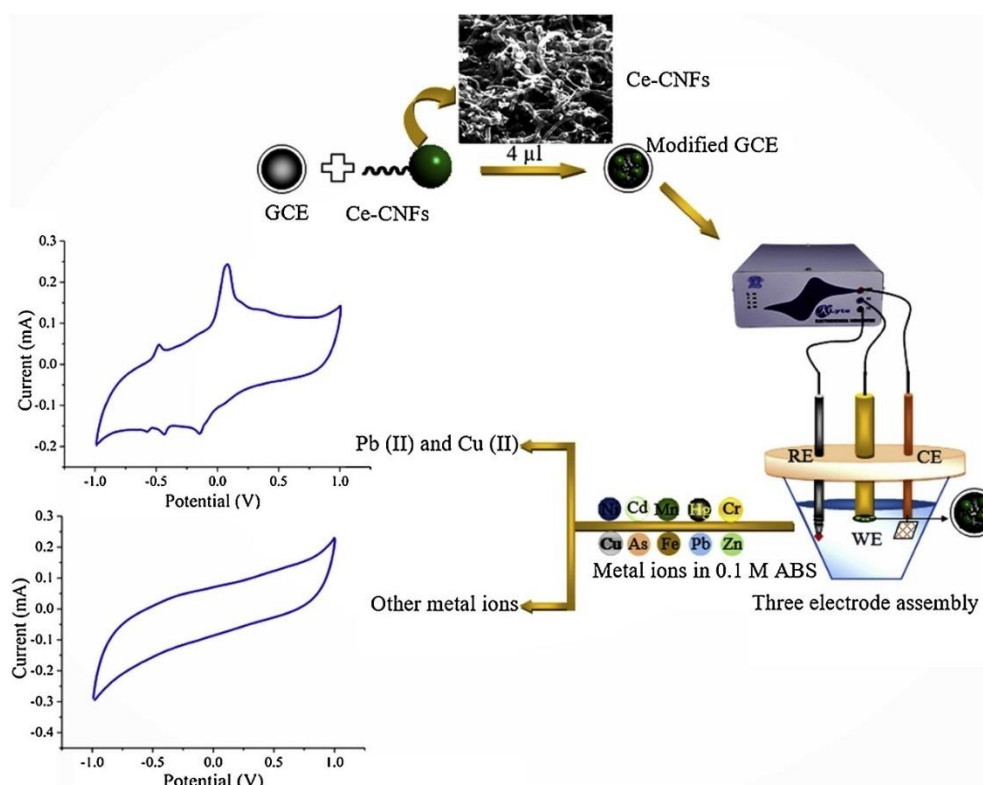


Figure 14. Schematic representation of steps involved in making Ce-CNFs based electrochemical sensor for real-time detection of Pb (II) and Cu (II). Reproduced from [163] with permission of Elsevier.

The cyclic voltammetry (CV) response of Ce-CNFs with Cu (II) metal/ions from the concentration of 0.3 ppb to 10 ppb exhibited significant reproducibility and linearity. It showed excellent linearity from 0.9 ppb to 2.1 ppb of Cu (II) metal/ions. Moreover, DPV analysis was also carried out from -0.7 to 0.0 V using optimized parameters. The LOD of Cu (II) was determined at 0.6 ppb.

Wang et al. [164] have reported $\text{Fe}_3\text{O}_4@\text{PDA}@\text{MnO}_2$ core-shell nanocomposites for electrochemical detection of Pb (II) ion. In this investigation, $\text{Fe}_3\text{O}_4@\text{PDA}@\text{MnO}_2$ core-shell magnetic nanocomposites were synthesized for the first time by the solvothermal method. Synthesized material was multi-parametrically tested for its structural, functional, magnetic, and morphological properties by XPS, FTIR, VSM, and TEM, respectively. A dense polydopamine (PDA) coating was formed on the surface of Fe_3O_4 to ensure high stability in acidic conditions. Redox activity between PDA and KMnO_4 is due to the introduction of a high adsorption capacity MnO_2 shell into the PDA surface. MnO_2 shell with a high adsorption capacity of HMIs was successfully prepared on the Fe_3O_4 surface via dopamine and used to detect Pb (II). Further, $\text{Fe}_3\text{O}_4@\text{PDA}@\text{MnO}_2$ core-shell magnetic NPs were synthesized to improve sensitivity and selectivity. Figure 15 shows a scheme of the fabrication of $\text{Fe}_3\text{O}_4@\text{PDA}@\text{MnO}_2$ core-shell magnetic NPs (A) and the capture, isolation, and detection of the target Pb(II) in the sample solution (B).

DPV technique was used to detect the target analyte. The fabricated sensor linearly detects Pb (II) in the range of 0.1–150 $\mu\text{g/L}$ with a LOD of 0.03 $\mu\text{g/L}$ at optimized electrochemical and chemical conditions such as pH, nanocomposite concentration, supporting electrolytes and preconcentration time. This method showed excellent repeatability with a relative standard deviation (RSD) value of 2.52 % and good stability for up to 4 weeks for 20 $\mu\text{g/L}$ Pb (II). The sensor based on $\text{Fe}_3\text{O}_4@\text{PDA}@\text{MnO}_2/\text{mGCE}$ can be used to directly monitor trace Pb (II) levels in natural water.

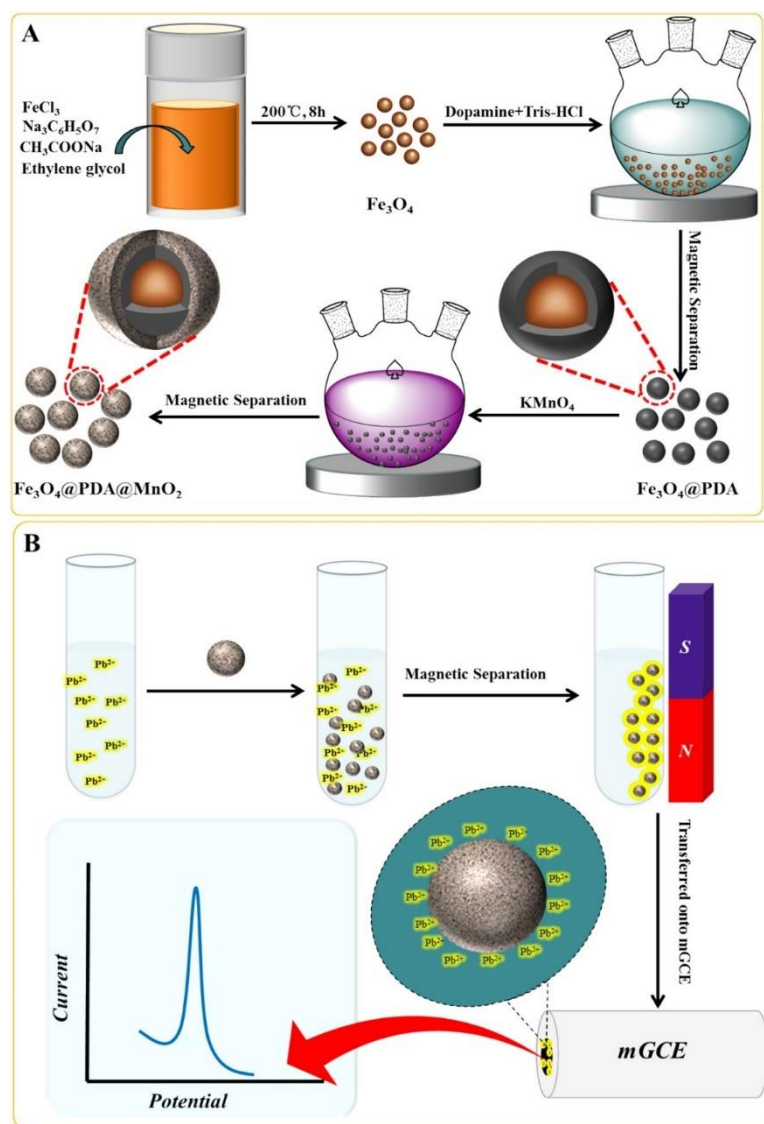


Figure 15. The scheme of the fabrication of Fe₃O₄@PDA@MnO₂ core-shell magnetic NPs (A) and the capture, isolation, and detection of the target Pb(II) in the sample solution (B). Reproduced from [164] with permission of Elsevier.

Padmalaya et al. [167] have reported a disposable modified screen-printed electrode using egg white/ZnO rice structured composite as a practical tool electrochemical sensor. A simple wet chemical technique was used to synthesize ZnO nanoparticles and chitosan/ZnO nanocomposite (NCPs). Synthesized NCPs were characterized using XRD and Fe-SEM for their structural and morphological parameters. A comparative electrochemical analysis was carried out using the cyclic voltammetry. The performance of the developed electrochemical sensor was investigated by employing DPV at various concentrations of formaldehyde. Although not a HMI, we have included formaldehyde in this review because of its toxic nature, and it can also be detected by electrochemical technique. The voltammogram was recorded by scanning the potential anodically in the range of 0 V–1.5 V (vs. Ag/AgCl), as shown in Figure 16(a). Figure 16(b) shows the sensor's calibration plot. The sensor exhibited linear aldehyde detection in the detection range of 1 μM to 5 μM with a sensitivity of 770.68 mM/μA and a LOD of 6.2 nM. The sensor proposed in this study demonstrated its potential for real-time analysis, as it could detect formaldehyde concentrations in urine samples using cyclic voltammetry. The reported sensor based on Egg white albumin/ZnO rice/SPCE shows highly selective behavior, with stability over several days, inexpensive, disposable, and simple to manufacture and operate. However, stability was not very significant, and it exhibited poor linearity at higher concentrations.

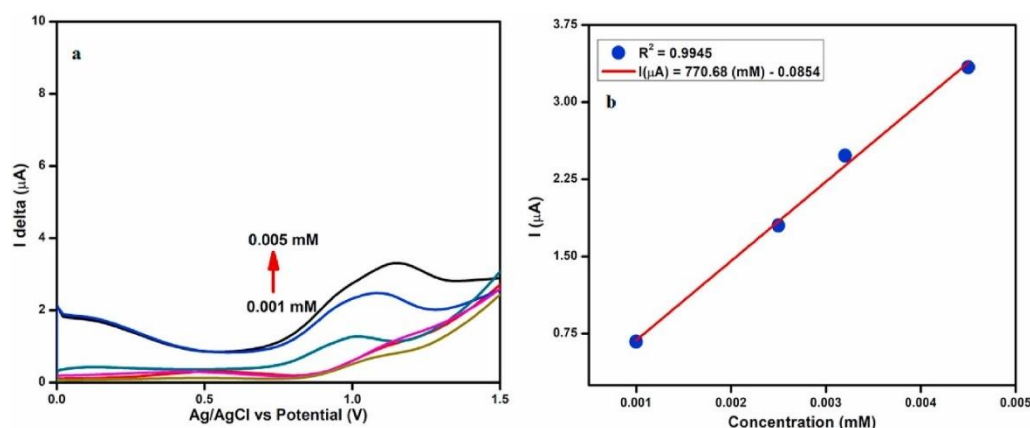


Figure 16. (a) DPV response of Egg albumin/ZnO rice structure/SPCE and (b) calibration plot for various formaldehyde concentrations. Reproduced from [167] with permission of Elsevier.

4.7. Chitosan-Based Nanocomposite

Chitosan-based nanocomposites have shown promise in detecting HMIs in water. These nanocomposites consist of chitosan and metal oxide nanoparticles, which can interact with HMIs through chelation. This interaction causes changes in the optical or electrical properties of the nanocomposite, which can be detected and measured. The use of chitosan (CH) as a base material for these nanocomposites provides several advantages, including biocompatibility, biodegradability, and ease of modification. Overall, chitosan-based nanocomposites have the potential to be an effective and affordable solution for detecting HMIs in water.

While chitosan-based nanocomposites offer promising potential for detecting HMIs, researchers may face several challenges in their development and application. Some of these challenges include:

- **Sensitivity:** Achieving a high level of sensitivity to detect trace amounts of HMIs in water, especially in complex or contaminated samples.
- **Stability:** Ensuring the nanocomposites remain stable and do not degrade or lose their effectiveness over time or under different environmental conditions.
- **Interference:** Dealing with potential interference from other substances in the water, such as organic matter, can affect detection accuracy.
- **Reproducibility:** Ensuring the detection results are consistent and reproducible over time and across different samples.

Therefore, to address these challenges, researchers are exploring different combinations of materials to form nanocomposites with chitosan, which has been proved as an excellent platform for detecting HMIs [105, 136, 138, 168-171].

Wang et al. [138] have reported the development of an electrochemical aptasensor for the sensitive detection of Pb^{2+} using a composite material consisting of chitosan, rGO, and titanium dioxide (TiO_2). The aptasensor was fabricated by immobilizing a specific aptamer for Pb^{2+} onto the composite material and measuring the changes in current upon binding of Pb^{2+} to the aptamer. The aptasensor showed high sensitivity and selectivity towards Pb^{2+} with a LOD of 0.33 ng/L, which is much lower than the maximum allowable limit set by the USEPA for Pb^{2+} in drinking water. The aptasensor was also tested on actual water samples and showed good accuracy and precision. The authors conclude that the developed aptasensor has excellent potential for practical applications in the detection of Pb^{2+} in environmental and biological samples. They have reported a composite containing chitosan, graphene, and titanium dioxide (CS/rGO/ TiO_2) for the detection of Pb^{2+} ions. The reported CV and EIS results confirmed that the CS/rGO/ TiO_2 could improve the electrochemical performance of the electrode and provide a better electrochemical sensing interface. The author reported the development of a novel and sensitive aptasensor for detecting Pb^{2+} using CS/rGO/ TiO_2 . The modified electrode surface was assembled with the complementary strand of the aptamer, which hybridizes with the Pb^{2+} aptamer to form a DNA double-strand structure. The optimization of

experimental parameters, such as the reaction time and the pH of the electrolyte, was performed by DPV.

Moreover, the electrochemical aptasensor was also used to determine the concentration of Pb^{2+} ions in actual samples with acceptable results. The optimized electrochemical biosensor exhibited a wide range of Pb^{2+} detection (1 ng/L to 1 $\mu\text{g/L}$) with a significantly low LOD of 0.33 ng/L, which is well below the maximum concentration level suggested by the USEPA and WHO. The DPV responses of the sensor for different concentrations of Pb^{2+} is shown in Figure 17 (A) and the calibration curve is shown in Figure 17 (B). The aptasensor exhibited excellent repeatability, specificity, and stability. Moreover, its performance was evaluated for detecting Pb^{2+} in food samples, and the results were comparable to those obtained from the ICP-MS method, demonstrating its potential for monitoring Pb^{2+} levels in food samples.

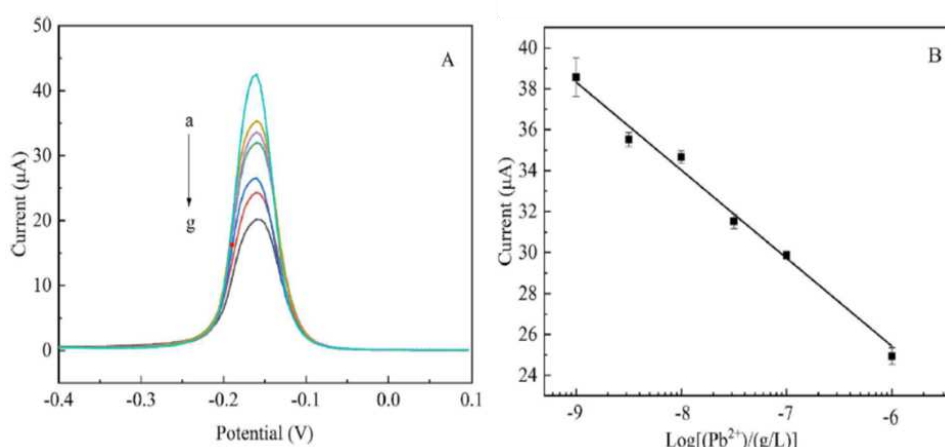


Figure 17. (A) DPV responses of different concentrations of Pb^{2+} . The concentration of Pb^{2+} (g/L): (a) 0; (b) 10^{-9} ; (c) 10^{-8} ; (d) 5×10^{-7} ; (e) 10^{-7} ; (f) 5×10^{-6} ; (g) 10^{-6} , (B) Calibration curve of Pb^{2+} . Reproduced from [138] with permission of Elsevier.

This article reported a novel electrochemical aptasensor for Pb^{2+} detection based on the specific binding of the apt towards the Pb^{2+} and CS/rGO/ TiO_2 composite material. This aptasensor offers the advantages of both rGO and CS properties. rGO provides high surface area and excellent electrocatalysis, which improves electrochemical sensitivity, while CS offers excellent chemical stability, good biocompatibility, and film-forming abilities.

Guo et al. [136] developed a nanocomposite-modified GCE using rGO/ MoS_2 /CS for detecting Pb^{2+} in tobacco leaves. The rGO was incorporated to enhance conductivity, while the nano-flowered MoS_2 provided a large specific surface area and active sites for heavy metal reactions. The CS was added to improve heavy metal enrichment and increase the electrocatalytic activity of the electrode. The sensor exhibited excellent performance in terms of reproducibility, stability, and anti-interference ability. The stripping behavior of Pb(II) was studied using square wave anodic stripping voltammetry (SWASV), and the sensor's application conditions were optimized. A schematic diagram of the sensor based on GCE modified with rGO/ MoS_2 /CS and the electrochemical analysis process for Pb(II) are presented in Figure 18. This work used the electrode modified by GO/ MoS_2 , rGO/ MoS_2 , and rGO/ MoS_2 /CS nanocomposites to determine Pb(II) in an aqueous solution, and the catalytic performance of these electrode-modified materials was evaluated in detail. Among them, the rGO/ MoS_2 /CS nanocomposites had the best electrocatalytic performance and sensitivity for Pb(II) detection. SWASV response of rGO/ MoS_2 /CS/GCE for Pb(II) in the tobacco sample was a in the Pb(II) concentration range from 0.005 to 2.0 μM . The LOD of the rGO/ MoS_2 /CS/GCE-based sensor was 1.6 nM. Moreover, the author used a sensor to determine tobacco leaves' Pb(II) content. This work provided a new approach to the determination of Pb(II) in actual tobacco leaf samples, and ICP-MS also verified the results. The LOD was below the maximum concentration level suggested by USEPA and WHO. The operating experimental conditions of the electrode were optimized, such as pH,

deposition potential, and deposition time. The interference study shows that the rGO/MoS₂/CS nanocomposite is highly selective towards the lead ions. Moreover, the sensor based on rGO/MoS₂/CS/GCE exhibited excellent performance in terms of reproducibility, stability, and anti-interference ability.

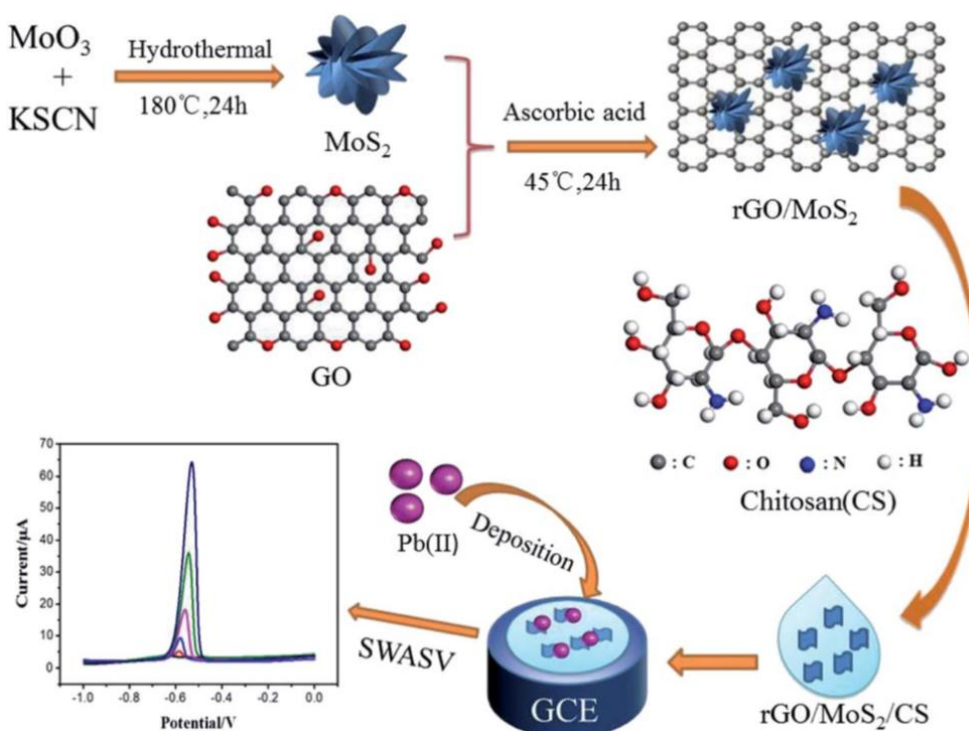


Figure 18. Schematic diagram of the constructed sensor based on GCE modified with rGO/MoS₂/CS and electrochemical analysis process for Pb(II). SWASV is the abbreviation of Square wave anodic stripping voltammetry [136].

4.8. Mxene-Based Nanocomposite

Mxene-based nanocomposites have emerged as a promising platform for detecting HMIs due to their high surface area, conductivity, and facile surface modification. These nanocomposites typically comprise mxene, a two-dimensional transition metal carbide or nitride, and various other materials, including metal oxides, metal sulfides, and carbon-based materials. The resulting nanocomposites exhibit enhanced sensing properties, such as increased sensitivity, selectivity, and stability, making them attractive candidates for environmental monitoring and biomedical applications. Various detection methods, including electrochemical, optical, and colorimetric, have been employed to detect HMIs using mxene-based nanocomposites. Overall, mxene-based nanocomposites hold great potential for the development of effective and efficient sensors for HMIs detection.

While mxenes have shown great promise for HMIs detection, their use still has limitations. The stability of mxene materials is an important factor that can impact their performance and suitability for various applications. Mxenes are two-dimensional transition metal carbides, nitrides, or carbonitrides, typically synthesized by selective etching of the A element (such as aluminium or silicon) from MAX phases (such as Ti₃AlC₂).

Mxenes have a high surface area, which makes them susceptible to oxidation and degradation in specific environments. Exposure to moisture or air can lead to the formation of oxide layers on the surface of mxenes, which can affect their electronic and mechanical properties. In addition, the presence of impurities or defects can also impact the stability of mxenes.

Researchers have explored various strategies to address these stability issues, such as surface functionalization, doping with other elements, and encapsulation in protective matrices. For example, surface functionalization of mxenes with hydrophobic or hydrophilic groups can improve their stability in different environments. Doping with other elements, such as nitrogen or boron, can

also enhance the stability of mxenes and improve their electrochemical performance. Encapsulation of mxenes in protective matrices, such as graphene or polymers, can also prevent their degradation and improve their stability.

Overall, while the stability of mxenes can be a challenge, various researchers have developed and adopted various strategies by synthesizing mxenes-based nanocomposite to address these issues and improve their performance for the detection of HMIs [172-183].

He et al. reported preparing and applying a bismuth/mxene nano-composite as an electrochemical sensor for detecting HMIs [172]. This article focuses on the development of a new type of electrochemical sensor for detecting HMIs. The authors synthesized a bismuth/multilayered mxene (Bi/mxene) composite through a simple and efficient method and investigated its performance as an electrochemical sensor for the detection of HMIs in water. A nano-form composite of mxenes ($\text{Ti}_3\text{C}_2\text{T}_x$, $\text{T}_x = -\text{O}, -\text{OH}, -\text{F}$) was synthesized by depositing bismuth-nanoparticle (BiNPs) onto $\text{Ti}_3\text{C}_2\text{T}_x$ sheets.

The results of the study showed that the $\text{BiNPs}/\text{Ti}_3\text{C}_2\text{T}_x$ nano-composite exhibited excellent electrochemical activity and high sensitivity towards HMIs such as Pb^{2+} , Cd^{2+} , and Hg^{2+} . The electrochemical sensor based on $\text{BiNPs}/\text{Ti}_3\text{C}_2\text{T}_x$ nano-composite also demonstrated good selectivity, stability, and reproducibility. The paper provides a detailed description of the synthesis and characterization of the $\text{BiNPs}/\text{Ti}_3\text{C}_2\text{T}_x$ nano-composite and the fabrication and testing of the electrochemical sensor. The authors also discussed the potential applications of the Bi/mxene composite-based sensor in environmental monitoring and water quality analysis.

The performance of the sensor-based $\text{BiNPs}@ \text{Ti}_3\text{C}_2\text{T}_x/\text{GCE}$ composite was investigated. Figure 19 (A) represents SWASV curves of Pb^{2+} at 0, 0.06, 0.08, 0.2, 0.4, and 0.6 μM in the presence of 0.4 μM Cd^{2+} and the corresponding linear calibration plot against Pb^{2+} is shown in the inset. Similarly, Figure 19(B) represents SWASV curves of Cd^{2+} at 0, 0.08, 0.1, 0.2, 0.4, and 0.6 μM in the presence of 0.2 μM Pb^{2+} at $\text{BiNPs}@ \text{Ti}_3\text{C}_2\text{T}_x/\text{GCE}$, and the corresponding linear calibration plot against Cd^{2+} is shown in the inset. This research paper presents a promising approach for developing highly sensitive and selective electrochemical sensors for detecting HMIs. The sensor based on $\text{BiNPs}@ \text{Ti}_3\text{C}_2\text{T}_x/\text{GCE}$ has the capability to simultaneously detect Pb^{2+} and Cd^{2+} with high sensitivity and good exactness. Utilizing $\text{BiNPs}@ \text{Ti}_3\text{C}_2\text{T}_x$ nano-composite, the sensor can be an excellent electrode-modification material for rapidly and straightforwardly determining UMIs in environment.

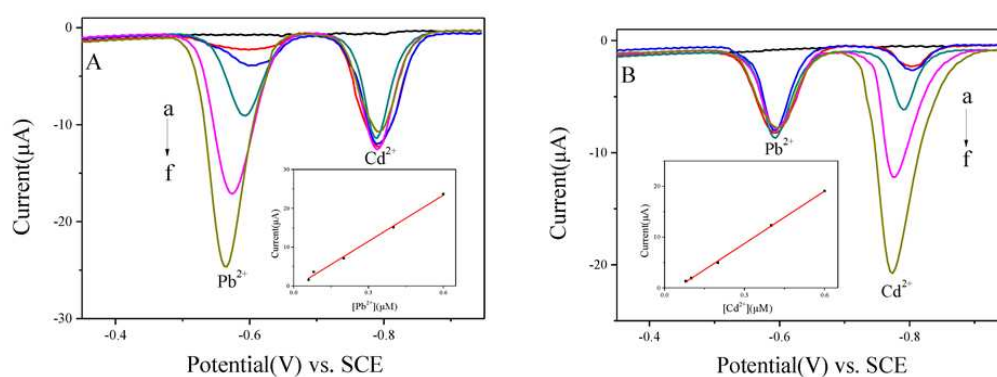


Figure 19. (A) SWASV curves of Pb^{2+} at 0, 0.06, 0.08, 0.2, 0.4, and 0.6 μM in the presence of 0.4 μM Cd^{2+} at $\text{BiNPs}@ \text{Ti}_3\text{C}_2\text{T}_x/\text{GCE}$ and the corresponding linear calibration plots against Pb^{2+} . (B) SWASV curves of Cd^{2+} at 0, 0.08, 0.1, 0.2, 0.4, and 0.6 μM in the presence of 0.2 μM Pb^{2+} at $\text{BiNPs}@ \text{Ti}_3\text{C}_2\text{T}_x/\text{GCE}$ and the corresponding linear calibration plots against Cd^{2+} [172].

4.9. Metal Nanoparticle and Other Material-Based Nanocomposites

Metal nanoparticles and other material-based nanocomposites have been extensively studied as potential materials for the detection of HMIs. Metal nanoparticles, such as gold, silver, and copper, have unique optical and electronic properties that make them suitable for sensing applications. They can be easily functionalized with specific ligands that bind selectively to target HMIs. Other

materials, such as graphene, carbon nanotubes, and MOFs, have also been investigated for their potential in HMIs detection.

The nanocomposites of nanoparticles and other materials, have also been studied for their sensing capabilities. Compared to individual nanoparticles or other materials alone, these composites can provide improved sensitivity and selectivity for HMIs detection.

Overall, metal nanoparticles and other material-based nanocomposites show promise to develop efficient and reliable sensing platforms for HMIs.

Researchers studying metal nanoparticles and other material-based nanocomposites for HMIs detection may face several challenges during their research. Some of these challenges include:

- Synthesis of metal nanoparticles and other nanocomposites with controlled properties can be challenging. Researchers must carefully control the nanoparticles' size, shape, and surface chemistry to ensure optimal sensing performance.
- Sensitivity and selectivity: Developing high-sensitivity and selectivity sensors for detecting HMIs can be challenging. Researchers must design nanocomposites that selectively bind to target ions while avoiding interference from other species.
- Stability: The stability of metal nanoparticles and other nanocomposites is important for sensing applications. Researchers must ensure the nanocomposites are stable over time and under different environmental conditions to maintain their sensing performance.
- Reproducibility: The reproducibility of sensing results is crucial for practical applications. Researchers need to ensure that the sensing performance of nanocomposites is consistent across different batches and under different conditions.

Therefore, to address these challenges, various possibilities of synthesizing nanocomposite based on metal nanoparticles and other materials have been explored by researchers for the detection of HMIs [184-203].

Naseri et al. [184] reported the development of a robust electrochemical sensor based on a butterfly-shaped silver nanostructure (AgNS/SPCE) for the concurrent quantification of heavy metals in water samples. The sensor is designed to detect four heavy metals, lead, cadmium, mercury, and copper, commonly found in water samples and can cause severe health hazards. The butterfly-shaped silver nanostructure provides a large surface area for enhanced sensing performance, while its robustness ensures stability and reproducibility of the sensor's response. In this work, silver nanostructure (AgNS) was electrodeposited on SPCE by applying cyclic voltammetry via sweeping potential between 0 and 1.2 V. The authors also investigated the electrochemical behavior of SPCE and AgNS/SPCE. The authors described the fabrication process of the sensor and provided details of its electrochemical characterization. They also demonstrate the sensor's performance in detecting heavy metals in natural water samples and compare its results with those obtained from standard analytical methods. The results show that the sensor exhibits excellent sensitivity, selectivity, and reproducibility for the quantification of heavy metals in water samples.

The performance of the sensor based on AgNS/SPCE was investigated for the simultaneous detection of four target metal ions. Figure 20 shows the DPSV responses of the sensor for Cd (II), Pb (II), Cu (II), and Hg (II). Four individual prominent peaks appeared at approximately -0.788 V, -0.536 V, -0.209 V, and 0.627 V for Cd (II), Pb (II), Cu (II), and Hg (II), respectively, can be seen in DPSV responses.

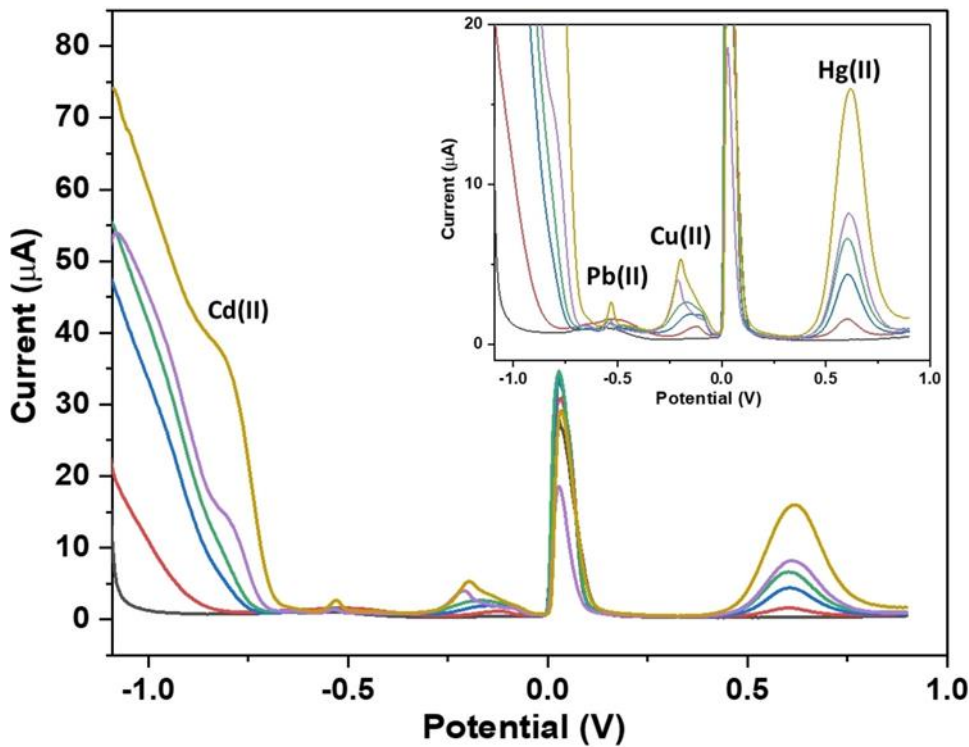


Figure 20. DPSPV responses of AgNS/SPCE using 0.1 M acetate buffer pH 4.4 containing different concentrations of Cd (II), Pb (II), Cu (II), and Hg (II) [184].

Overall, the study presents a promising approach for the development of robust and efficient electrochemical sensors for the quantification of heavy metals in water samples, which can have significant implications for environmental monitoring and public health.

A summary of nanocomposites used, the methodology utilized for detection, and outcomes of electrochemical sensors regarding sensitivity, the limit of detection (LOD), stability, repeatability, reproducibility, and linearity reported by various researchers is illustrated in Table 3.

Table 3. Summary of the properties of the sensors based on nanocomposites for detection of HMIs.

HMIs	Nanocomposite	Method of detection	LOD	Stability, repeatability, reproducibility	Linear range	Ref.
Hg(II)	Sucrose sensor using platinum ultra-microelectrode	CV	5×10^{-10} M	57 days, No, Yes	$(5 - 12.5) \times 10^{-10}$ M	[4]
Pb(II) Cd(II)	Graphene-MWCNTs	DPASV	0.2 µg/L	No	0.5–30 µg/L	[12]
Cd(II) Pb(II) Cu(II) Hg(II)	Hydrosulphonyl functional COF (COF-SH)	SWV	Cd: 0.3 µg/L Pb: 0.2 µg/L Cu: 0.2 µg/L Hg: 1.1 µg/L	Yes, Yes, No	Cd: 1–1000 µg/L Pb: 1–800 µg/L Cu: 1–800 µg/L Hg: 5–1000 µg/L	[13]
Cd(II) Pb(II)	Yb-MOF	DPASV	Cd: 3.0 ppb Pb: 1.6 ppb	Yes, Yes, Yes	--	[15]

Cd(II) Pb(II) Cu(II) Zn(II)	trGNO/Fc-NH ₂ - UiO-66	DPASV	Cd: 8.5 nM Pb: 0.6 nM Cu: 0.8 nM Zn: 0.11 µg/L	20 days, No, Yes	Cd: 0.01–2 µM Pb: 0.001–0.1 µM Cu: 0.001–0.1 µM	[16]
Cd(II), Pb(II)	Fe ₂ O ₃ /G/Bi	DPASV	Cd: 0.08 µg/L Pb: 0.07 µg/L	Yes, Yes, No	1–100 µg/L	[17]
Pb(II)	Au/SWNTs@MO F-199	DPV	25 pM	No, Yes, Yes	0.1 mM–1 pM	[19]
Cu(II) Pb(II)	PEDOT:PSS/rGO	FET	Cu: 0.33 µg/L Pb: 2.36 µg/L	No	1–60 µg/L	[20]
Cd(II) Hg(II) Pb(II)	rGO/MoS ₂	DPV	5 µM	No, No, No	5 – 160 µM	[65]
Cd(II), Cu(II), Hg(II), Pb(II)	rGO/SMOF/PEI modified SPCEs	DPV	Cd: 0.296 µM Cu: 0.055 µM Hg: 0.351 µM Pb: 0.025 µM	–	Cd: 0.50–15.0 µM, Cu: 0.50–13.0 µM, Hg: 1.0–5.0 µM Pb: 0.50–13.0 µM	[67]
Cd(II), Pb(II) and Hg(II)	nano-Au- modified electrode	ICP-MS	Cd: 1.1 µg/L Pb: 1.0 µg/L Hg: 1.2 µg/L	–	0-200 µg/L	[68]
Pb(II)	nano-Cu WE	SWV	45 nM	–	0.5–1 µM	[69]
Zn(II), Cu(II), Hg(II), Pb(II)	DEP chips	DPV	Pb: 2.2 µg/L Hg: 2.5 µg/L Cu: 15.5 µg/L Zn: 10 µg/L	–	Pb: 10–500 ppb Hg: 25–1000ppb Cu: 25–500 ppb Zn: 10–300 ppb	[72]
Cd(II), Pb(II)	gold/bismuth film	(SWASV)	2.20 µg/L	Yes	0–300 µg/L	[73]
Zn, Cr, Cu, Pb, Mn	Colorimetric paper strip	ICP-OES	Zn: 0.63 mg/L Cr: 0.07 mg/L Cu: 0.17 mg/L Pb: 0.03 mg/L Mn: 0.11 mg/L	7 days, Yes, No	–	[74]
As(III)	GO/MOF	DPASV	0.06 ppb	No, No, Yes	0.2–25 ppb	[78]
Cu(II)	Porphyrinic MOF/rGO nanocomposite	DPV	1.5 µM	21 days, No, No	5–150 µM	[79]

Ni(II)	ZIF-8@DMG/ β -CD/RGO	DPASV	0.005 μ M	–	0.01–1.0 μ M	[81]
Cd(II), Hg(II), Cu(II), and Pb(II)	UiO-66-NH ₂ /SPCE	DPV	Cd: 10.90 fM, Pb: 5.98 fM Cu: 2.89 fM Hg: 3.1 fM	–	0.01–0.35 pM	[82]
Cd(II), Pb(II), Cu(II), Hg(II)	Co-TIC4R-I	SWASV	Cd: 17 nM Pb: 8 nM Cu: 16 nM Hg: 7 nM	Yes	Cd: 0.10–17.00 μ M Pb: 0.05–16.00 μ M Cu: 0.05–10.00 μ M Hg: 0.80–15.00 μ M	[83]
Cd(II) Pb(II)	CUiO-66/Bi/GCE	SWASV	Cd: 1.16 μ g/L Pb: 1.14 μ g/L	Yes	Cd: 10–50 μ g/L Pb: 10 – 50 μ g/L	[84]
Hg(II)	Zr-DMBD MOFs/3D-KSC	SWASV	0.05 μ M	Yes	0.25–3.5 μ M	[86]
Hg(II)	Cu-MOF	DPV	0.063 nM	Yes	0.1–50 nM	[87]
Cd(II), Pb(II), Cu(II) , Hg(II)	GaOOH-UiO-MOFs	DPV	Cd: 0.016 μ M Pb: 0.028 μ M Cu: 0.006 μ M Hg: 0.019 μ M Pb: 0.315 μ g/L	Yes	Cd: 0.35–1.60 μ M Pb: 0.55–2.50 μ M Cu: 0.30–1.40 μ M Hg: 0.10–0.45 μ M	[88]
Pb (II) Cu (II)	NH ₂ -MIL-53(Al)/PPy	DPV	μ g/L Cu: 0.244 μ g/L	Yes	1–400 μ g/L	[89]
As(III)	GO/UiO-67@PtNPs	SWASV	0.48 nM	Yes	2.7–33.4 nM	[90]
Cd(II) Pb(II)	Co@NC/MWCNT	SWASV	Cd: 4.5 nM Pb: 4.9 nM	No	0.12–2.5 μ M	[91]
Pb(II) Cd(II)	Gly/rGO/PANI	SWASV	Pb: 0.07 nM Cd: 0.072 nM	Yes	Pb: 0–1.0 μ M Cd: 0 –1.0 μ M	[92]
Cd(II) Pb(II)	Bi-PPy/MWCNT/CP E	SWASV	Cd: 0.157 μ g/L Pb: 0.099 μ g/L	Yes	Cd: 0.16–120 μ g/L Pb: 0.11–120 μ g/L	[93]
Cd(II), Pb(II), Cu(II)	rGO/Ala/PANI	SWASV	Cd: 0.03 nM Pb: 0.063 nM Cu: 0.045 nM	Yes	80 pM–100 nM	[94]
Hg(II)	Pt/g-C ₃ N ₄ /PTh NCs	DPV	0.009 nM	No	1–500 nM	[95]

Hg(II)	Pt/g-C ₃ N ₄ /PANI NCs	DPV	0.014 nM	No	1–500 nM	[96]
Cd(II)	3DGO-Py10	SWASV	3.6 µg/L	Yes	5–400 µg/L	[97]
Mn(II)	PMMA–SWCNT NCs/GCE	DPV	92.67 ± 4.63 pM	7 days	0.1 nM – 0.01 mM	[98]
Cu(II)	EDTA-PANI/SWNTs	DPV	1.4 µM	Yes	0–2 nM	[102]
Pb(II) and Cu(II)	66@ZIF-8/ /multi-walled carbon nanotubes	DPV	Pb: 1 nM Cu: 10 nM	21 days, Yes, Yes	Pb: 0–80 mM Cu: 0–50 mM	[123]
Hg(II), Pb(II), Cu(II)	ZnFe ₂ O ₄	DPASV	Hg: 1.61 nM Pb: 7.38 nM Cu: 12.03 nM	7 days, No, Yes	0.1–1 mM	[124]
Pb(II)	Gold modified graphene	Amperometric	1.67 pM	14 days, No, Yes	1 nM–1 mM	[125]
Pb(II), Cd(II)	GO-Fe ₃ O ₄ -PAMAM	SWASV	Pb: 130 ng/L Cd: 70 ng /L	3 weeks, Yes, Yes	Pb: 0.4–120 µg/L Cd: 0.2–140 µg/L	[126]
Cd(II), Pb(II)	porous graphene/carboxymethyl cellulose/fondaparinux	SWASV	Cd: 0.28 nM Pb: 0.17 nM	20 days, No, Yes	2 – 20 nM	[127]
Cu(II), Cd(II), Hg(II), Zn(II), Cd(II), Pb(II), Cu(II), Hg(II)	reduced graphene oxide/silver	DPV	Cu: 10–15 M Cd: 10–21 M Hg: 10–29 M Zn: 0.08 µg/L Cd: 0.09 µg/L Pb: 0.05 µg/L Cu: 0.19 µg/L Hg: 0.01 µg/L	–, No, No 30 days, Yes, Yes twelve successive cycles, No, Yes	– Zn: 6–7000 µg/L Cd: 4–6000 µg/L Pb: 6–5000 µg/L Cu: 4–4000 µg/L Hg: 6–5000 µg/L	[128] [130]
Hg(II)	SN-rGO	SWASV	8.93 nM	twelve successive cycles, No, Yes	0.4–12 000 nM	[133]
Cd(II), Cu(II), Hg(II)	NCO/N, S-rGO	DPASV	Cd: 123 nM Cu: 14.4 nM Hg: 67 nM	–	–	[134]

Cd(II), Pb(II), Cu(II), Hg(II)	rGO/ZnO-NPs- EDTA	SWV	Cd: 5.6 µM Pb: 6.8 µM Cu: 2.5 µM Hg: 10 µM	–, No, Yes	Cd: 18.5–500 µM Pb: 22.4–700 µM Cu: 8.3–200 µM Hg: 3.3–300 µM	[135]
Pb(II)	rGO/MoS ₂ /CS	SWASV	0.0016 µM	15 days, No, Yes	0.005–0.05–2.0 µM	[136]
Cd (II)	SnO ₂ @BCG	DPV	1 × 10 ⁻⁴ ppm	–	0.001–0.4 ppm	30 Days, No, Yes
Pb(II)	CS/rGO/TiO ₂	DPV	0.33 ng /L	Yes, Yes, Yes	1 ng–1000 ng/L	[138]
Pb(II)	rGO/AuNPs/ssD NA	CV	1.52 nM	30 days, No, Yes	5–50 nM	[139]
Pb(II), Cd(II)	Bi/g-C ₃ N ₄	SWASV	Cd: 21.8 µg /L Pb: 10.4 µg /L	No, No, No	Cd: 30 –120 µg/L Pb: 30 – 110 µg/L	[140]
Pb(II)	Au/N-deficient- C ₃ N ₄	SWASV	0.029 µM	Yes, No, Yes	0.2–0.8 µM	[141]
Cd(II), Hg(II), Pb(II), Zn(II)	g-C ₃ N ₄ /O- MWCNTs	DPSV	Hg: 0.04 ng/L Pb: 0.008 ng/L Cd: 0.03 ng/L Zn: 0.06 ng/L	Yes, No, Yes	Hg: 4.8 – 93.0 ng/L Pb: 6.5 – 110 ng/L Cd: 4.25 – 79.0 ng/L Zn: 4.2 – 202.0 ng/L	[142]
Cr (VI), Cu (II), Pb(II)	carbon dots@ graphitic-carbon nitride (CDs@g-C ₃ N ₄) nanocomposite graphene carbon nitride doped	Fluorescenc e	Cr: 0.54 nM Cu: 0.18 nM Pb: 0.2 nM	–	Cr: 0 –10 nM Cu: 0 –10 nM Pb: 0 – 50 nM	[143]
Cr(VI)	silver molybdate immobilized nafion (g- C ₃ N ₄ /AgM/Nf	CV	0.0016 µM	15 days Yes, Yes	10 – 100 µM	[144]
Cd(II), Pb(II), Hg(II)	metal-free g- C ₃ N ₄ /carbon black (CB) composite	DPASV	Cd: 2.1 nM Pb: 0.26 nM Hg: 0.22 nM	–, No, Yes	Cd: 0–700 nM Pb: 0–300 nM Hg: 0–500 nM	[145]

Cd(II), Pb(II), Hg(II)	metal-free g- C ₃ N ₄ /carbon black composite	DPASV	Cd: 2.1 nM Pb: 0.26 nM Hg: 0.22 nM	–, No, Yes	Cd: 0–700 nM Pb: 0–300 nM Hg: 0–500 nM	[146]
Cd(II), Pb(II)	Fe ₃ O ₄ /Bi ₂ O ₃ /C ₃ N ₄ / GCE	SWASV	Cd: 3 nM Pb: 1 nM	15 days, Yes, Yes	0 – 3 µM	[147]
Pb(II), Cd(II)	M/g-C ₃ N ₄ /ASPE	DPV	Pb: 0.008 µM Cd: 0.02 µM	7 days, No, Yes	0.1 – 1.0 µM	[148]
Cd(II), Pb(II)	pg- C ₃ N ₄ /CoMn ₂ O ₄	SWASV	Cd: 0.021 µM Pb: 0.014 µM	excellent stability, Yes, Yes	Cd: 0.5–7.0 µM Pb: 0.2–4.4 µM	[149]
Cd(II)	MnO ₂ /rGO	DPASV	1.12 µg/L	14 days	4.0 – 130 µg/L	[150]
Pb(II), Cd(II), Cu(II), Hg(II)	NiO/rGO	SWASV	0.01 µM	–, No, Yes	-	[151]
Cd(II), Pb(II)	r-CeO ₂ /EG composite	DPV	Cd: 0.39 µg/L Pb: 0.21 µg/L	–, No, No	0–100 µg/L	[153]
Hg(II)	sepiolite/pyrite (Sep/FeS ₂)	SWASV	4.12 nM	good reproducibility	10 – 120 nM	[154]
Pb(II)	α-Fe ₂ O ₃ /NiO heterostructure	SWASV	0.02 µM	30 days , No, good reproducibility	0.05 – 0.9 µM	[155]
Hg(II)	Co ₃ O ₄ /ZnO	SWASV	0.3 µM	20 days, No, No	0 – 2.1 µM	[156]
Pb(II), Cu(II), Hg(II)	Zr/ZrO ₂	DPV	Pb: 0.8 nM Cu: 0.5 nM Hg: 0.4 nM	–	Pb: 0.8 nM – 10 µM Cu: 0.5 nM – 2 µM Hg: 0.4 nM –10 µM	[157]
Cd(II), Pb(II)	SnS-Bi ₂ O ₃	SWASV	Cd: 1.50 nM Pb: 1.40 nM	–, No, No	0 – 1 µM	[158]
Hg(II)	Ru/CeO ₂	SWASV	0.019 µM	–, No, No	0 – 0.9 µM	[159]
Pb(II), Hg(II)	MgO–SiO ₂	SWASV	Pb: 0.019 µM Hg: 0.041 µM	–	–	[160]
Pb(II), Cd(II)	Fe ₃ O ₄ @G2-PAD	SWASV	Pb: 0.17 µg/L Cd: 0.21 µg/L	–	0.5 – 80 µg/L	[161]

Hg(II)	CuO/PVA	DPV	0.42 nM	–, No, Yes,	10–70 µM	[162]
Pb(II), Cu(II)	Cerium oxide	CV, DPV	Pb: 0.6 ppb Cu: 0.3 ppb	No, Yes, No	Pb: 0.6 – 12 ppb Cu: 0.3 – 10 ppb	[163]
Pb(II)	Fe ₃ O ₄ @ PDA@ MnO ₂	DPV	0.03 µg/L	28 days, Yes, No	0.1 – 150 µg/L	[164]
Cd(II), Pb(II), Cu(II)	Zn/Fe nanocomposite	CV	Cd: 0.14 mg/L Pb: 0.07 mg/L Cu: 0.04 mg/L	No, No, Yes	0 – 16.5 mg/L	[165]
Cd(II), Pb(II)	Fe ₂ O ₃ /Bi ₂ O ₃	SWASV	Cd: 0.56 nM Pb: 0.36 nM	21 days, Yes, Yes	0.002 – 4 µM	[166]
Zn(II), Cd(II), Pb(II)	Bi/Chitosan	SWASV	Zn: 0.1 ppb Cd: 0.1 ppb Pb: 0.2 ppb	No, Yes, Yes	Zn: 1 – 5 ppb Cd: 1 – 5 ppb Pb: 1 – 10 ppb	[168]
Cu(II)	Chitosan/GO	DPASV	0.15 µM	No, Yes, Yes	0.5 – 100 µM	[169]
Cd(II)	Chitosan/Au/Gra phene	DPV	0.162 nM	30 days, Yes, No	0.1 – 0.9 µM	[170]
Pb(II)	PVA/Chitosan/rG O	SWASV	0.05 ppb	No, Yes, Yes	1 – 50 ppb	[171]
Pb(II), Cd(II)	Bi/MXene	SWASV	Pb: 10.8 nM, Cd: 12.4 nM	42 days, Yes, Yes	Pb: 0.06 – 0.6 µM Cd: 0.08 – 0.8 µM	[172]
Pb(II), Cd(II), Zn(II)	Bi/MXene	SWASV	Pb: 0.2 µg/L Cd: 0.4 µg/L Zn: 0.5 µg/L	14 days, Yes, Yes	1 – 20 µg/L	[173]
Cd(II), Pb(II)	Ti ₃ C ₂ MXene/ Carbon heterostructure	SWASV	Cd: 2.55 nM, Pb: 1.10 nM	7 days, Yes, Yes	Cd: 0.1– 8 µM, Pb: 0.25 – 2 µM	[177]
Zn(II), Cd(II), Pb(II)	Melamine/rGO/M Xene aerogel	DPASV	Zn: 0.48 µg/L Cd: 0.45 µg/L Pb: 0.29 µg/L	No, Yes, Yes	3–900 µg/L	[178]
Cd(II), Pb(II), Cu(II),Hg(II))	Alk- Ti ₃ C ₂	SWASV	Cd: 0.098 µM Pb: 0.041 µM Cu: 0.032 µM Hg: 0.130 µM	21 Days, No, Yes	Cd: 0.1 – 1 µM, Pb: 0.1 – 0.55 µM Cu: 0.1 – 1.4 µM Hg: 0 – 1.9 µM	[180]

Cd(II), Pb(II), Cu(II), Hg(II)	AgNs/SPCE	DPSV	Cd: 0.4 ppb Pb: 2.5 ppb Cu: 7.3 ppb Hg: 0.7 ppb	–, No, Yes	Cd: 5 – 300 ppb Pb: 5 – 300 ppb Cu: 50 – 500 ppb Hg: 5 –100 ppb	[184]
Cd(II), Pb(II)	FeNi ₃ / CuS/ BiOC	SWASV	Cd: 0.4 µg/L Pb: 0.1 µg/L	30 days, Yes, Yes	Cd: 1 – 150.0 µg/L Pb: 0.5 – 120.0 µg/L	[186]
Pb(II)	Cu-chitosan nanocomposite	SWSAV	0.72 ppb	–	0 – 60 ppb	[187]
Pb(II), Cd(II)	BiNPs/CoFe ₂ O ₄	SWASV	Pb: 7.3 nM Cd: 8.2 nM	42 days, No, Yes	Pb: 0.06 – 0.6 µM Cd: 0.08 – 0.8 µM	[188]
Pb(II), Hg(II)	Ni NMO - GR	SWASV	Pb: 0.050 µM Hg: 0.027 µM	–	Pb: 1.4 – 7.7 µM Hg: 0.7 – 607 µM	[189]
Pb(II)	Ternary nanocomposites CNW,CNW:Ag, AgNPs	EIS	10 nM	–	10 nM – 1 mM	[191]
Cd(II), Cu(II), Hg(II), Pb(II)	Mg(II)/Al(II)	SWASV	Cd: 250 ng/L Cu: 25 ng/L Hg: 250 ng/L Pb: 16 ng/L	–, Yes, Yes	Cd: 0.5 – 0.20 µg/L Cu: 0.05 – 0.20 µg/L Hg: 0.5 – 20 µg/L Pb: 0.05 – 0.20 µg/L	[192]
Cd(II)	CA functionalized ZnO	CV, SWV	0.41 µM	30 days, No, No	0.1 – 0.50 µM	[193]
Pb(II), Cu(II)	BFS	DPV	Pb: 0.084 µM Cu: 0.44 µM	–	0–80 µM	[194]
Cu(II)	Ni/NiO/MoO ₃ /Ch itosan	DPV	5.69 nM	–	0 – 25 µM	[195]
Pb(II)	Aptazyme driven DNA	DPV	0.034 nM	28 days	0 – 0.5 µM	[196]
Cr(VI)	polyoxometalates	DPV	0.174 µM	–	2 – 2.61 mM	[197]
Cu(II)	Eggshell membrane	DPV	0.63 µM	–	1 – 300 µM	[198]
Cu(II)	PIE/BP	SWASV	0.02 µM	–	0.25 – 177 µM	[199]
Cu(II), Hg(II)	CSs	DPASV	405 nM	–	12.5 nM	[200]

As(III)	Ag, Au alloy NPs	DPV	0.003 µg/L	–, Yes, Yes	0.01 – 10 µg/L	[201]
Pb(II)	Ag, Au alloy NPs	CV, DPV	0.3 ng/L	20 days, No, Yes	0.01 – 10 µg/L	[202]
Hg(II)	DETTDC2	Amperometric	12.80 ± 0.64 pM	Yes	0.1 nM – 0.01 M	[106]
As(III)	Ag@SiO ₂ /PANI NFs	SWASV	0.013 µg/L	Yes	0.1 – 100 µg/L	[107]
Pb(II)	rGO@CNT@Fe ₂ O ₃ /GCE	SWASV	0.1 nM	Yes	0.02 – 0.26 µM	[108]
Pb(II)	PPy/CNFs/CPE	SWASV	0.05 µg/L	Yes	0.2 – 130 µg/L	[109]
Pb(II)	sGO/PPy-SPE	DPASV	0.07 ppb	Yes	1.4–28 ppb	[110]
Pb(II)	PPy/CNT/NH ₂ -ITO	DPV	2.9 nM	No	10 nM – 0.1 µM	[111]
Cd(II), Pb(II)	GO@Fe ₃ O ₄ @2-CBT	SWASV	Cd: 0.03 µg/L Pb: 0.02 µg/L	Yes	0.08 – 90 µg/L	[112]
Pb(II), Cu(II), Cd(II)	ITO-AP-PPy-ABS	DPV	PB: 11.1 nM Cu: 8.95 nM Cd: 0.99 nM	Yes	–	[114]
Pb(II)	DTA-Ppy/SWNTs	DPV	0.07 µM	Yes	0.15 – 800 µM	[115]
Cd(II), Pb(II), Cu(II), Hg(II)	Fe ₃ O ₄ /F-MWCNTs	SWASV	Cd: 0.05 nM Pb: 0.08 nM Cu: 0.02 nM Hg: 0.05 nM	Yes	Cd: 0.5–30.0 µM Pb: 0.5–30.0 µM Cu: 0.5–30.0 µM Hg: 0.5–20.0 µM	[116]
Cd(II), Pb(II)	Fe ₃ O ₄ /MWCNTs/LSG/CS/GCE	SWASV	Cd: 0.1 µg/L Pb: 0.07 µg/L	No	1 –200 µg/L	[117]
Cd(II), Pb(II)	Sb ₂ O ₃ /MWCNTs	LSASV	Cd: 11.23 ppb Pb: 2.68 ppB	–	Cd: 80–150 ppb Pb: 5–35 ppb	[118]
Hg(II)	Sr@FeNi-S/SWCNTs	DPV	0.52 nM	Yes	0.05–279 µM	[119]

Fe ³⁺	PPCOT/NF/C-SWCNT	Amperometric	97.08 ± 4.85 μM	Yes	0.1 nM – 0.01 mM.	[120]
Zn(II), Cd(II), Pb(II), Cu(II),	BiNP/MWCNT-NNaM/PGE	SWASV	Zn: 0.707 μM Cd: 0.097 μM Pb: 0.008 μM Cu: 0.157 μM	–	Zn: 2.36–40; 40–180 μM Cd: 0.32–2; 2–240 μM, Pb: 0.03–5; 5–80 μM Cu: 0.52–10; 10–40 μM	[121]
Cd(II)	CNTs–UiO-66-NH ₂ /GCE	DPV	0.2 μM	Yes	0.3 – 150 μM	[122]
Cd(II), Pb(II)	MOF-derived BCN material.	SWASV	Cd: 0.41 μg/L Pb: 0.93 μg/L	good repeatability, stability, and specificity	Cd: 1–150 μg/L Pb: 2–150 μg/L	[46]
Pb(II)	transition metal ion assisted PVG	PVG	0.005 ng/g	–	0.005 – 100 ng/g	[47]
Pb(II)	Polytetrafluoroethylene (PTFE)	AAS	0.2 μg/L	–	0.0–8.0 μg/L	[48]
As(III))	5,10,15,20-tetrakis (4-methoxyphenyl) porphyrinatocobalt(II) (TMOPP-Co)	FET	>10 ⁻¹⁰ M	–	0.1 nM – 0.1 mM	[61]

It can be concluded from the Table 3 that the most advantageous approaches for sensor preparation for detection of various HMIs involve the utilization of composite of various nanostructured materials. These approaches employ composite of various nanomaterials, which offer high surface area-to-volume ratios and enhanced sensitivity. Functionalization of these nanomaterials with selective ligands or receptors allows for specific binding and detection of HMIs. Additionally, the integration of nanomaterials with microfluidic systems enables rapid and efficient sample handling, enhancing the sensor's performance. Another promising approach is the development of electrochemical sensors that utilize modified electrodes. By functionalizing the electrode surfaces with selective materials, such as polymers or MOFs, HMIs can be selectively captured and quantified. These approaches provide a powerful platform for the preparation of sensors that offer high sensitivity, selectivity, and rapid response, making them valuable tools for HMIs detection in various environmental and analytical applications.

5. Summary and Future Prospects

5.1. Summary

This review article explored the application of various nanocomposite materials in the electrochemical detection of heavy metal ions (HMIs). The nanocomposite materials discussed in this review include metal-organic framework (MOF), organic conducting polymers (OCP), carbon nanotubes, graphene / reduced graphene oxide, graphitic carbon nitride, metal oxide, chitosan, mxenes and metal nanoparticles-based nanocomposites.

The advantages and limitations of each material and its nanocomposites for the detection of HMIs, highlighting their sensitivity, selectivity, and stability, have been comprehensively discussed.

For example, MOFs have a high surface area, increasing the electrochemical sensor's sensitivity. The highly porous structure of the MOF provides many binding sites for HMIs. Moreover, MOFs can be designed with specific functional groups to selectively bind to certain HMIs, allowing their selective detection complex samples. However, MOFs can be unstable in aqueous solutions, affecting the electrochemical sensor's reliability and reproducibility. The synthesis of MOFs can be challenging, and their electrochemical properties can depend highly on the synthesis conditions. Despite their high surface area and porosity, MOFs may not always provide the required sensitivity for trace-level detection of HMIs.

OCPs have high sensitivity towards HMIs, making them suitable for trace-level detection. OCPs can be designed with specific functional groups to selectively bind to certain HMIs, allowing their selective detection in complex samples. OCPs are flexible and easily fabricated into different shapes and sizes, making them suitable for various applications. However, OCPs can be unstable in aqueous solutions, affecting the electrochemical sensor's reliability and reproducibility. Other compounds in the sample matrix may interfere with the electrochemical detection of HMIs, affecting the accuracy of the results. Stability can be one of the significant challenges while using OCP for the detection of HMIs.

Similarly, carbon nanotubes (CNTs) have a high surface area-to-volume ratio, which results in a high sensitivity for detecting HMIs. CNT-based electrodes can be modified with specific chemical groups to selectively detect HMIs in the presence of other ions. Electrochemical detection using CNT-based electrodes can provide real-time analysis and can be conducted rapidly, making it an attractive option for environmental monitoring and industrial applications. The electrochemical detection of HMIs using CNT-based electrodes can achieve a low detection limit due to the high sensitivity and selectivity of the method. CNT-based electrodes are highly stable and can be reused for multiple detections, making them cost-effective. However, preparing CNT-based electrodes is time-consuming and requires expertise in synthesizing and functionalizing of CNTs. The presence of other ions can interfere with the detection of HMIs, reducing the accuracy and specificity of the method. The reproducibility of CNT-based electrodes can be affected by variations in the synthesis and functionalization of CNTs, leading to inconsistencies in the results. The disposal of CNTs can pose environmental risks, as they are not readily biodegradable.

This review comprehensively covers the different methods used for synthesizing and functionalizing these nanocomposite materials to address the abovementioned challenges and improve their electrochemical properties for HMIs detection. Several options have been explored to form nanocomposites to address these challenges so that highly sensitive and selective, stable, repeatable, and reproducible sensors can be developed for the detection of HMIs.

5.2. Future Prospects

The electrochemical detection of HMIs based on nanocomposite materials is an emerging field with great potential for future applications.

The challenging issues of the materials can be intelligently tackled. The properties of the nanocomposites can be further fine-tuned, and sensors with enhanced stability, sensitivity, and selectivity can be developed for HMIs detection. Moreover, the following technological aspects can also be achieved. Further directions can be focused also on application of nucleic acid aptamers as receptors immobilized at nanocomposite materials for selective detection of HMIs [202,203].

Miniaturization: Nanocomposite-based sensors can be miniaturized, making them suitable for point-of-care testing and on-site monitoring and allowing for portable and on-site monitoring of HMIs. The development of nanocomposite-based sensors with small form factors and low power consumption can lead to widespread use in various fields.

Multi-metal Detection: Nanocomposite materials can be engineered to simultaneously detect multiple HMIs. The development of nanocomposite-based sensors with multi-metal detection capabilities can lead to more efficient and cost-effective monitoring of heavy metal contamination.

Industrial Applications: The electrochemical detection of HMIs based on nanocomposite materials can be used in various industrial applications, such as quality control and process monitoring. The development of nanocomposite-based sensors for industrial applications can lead to improved product quality and increased efficiency.

Overall, the future of electrochemical detection of HMIs based on nanocomposite materials looks promising, and further research and development in this field can lead to innovative and practical applications.

Author Contributions: Conceptualization, M.D.S. and T.H.; writing—original draft, M.D.S.; writing—review & editing, M.D.S. All authors have read and agreed to the published version of the manuscript.

Institutional Review Board Statement: Not applicable.

Informed Consent Statement: Not applicable.

Data Availability Statement: Not applicable.

Acknowledgement: Mahendra D, Shirsat gratefully acknowledges the Slovak Academic Information Agency (SAIA) and Department of Nuclear Physics and Biophysics, Faculty of Mathematics, Physics and Informatics, Comenius University, Bratislava, Slovak Republic, for the sanction of scholarship under the framework of National Scholarship Program (NSP) of Slovak republic. Moreover, Mahendra D. Shirsat also gratefully acknowledges Dr Babasaheb Ambedkar Marathwada University, Aurangabad, MS, India, for the sanctioned study, leave to visit Comenius University, Bratislava, Slovak Republic.

Conflicts of Interest: The authors declare no conflict of interest.

References

1. Sharma, S.K. *Heavy Metals in Water: Presence, Removal and Safety*; Royal Society of Chemistry, London, UK, 2014. <https://doi.org/10.1039/9781782620174>.
2. Shadman, S.M.; Daneshi, M.; Shafiei, F.; Azimimehr, M.; Khorasgani, M.R.; Sadeghian, M.; Motaghi, H.; Mehrgardi, M.A. Aptamer-based electrochemical biosensors. In *Electrochemical Biosensors*; Ensafi, A.A. Ed.; Elsevier: Amsterdam, The Netherlands, 2019; pp. 213-251. <https://doi.org/10.1016/B978-0-12-816491-4.01001-9>.
3. Valko, M.; Morris, H.; Cronin, M. Metals, toxicity and oxidative stress. *Current Medic. Chem.* **2005**, *12*, 1161-1208. <https://doi.org/10.2174/0929867053764635>.
4. Bagal-Kestwal, D.; Karve, M.S.; Kakade, B.; Pillai, V.K. Invertase inhibition based electrochemical sensor for the detection of heavy metal ions in aqueous system: Application of ultra-microelectrode to enhance sucrose biosensor's sensitivity. *Biosens. Bioelectron.* **2008**, *24*, 657-664. <https://doi.org/10.1016/j.bios.2008.06.027>.
5. Zularisam, A.; Ismail, A.; Salim, R. Behaviours of natural organic matter in membrane filtration for surface water treatment—a review. *Desalination* **2006**, *194*, 211-231. <https://doi.org/10.1016/j.desal.2005.10.030>.
6. Vetrimurugan, E.; Brindha, K.; Elango, L.; Ndwandwe, O.M. Human exposure risk to heavy metals through groundwater used for drinking in an intensively irrigated river delta. *Appl. Water Sci.* **2017**, *7*, 3267-3280. <https://doi.org/10.1007/s13201-016-0472-6>.
7. National Primary Drinking Water Regulations, USEPA. **2015**.
8. Ferrari, A.G.-M.; Carrington, P.; Rowley-Neale, S.J.; Banks, C.E. Recent advances in portable heavy metal electrochemical sensing platforms. *Environmental Sci.: Water Research & Technology* **2020**, *6*, 2676-2690. <https://doi.org/10.1039/D0EW00407C>.
9. Srivastav, A.L. Chemical fertilizers and pesticides: role in groundwater contamination. In *Agrochemicals Detection, Treatment and Remediation*; Elsevier: 2020; pp. 143-159. <https://doi.org/10.1016/B978-0-08-103017-2.00006-4>.
10. Liu, Y.; Deng, Y.; Dong, H.; Liu, K.; He, N. Progress on sensors based on nanomaterials for rapid detection of heavy metal ions. *Sci. China Chem.* **2017**, *60*, 329-337. <https://doi.org/10.1007/s11426-016-0253-2>.

11. Joshi, N.C.; Gururani, P. Advances of graphene oxide based nanocomposite materials in the treatment of wastewater containing heavy metal ions and dyes. *Current Res. in Green and Sust. Chem.* **2022**, 100306. <https://doi.org/10.1016/j.crgsc.2022.100306>.
12. Huang, H.; Chen, T.; Liu, X.; Ma, H. Ultrasensitive and simultaneous detection of heavy metal ions based on three-dimensional graphene-carbon nanotubes hybrid electrode materials. *Anal. Chim. Acta* **2014**, 852, 45-54. <https://doi.org/10.1016/j.aca.2014.09.010>.
13. Pan, F.; Tong, C.; Wang, Z.; Han, H.; Liu, P.; Pan, D.; Zhu, R. Nanocomposite based on graphene and intercalated covalent organic frameworks with hydrosulphonyl groups for electrochemical determination of heavy metal ions. *Microchim. Acta* **2021**, 188, 295. <https://doi.org/10.1007/s00604-021-04956-1>.
14. Devaraj, M.; Sasikumar, Y.; Rajendran, S.; Ponce, L.C. Metal organic framework based nanomaterials for electrochemical sensing of toxic heavy metal ions: progress and their prospects. *J. Electrochem. Soc.* **2021**, 168, 037513. <https://doi.org/10.1149/1945-7111/abec97>.
15. Nguyen, M.B.; Nga, D.T.N.; Thu, V.T.; Piro, B.; Truong, T.N.P.; Yen, P.T.H.; Le, G.H.; Hung, L.Q.; Vu, T.A.; Ha, V.T.T. Novel nanoscale Yb-MOF used as highly efficient electrode for simultaneous detection of heavy metal ions. *J. Mat. Sci.* **2021**, 56, 8172-8185. <https://doi.org/10.1007/s10853-021-05815-3>.
16. Wang, X.; Qi, Y.; Shen, Y.; Yuan, Y.; Zhang, L.; Zhang, C.; Sun, Y. A ratiometric electrochemical sensor for simultaneous detection of multiple heavy metal ions based on ferrocene-functionalized metal-organic framework. *Sens. Actuat. B: Chemical* **2020**, 310, 127756. <https://doi.org/10.1016/j.snb.2020.127756>.
17. Lee, S.; Oh, J.; Kim, D.; Piao, Y. A sensitive electrochemical sensor using an iron oxide/graphene composite for the simultaneous detection of heavy metal ions. *Talanta* **2016**, 160, 528-536. <https://doi.org/10.1016/j.talanta.2016.07.034>.
18. Akanji, S.P.; Ama, O.M.; Ray, S.S.; Osifo, P.O. Metal oxide nanomaterials for electrochemical detection of heavy metals in water. In *Nanostructured Metal-Oxide Electrode Materials for Water Purification: Fabrication, Electrochemistry and Applications*; Ama, O., Ray, S. Eds.; Springer: Cham, Germany **2020**; pp. 113-126. https://doi.org/10.1007/978-3-030-43346-8_7.
19. Bodkhe, G.A.; Hedau, B.S.; Deshmukh, M.A.; Patil, H.K.; Shirsat, S.M.; Phase, D.M.; Pandey, K.K.; Shirsat, M.D. Selective and sensitive detection of lead Pb (II) ions: Au/SWNT nanocomposite-embedded MOF-199. *J. Mat. Sci.* **2021**, 56, 474-487. <https://doi.org/10.1007/s10853-020-05285-z>.
20. Sayyad, P.W.; Ingle, N.N.; Al-Gahouari, T.; Mahadik, M.M.; Bodkhe, G.A.; Shirsat, S.M.; Shirsat, M.D. Sensitive and selective detection of Cu²⁺ and Pb²⁺ ions using field effect transistor (FET) based on L-Cysteine anchored PEDOT: PSS/rGO composite. *Chem. Phys. Lett.* **2020**, 761, 138056. <https://doi.org/10.1016/j.cplett.2020.138056>.
21. Sayyad, P.W.; Ingle, N.N.; Al-Gahouari, T.; Mahadik, M.M.; Bodkhe, G.A.; Shirsat, S.M.; Shirsat, M.D. Selective Hg²⁺ sensor: rGO-blended PEDOT: PSS conducting polymer OFET. *Appl. Physics A* **2021**, 127, 1-10. <https://doi.org/10.1007/s00339-021-04314-1>.
22. Bodkhe, G.A.; Hedau, B.S.; Deshmukh, M.A.; Patil, H.K.; Shirsat, S.M.; Phase, D.M.; Pandey, K.K.; Shirsat, M.D. Detection of Pb (II): Au nanoparticle incorporated CuBTC MOFs. *Frontiers in Chem.* **2020**, 8, 803. <https://doi.org/10.3389/fchem.2020.00803>.
23. Sayyad, P.W.; Shaikh, Z.A.; Ingle, N.N.; Al-Gahouari, T.; Mahadik, M.M.; Bodkhe, G.A.; Shirsat, S.M.; Shirsat, M.D. Simultaneous reduction of graphene oxide (GO) and formation of rGO/Gly-Gly composite for sensitive detection of Cu²⁺ ions. *J. Phys.: Conf. Ser.* **2020**, 1644, 012001. <https://doi.org/10.1088/1742-6596/1644/1/012001>.
24. Mahadik, M.; Patil, H.; Bodkhe, G.; Ingle, N.; Sayyad, P.; Al-Gahouari, T.; Shirsat, S.M.; Shirsat, M. EDTA modified PANI/GO composite based detection of Hg (II) ions. *Frontiers in Materials* **2020**, 7, 81. <https://doi.org/10.1088/1742-6596/1644/1/012001>.
25. Al-Gahouari, T.; Bodkhe, G.; Sayyad, P.; Ingle, N.; Mahadik, M.; Shirsat, S.M.; Deshmukh, M.; Musahwar, N.; Shirsat, M. Electrochemical sensor: L-cysteine induced selectivity enhancement of electrochemically reduced graphene oxide-multiwalled carbon nanotubes hybrid for detection of lead (Pb²⁺) ions. *Frontiers in Materials* **2020**, 7, 68. <https://doi.org/10.3389/fmats.2020.00068>.
26. Patil, H.K.; Deshmukh, M.A.; Bodkhe, G.A.; Shirsat, S.M.; Asokan, K.; Shirsat, M.D. Dimethylglyoxime modified swift heavy oxygen ions irradiated polyaniline/single walled carbon nanotubes composite electrode for detection of cobalt ions. *Materials Research Express* **2018**, 5, 065048. <https://doi.org/10.1088/2053-1591/aacbb3>.
27. Deshmukh, M.A.; Celiesiute, R.; Ramanaviciene, A.; Shirsat, M.D.; Ramanavicius, A. EDTA_PANI/SWCNTs nanocomposite modified electrode for electrochemical determination of copper (II), lead (II) and mercury (II) ions. *Electrochim. Acta* **2018**, 259, 930-938. <https://doi.org/10.1016/j.electacta.2017.10.131>.
28. Deshmukh, M.A.; Patil, H.K.; Bodkhe, G.A.; Yasuzawa, M.; Koinkar, P.; Ramanavicius, A.; Pandey, S.; Shirsat, M.D. EDA modified PANI/SWNTs nanocomposite for determination of Ni (II) metal ions. *Coll. Surf. A: Physicochemical and Engineering Aspects* **2018**, 537, 303-309. <https://doi.org/10.1016/j.colsurfa.2017.10.026>.

29. Deore, K.B.; Patil, S.S.; Narwade, V.N.; Takte, M.A.; Khune, A.S.; Mohammed, H.Y.; Farea, M.; Sayyad, P.W.; Tsai, M.-L.; Shirsat, M.D. Chromium-benzenedicarboxylates metal organic framework for supersensitive and selective electrochemical sensor of Toxic Cd²⁺, Pb²⁺, and Hg²⁺ metal ions: Study of their interactive mechanism. *J. Electrochem. Soc.* **2023**, *170*, 046505. <https://doi.org/10.1149/1945-7111/acc9df>.
30. Malik, L.A.; Bashir, A.; Qureashi, A.; Pandith, A.H. Detection and removal of heavy metal ions: a review. *Environmen. Chem. Lett.* **2019**, *17*, 1495-1521. <https://doi.org/10.1007/s10311-019-00891-z>.
31. Rubino, A.; Queirós, R. Electrochemical determination of heavy metal ions applying screen-printed electrodes based sensors. A review on water and environmental samples analysis. *Talanta* **2023**, *7*, 100203. <https://doi.org/10.1016/j.talo.2023.100203>.
32. Kajal, N.; Singh, V.; Gupta, R.; Gautam, S. Metal organic frameworks for electrochemical sensor applications: A review. *Environmen. Res.* **2022**, *204*, 112320. <https://doi.org/10.1016/j.envres.2021.112320>.
33. Nemiwal, M.; Kumar, D. Recent progress on electrochemical sensing strategies as comprehensive point-care method. *Chemical Monthly* **2021**, *152*, 1-18. <https://doi.org/10.1007/s00706-020-02732-0>.
34. Munonde, T.S.; Nomngongo, P.N. Nanocomposites for electrochemical sensors and their applications on the detection of trace metals in environmental water samples. *Sensors* **2020**, *21*, 131. <https://doi.org/10.3390/s21010131>.
35. Buledi, J.A.; Amin, S.; Haider, S.I.; Bhangar, M.I.; Solangi, A.R. A review on detection of heavy metals from aqueous media using nanomaterial-based sensors. *Environment. Sci. Pollut. Res.* **2021**, *28*, 58994-59002. <https://doi.org/10.1007/s11356-020-07865-7>.
36. Sinha, A.; Kalambate, P.K.; Mugo, S.M.; Kamau, P.; Chen, J.; Jain, R. Polymer hydrogel interfaces in electrochemical sensing strategies: A review. *TrAC Trends Anal. Chem.* **2019**, *118*, 488-501. <https://doi.org/10.1016/j.trac.2019.06.014>.
37. Wang, H.; Xu, C.; Yuan, B. Polymer-based electrochemical sensing platform for heavy metal ions detection—A critical review. *Int. J. Electrochem. Sci* **2019**, *14*, 8760-8771. <https://doi.org/10.20964/2019.09.22>.
38. Shoaie, N.; Daneshpour, M.; Azimzadeh, M.; Mahshid, S.; Khoshfetrat, S.M.; Jahanpeyma, F.; Gholaminejad, A.; Omidfar, K.; Foruzandeh, M. Electrochemical sensors and biosensors based on the use of polyaniline and its nanocomposites: A review on recent advances. *Microchim. Acta* **2019**, *186*, 1-29. <https://doi.org/10.1007/s00604-019-3588-1>.
39. Ahmad, R.; Tripathy, N.; Khosla, A.; Khan, M.; Mishra, P.; Ansari, W.A.; Syed, M.A.; Hahn, Y.-B. Recent advances in nanostructured graphitic carbon nitride as a sensing material for heavy metal ions. *J. Electrochem. Soc.* **2019**, *167*, 037519. <https://doi.org/10.1149/2.0192003JES>.
40. Sawan, S.; Maalouf, R.; Errachid, A.; Jaffrezic-Renault, N. Metal and metal oxide nanoparticles in the voltammetric detection of heavy metals: A review. *TrAC Trends Anal. Chem.* **2020**, *131*, 116014. <https://doi.org/10.1016/j.trac.2020.116014>.
41. Kumunda, C.; Adekunle, A.S.; Mamba, B.B.; Hlongwa, N.W.; Nkambule, T.T. Electrochemical detection of environmental pollutants based on graphene derivatives: A review. *Frontiers in Materials* **2021**, *7*, 616787. <https://doi.org/10.3389/fmats.2020.616787>.
42. Tajik, S.; Beitollahi, H.; Nejad, F.G.; Dourandish, Z.; Khalilzadeh, M.A.; Jang, H.W.; Venditti, R.A.; Varma, R.S.; Shokouhimehr, M. Recent developments in polymer nanocomposite-based electrochemical sensors for detecting environmental pollutants. *Industrial Eng. Chem. Res.* **2021**, *60*, 1112-1136. <https://doi.org/10.1021/acs.iecr.0c04952>.
43. Langari, M.M.; Antxustegi, M.M.; Labidi, J. Nanocellulose-based sensing platforms for heavy metal ions detection: A comprehensive review. *Chemosphere* **2022**, *134823*. <https://doi.org/10.1016/j.chemosphere.2022.134823>.
44. Raju, C.V.; Cho, C.H.; Rani, G.M.; Manju, V.; Umapathi, R.; Huh, Y.S.; Park, J.P. Emerging insights into the use of carbon-based nanomaterials for the electrochemical detection of heavy metal ions. *Coordinat. Chem. Rev.* **2023**, *476*, 214920. <https://doi.org/10.1016/j.ccr.2022.214920>.
45. Meng, R.; Zhu, Q.; Long, T.; He, X.; Luo, Z.; Gu, R.; Wang, W.; Xiang, P. The innovative and accurate detection of heavy metals in foods: A critical review on electrochemical sensors. *Food Control* **2023**, 109743. <https://doi.org/10.1016/j.foodcont.2023.109743>.
46. Huang, R.; Lv, J.; Chen, J.; Zhu, Y.; Zhu, J.; Wågberg, T.; Hu, G. Three-dimensional porous high boron-nitrogen-doped carbon for the ultrasensitive electrochemical detection of trace heavy metals in food samples. *J. Hazard. Mat.* **2023**, *442*, 130020. <https://doi.org/10.1016/j.jhazmat.2022.130020>.
47. Gao, Y.; Xu, M.; Sturgeon, R.E.; Mester, Z.; Shi, Z.; Galea, R.; Saull, P.; Yang, L. Metal ion-assisted photochemical vapor generation for the determination of lead in environmental samples by multicollector-ICPMS. *Anal. Chem.* **2015**, *87*, 4495-4502. <https://doi.org/10.1021/acs.analchem.5b00533>.
48. Barbosa Jr, F.; Krug, F.J.; Lima, É.C. On-line coupling of electrochemical preconcentration in tungsten coil electrothermal atomic absorption spectrometry for determination of lead in natural waters. *Spectrochim. Acta Part B: Atomic Spectroscopy* **1999**, *54*, 1155-1166. [https://doi.org/10.1016/S0584-8547\(99\)00055-5](https://doi.org/10.1016/S0584-8547(99)00055-5).

49. Rahmalan, A.; Abdullah, M.Z.; Sanagi, M.M.; Rashid, M. Determination of heavy metals in air particulate matter by ion chromatography. *J. Chromatography A* **1996**, *739*, 233-239. [https://doi.org/10.1016/0021-9673\(96\)00025-8](https://doi.org/10.1016/0021-9673(96)00025-8).
50. Nyholm, L. Electrochemical techniques for lab-on-a-chip applications. *Analyst* **2005**, *130*, 599-605. <https://doi.org/10.1039/B415004J>.
51. Piliarik, M.; Párová, L.; Homola, J. High-throughput SPR sensor for food safety. *Biosens. Bioelectron.* **2009**, *24*, 1399-1404. <https://doi.org/10.1016/j.bios.2008.08.012>.
52. Li, Y.; Chen, M.; Han, Y.; Feng, Y.; Zhang, Z.; Zhang, B. Fabrication of a new corrole-based covalent organic framework as a highly efficient and selective chemosensor for heavy metal ions. *Chem. Materials* **2020**, *32*, 2532-2540. <https://doi.org/10.1021/acs.chemmater.9b05234>.
53. Lv, M.; Zhou, W.; Tavakoli, H.; Bautista, C.; Xia, J.; Wang, Z.; Li, X. Aptamer-functionalized metal-organic frameworks (MOFs) for biosensing. *Biosens. Bioelectron.* **2021**, *176*, 112947. <https://doi.org/10.1016/j.bios.2020.112947>.
54. Vlasov, Y.; Legin, A.; Rudnitskaya, A. Cross-sensitivity evaluation of chemical sensors for electronic tongue: determination of heavy metal ions. *Sens. Actuat. B: Chemical* **1997**, *44*, 532-537. [https://doi.org/10.1016/S0925-4005\(97\)00241-4](https://doi.org/10.1016/S0925-4005(97)00241-4).
55. Falina, S.; Syamsul, M.; Rhaffor, N.A.; Sal Hamid, S.; Mohamed Zain, K.A.; Abd Manaf, A.; Kwarada, H. Ten years progress of electrical detection of heavy metal ions (hmis) using various field-effect transistor (fet) nanosensors: A review. *Biosensors* **2021**, *11*, 478. <https://doi.org/10.3390/bios11120478>.
56. Mohamad Nor, N.; Ramli, N.H.; Poobalan, H.; Qi Tan, K.; Abdul Razak, K. Recent advancement in disposable electrode modified with nanomaterials for electrochemical heavy metal sensors. *Critical Rev. Anal. Chem.* **2023**, *53*, 253-288. <https://doi.org/10.1080/10408347.2021.1950521>.
57. Bansod, B.; Kumar, T.; Thakur, R.; Rana, S.; Singh, I. A review on various electrochemical techniques for heavy metal ions detection with different sensing platforms. *Biosens. Bioelectron.* **2017**, *94*, 443-455. <https://doi.org/10.1016/j.bios.2017.03.031>.
58. Heidari, G.; Fallah, Z.; Zare, E.N. One-Dimensional Polymeric nanocomposites for heavy metal detection. In *One-Dimensional Polymeric Nanocomposites: Synthesis to Emerging Applications*, 1st ed.; Gupta, R.K., Nguyen, T.A. Eds.; CRC Press: London, UK, **2023**, pp. 1-20. <https://doi.org/10.1201/9781003223764>.
59. Jose, J.; Prakash, P.; Jeyaprabha, B.; Abraham, R.; Mathew, R.M.; Zacharia, E.S.; Thomas, V.; Thomas, J. Principle, design, strategies, and future perspectives of heavy metal ion detection using carbon nanomaterial-based electrochemical sensors: a review. *J. Iranian Chem. Soc.* **2023**, *20*, 775-791. <https://doi.org/10.1007/s13738-022-02730-5>.
60. Shen, Y.; Gao, X.; Lu, H.-J.; Nie, C.; Wang, J. Electrochemiluminescence-based innovative sensors for monitoring the residual levels of heavy metal ions in environment-related matrices. *Coordinat. Chem. Rev.* **2023**, *476*, 214927. <https://doi.org/10.1016/j.ccr.2022.214927>.
61. Tatavarthi, S.S.; Wang, S.-L.; Wang, Y.-L.; Chen, J.-C. Rapid and highly sensitive extended gate FET-based sensors for Arsenite detection using a handheld device. *ECS J. Solid State Sci. Technol.* **2020**, *9*, 115014. <https://doi.org/10.1149/2162-8777/abab18>.
62. Krishnan, S.K.; Nataraj, N.; Meyyappan, M.; Pal, U. Graphene-based field-effect transistors in biosensing and neural interfacing applications: Recent advances and prospects. *Anal. Chem.* **2023**, *95*, 2590-2622. <https://doi.org/10.1021/acs.analchem.2c03399>.
63. Farahmandpour, M.; Kordrostami, Z.; Rajabzadeh, M.; Khalifeh, R. Flexible bio-electronic hybrid metal-oxide channel FET as a glucose sensor. *IEEE Transactions on NanoBioscience* **2023**. <https://doi.org/10.1109/TNB.2023.3236460>.
64. Zhang, X.; Pu, Z.; Su, X.; Li, C.; Zheng, H.; Li, D. Flexible organic field-effect transistors-based biosensors: progress and perspectives. *Anal. Bioanal. Chem.* **2023**, *415*, 1607-1625. <https://doi.org/10.1007/s00216-023-04553-6>.
65. Jiang, D.; Sheng, K.; Gui, G.; Jiang, H.; Liu, X.; Wang, L. A novel smartphone-based electrochemical cell sensor for evaluating the toxicity of heavy metal ions Cd²⁺, Hg²⁺, and Pb²⁺ in rice. *Anal. Bioanal. Chem.* **2021**, *413*, 4277-4287. <https://doi.org/10.1007/s00216-021-03379-4>.
66. Sivakumar, R.; Lee, N.Y. Recent progress in smartphone-based techniques for food safety and the detection of heavy metal ions in environmental water. *Chemosphere* **2021**, *275*, 130096. <https://doi.org/10.1016/j.chemosphere.2021.130096>.
67. Xu, Z.; Liu, Z.; Xiao, M.; Jiang, L.; Yi, C. A smartphone-based quantitative point-of-care testing (POCT) system for simultaneous detection of multiple heavy metal ions. *Chem. Eng. J.* **2020**, *394*, 124966. <https://doi.org/10.1016/j.cej.2020.124966>.
68. Zhang, W.; Liu, C.; Liu, F.; Zou, X.; Xu, Y.; Xu, X. A smart-phone-based electrochemical platform with programmable solid-state-microwave flow digestion for determination of heavy metals in liquid food. *Food Chem.* **2020**, *303*, 125378. <https://doi.org/10.1016/j.foodchem.2019.125378>.

69. Liao, J.; Chang, F.; Han, X.; Ge, C.; Lin, S. Wireless water quality monitoring and spatial mapping with disposable whole-copper electrochemical sensors and a smartphone. *Sens. Actuat. B: Chemical* **2020**, *306*, 127557. <https://doi.org/10.1016/j.snb.2019.127557>.
70. Nemiroski, A.; Christodouleas, D.C.; Hennek, J.W.; Kumar, A.A.; Maxwell, E.J.; Fernández-Abedul, M.T.; Whitesides, G.M. Universal mobile electrochemical detector designed for use in resource-limited applications. *Proc. Nat. Acad. Sci.* **2014**, *111*, 11984-11989. <https://doi.org/10.1073/pnas.1405679111>.
71. Li, Y.; Chen, Y.; Yu, H.; Tian, L.; Wang, Z. Portable and smart devices for monitoring heavy metal ions integrated with nanomaterials. *TrAC Trends in Analytical Chemistry* **2018**, *98*, 190-200. <https://doi.org/10.1016/j.trac.2017.11.011>.
72. Li, Z.; Xu, D.; Zhang, D.; Yamaguchi, Y. A portable instrument for on-site detection of heavy metal ions in water. *Anal. Bioanal. Chem.* **2021**, *413*, 3471-3477. <https://doi.org/10.1007/s00216-021-03292-w>.
73. Xu, G.; Li, X.; Cheng, C.; Yang, J.; Liu, Z.; Shi, Z.; Zhu, L.; Lu, Y.; Low, S.S.; Liu, Q. Fully integrated battery-free and flexible electrochemical tag for on-demand wireless in situ monitoring of heavy metals. *Sens. Actuat. B: Chemical* **2020**, *310*, 127809. <https://doi.org/10.3390/mi14010142>.
74. Muhammad-Aree, S.; Teepoo, S. On-site detection of heavy metals in wastewater using a single paper strip integrated with a smartphone. *Anal. Bioanal. Chem.* **2020**, *412*, 1395-1405. <https://doi.org/10.1007/s00216-019-02369-x>.
75. Fang, X.; Chen, X.; Liu, Y.; Li, Q.; Zeng, Z.; Maiyalagan, T.; Mao, S. Nanocomposites of Zr (IV)-based metal-organic frameworks and reduced graphene oxide for electrochemically sensing ciprofloxacin in water. *ACS Appl. Nano Mat.* **2019**, *2*, 2367-2376. <https://doi.org/10.1021/acsanm.9b00243>.
76. Dehdashtian, S.; Hashemi, B.; Aeenmehr, A. The application of perlite/cobalt oxide/reduced graphene oxide (PC-rGO)/metal organic framework (MOF) composite as electrode modifier for direct sensing of anticancer drug idarubicin. *IEEE Sensors J.* **2019**, *19*, 11739-11745. <https://doi.org/10.1109/JSEN.2019.2937400>.
77. Altass, H.M.; Morad, M.; Khder, A.E.-R.S.; Mannaa, M.A.; Jassas, R.S.; Alsimaree, A.A.; Ahmed, S.A.; Salama, R.S. Enhanced catalytic activity for CO oxidation by highly active Pd nanoparticles supported on reduced graphene oxide/copper metal organic framework. *J. Taiwan Inst. Chem. Eng.* **2021**, *128*, 194-208. <https://doi.org/10.1016/j.jtice.2021.08.034>.
78. Baghayeri, M.; Ghanei-Motlagh, M.; Tayebie, R.; Fayazi, M.; Narenji, F. Application of graphene/zinc-based metal-organic framework nanocomposite for electrochemical sensing of As (III) in water resources. *Anal. Chim. Acta* **2020**, *1099*, 60-67. <https://doi.org/10.1016/j.aca.2019.11.045>.
79. Huang, Y.; Niu, Q.; Jian, L.; Zhao, W.; Li, Y.; Dong, W.; Zhang, K.; Liang, W.; Yang, C. Synthesis of porphyrinic metal-organic framework/rGO nanocomposite for electrochemical recognition of copper ions in water. *J. Organometal. Chem.* **2023**, *985*, 122597. <https://doi.org/10.1016/j.jorganchem.2022.122597>.
80. Li, D.; Yan, D.; Zhang, X.; Li, J.; Lu, T.; Pan, L. Porous CuO/reduced graphene oxide composites synthesized from metal-organic frameworks as anodes for high-performance sodium-ion batteries. *J. Coll. Interface Sci.* **2017**, *497*, 350-358. <https://doi.org/10.1016/j.jcis.2017.03.037>.
81. Cui, X.; Yang, B.; Zhao, S.; Li, X.; Qiao, M.; Mao, R.; Wang, Y.; Zhao, X. Electrochemical sensor based on ZIF-8@ dimethylglyoxime and β -cyclodextrin modified reduced graphene oxide for nickel (II) detection. *Sens. Act. B: Chemical* **2020**, *315*, 128091. <https://doi.org/10.1016/j.snb.2020.128091>.
82. Huo, D.; Zhang, Y.; Li, N.; Ma, W.; Liu, H.; Xu, G.; Li, Z.; Yang, M.; Hou, C. Three-dimensional graphene/amino-functionalized metal-organic framework for simultaneous electrochemical detection of Cd (II), Pb (II), Cu (II), and Hg (II). *Anal. Bioanal. Chem.* **2022**, *414*, 1475-1585. <https://doi.org/10.1007/s00216-021-03779-6>.
83. Guo, T.-T.; Cao, X.-Y.; An, Y.-Y.; Zhang, X.-L.; Yan, J.-Z. Sulfur-bridged Co (II)-thiacalix [4] arene metal-organic framework as an electrochemical sensor for the determination of toxic heavy metals. *Inorganic Chem.* **2023**, *438*, 135-639. <https://doi.org/10.1016/j.cej.2022.135639>.
84. Ding, Y.; Wei, F.; Dong, C.; Li, J.; Zhang, C.; Han, X. UiO-66 based electrochemical sensor for simultaneous detection of Cd (II) and Pb (II). *Inorganic Chem. Commun.* **2021**, *131*, 108785. <https://doi.org/10.1016/j.inoche.2021.108785>.
85. Yang, S.; Yang, M.; Yao, X.; Fa, H.; Wang, Y.; Hou, C. A zeolitic imidazolate framework/carbon nanofiber nanocomposite based electrochemical sensor for simultaneous detection of co-existing dihydroxybenzene isomers. *Sens. Actuat. B: Chemical* **2020**, *320*, 128294. <https://doi.org/10.1016/j.snb.2020.128294>.
86. Yang, H.; Peng, C.; Han, J.; Song, Y.; Wang, L. Three-dimensional macroporous Carbon/Zr-2, 5-dimercaptoterephthalic acid metal-organic frameworks nanocomposites for removal and detection of Hg (II). *Sens. Actuat. B: Chemical* **2020**, *320*, 128447. <https://doi.org/10.1016/j.snb.2020.128447>.
87. Singh, S.; Numan, A.; Zhan, Y.; Singh, V.; Van Hung, T.; Nam, N.D. A novel highly efficient and ultrasensitive electrochemical detection of toxic mercury (II) ions in canned tuna fish and tap water based on a copper metal-organic framework. *J. Hazardous Mat.* **2020**, *399*, 123042. <https://doi.org/10.1016/j.jhazmat.2020.123042>.

88. Ru, J.; Wang, X.; Cui, X.; Wang, F.; Ji, H.; Du, X.; Lu, X. GaOOH-modified metal-organic frameworks UiO-66-NH₂: Selective and sensitive sensing four heavy-metal ions in real wastewater by electrochemical method. *Talanta* **2021**, *234*, 122679. <https://doi.org/10.1016/j.talanta.2021.122679>.
89. Wang, N.; Zhao, W.; Shen, Z.; Sun, S.; Dai, H.; Ma, H.; Lin, M. Sensitive and selective detection of Pb (II) and Cu (II) using a metal-organic framework/polypyrrole nanocomposite functionalized electrode. *Sens. Actuat. B: Chemical* **2020**, *304*, 127286. <https://doi.org/10.1016/j.snb.2019.127286>.
90. Ru, J.; Wang, X.; Zhao, J.; Yang, J.; Zhou, Z.; Du, X.; Lu, X. Evaluation and development of GO/UiO-67@PtNPs nanohybrid-based electrochemical sensor for invisible arsenic (III) in water samples. *Microchem. J.* **2022**, *181*, 107765. <https://doi.org/10.1016/j.microc.2022.107765>.
91. Zhao, J.; Long, Y.; He, C.; Yang, H.; Zhao, S.; Luo, X.; Huo, D.; Hou, C. Simultaneous Electrochemical detection of Cd²⁺ and Pb²⁺ based on an MOF-derived carbon composite linked with multiwalled carbon nanotubes. *ACS Sustainable Chem. Eng.* **2023**, *11*, 2160-2171. <https://doi.org/10.1021/acssuschemeng.2c05240>.
92. Hanif, F.; Tahir, A.; Akhtar, M.; Waseem, M.; Haider, S.; Aboud, M.F.A.; Shakir, I.; Imran, M.; Warsi, M.F. Ultra-selective detection of Cd²⁺ and Pb²⁺ using glycine functionalized reduced graphene oxide/polyaniline nanocomposite electrode. *Synthetic Metals* **2019**, *257*, 116185. <https://doi.org/10.1016/j.synthmet.2019.116185>.
93. Oularbi, L.; Turmine, M.; El Rhazi, M. Preparation of novel nanocomposite consisting of bismuth particles, polypyrrole and multi-walled carbon nanotubes for simultaneous voltammetric determination of cadmium (II) and lead (II). *Synthetic Metals* **2019**, *253*, 1-8. <https://doi.org/10.1016/j.synthmet.2019.04.011>.
94. Akhtar, M.; Tahir, A.; Zulfiqar, S.; Hanif, F.; Warsi, M.F.; Agboola, P.O.; Shakir, I. Ternary hybrid of polyaniline-alanine-reduced graphene oxide for electrochemical sensing of heavy metal ions. *Synthetic Metals* **2020**, *265*, 116410. <https://doi.org/10.1016/j.synthmet.2020.116410>.
95. Mahmoudian, M.; Basirun, W.; Alias, Y.; MengWoi, P. Investigating the effectiveness of g-C₃N₄ on Pt/g-C₃N₄/polythiophene nanocomposites performance as an electrochemical sensor for Hg²⁺ detection. *J. Environmental Chem. Eng.* **2020**, *8*, 104204. <https://doi.org/10.1016/j.jece.2020.104204>.
96. Mahmoudian, M.; Alias, Y.; Woi, P.M.; Yousefi, R.; Basirun, W. An electrochemical sensor based on Pt/g-C₃N₄/polyaniline nanocomposite for detection of Hg²⁺. *Adv. Powder Technol.* **2020**, *31*, 3372-3380. <https://doi.org/10.1016/j.appt.2020.06.024>.
97. Guo, X.; Cui, R.; Huang, H.; Li, Y.; Liu, B.; Wang, J.; Zhao, D.; Dong, J.; Sun, B. Insights into the role of pyrrole doped in three-dimensional graphene aerogels for electrochemical sensing Cd (II). *J. Electroanal. Chem.* **2020**, *871*, 114323. <https://doi.org/10.1016/j.jelechem.2020.114323>.
98. Katowah, D.F.; Alsulami, Q.A.; Alam, M.; Ismail, S.H.; Asiri, A.M.; Mohamed, G.G.; Rahman, M.M.; Hussein, M.A. The performance of various SWCNT loading into CuO-PMMA nanocomposites towards the detection of Mn²⁺ ions. *J. Inorganic Organometal. Polymers Mat.* **2020**, *30*, 5024-5041. <https://doi.org/10.1007/s10904-020-01591-w>.
99. Deshmukh, M.A.; Shirsat, M.D.; Ramanaviciene, A.; Ramanavicius, A. Composites based on conducting polymers and carbon nanomaterials for heavy metal ion sensing. *Critical Rev. Anal. Chem.* **2018**, *48*, 293-304. <https://doi.org/10.1080/10408347.2017.1422966>.
100. El Rhazi, M.; Majid, S.; Elbasri, M.; Salih, F.E.; Oularbi, L.; Lafdi, K. Recent progress in nanocomposites based on conducting polymer: application as electrochemical sensors. *Int. Nano Lett.* **2018**, *8*, 79-99. <https://doi.org/10.1007/s40089-018-0238-2>.
101. Kaur, G.; Kaur, A.; Kaur, H. Review on nanomaterials/conducting polymer based nanocomposites for the development of biosensors and electrochemical sensors. *Polymer-Plastics Technol. Mat.* **2021**, *60*, 504-521. <https://doi.org/10.1080/25740881.2020.1844233>.
102. Deshmukh, M.A.; Patil, H.K.; Bodkhe, G.A.; Yasuzawa, M.; Koinkar, P.; Ramanaviciene, A.; Shirsat, M.D.; Ramanavicius, A. EDTA-modified PANI/SWNTs nanocomposite for differential pulse voltammetry based determination of Cu (II) ions. *Sens. Actuat. B: Chemical* **2018**, *260*, 331-338. <https://doi.org/10.1016/j.snb.2017.12.160>.
103. Bashir, S.; Ramesh, S.; Ramesh, K.; Numan, A.; Iqbal, J. Conducting polymer composites in electrochemical sensors. *Conducting Polymer Composites* Central West Publishing, Australia **2018**, 41-68.
104. Kumar, H.; Kumari, N.; Sharma, R. Nanocomposites (conducting polymer and nanoparticles) based electrochemical biosensor for the detection of environment pollutant: Its issues and challenges. *Environment. Impact Assess. Rev.* **2020**, *85*, 106438. <https://doi.org/10.1016/j.eiar.2020.106438>.
105. Rashed, M.A.; Ahmed, J.; Faisal, M.; Alsareii, S.; Jalalah, M.; Harraz, F.A. Highly sensitive and selective thiourea electrochemical sensor based on novel silver nanoparticles/chitosan nanocomposite. *Coll. Surf. A: Physicochemical and Engineering Aspects* **2022**, *644*, 128879. <https://doi.org/10.1016/j.colsurfa.2022.128879>.
106. Rahman, M.M.; Alamry, K.A.; Awual, M.R.; Mekky, A.E. Efficient Hg (II) ionic probe development based on one-step synthesized diethyl thieno [2, 3-b] thiophene-2, 5-dicarboxylate (DETTDC2) onto glassy carbon electrode. *Microchem. J.* **2020**, *152*, 104291. <https://doi.org/10.1016/j.microc.2019.104291>.

107. Feng, T.; Chen, K.; Zhong, J.; Cheng, Y.; Zhao, H.; Lan, M. In-situ polymerization of dendritic polyaniline nanofibers network embedded with Ag@SiO₂ core-shell nanoparticles for electrochemical determination of trace arsenic (III). *Sens. Actuat. B: Chemical* **2022**, 369, 132265. <https://doi.org/10.1016/j.snb.2022.132265>.
108. Fall, B.; Diaw, A.K.; Fall, M.; Sall, M.L.; Lo, M.; Gningue-Sall, D.; Thotiyil, M.O.; Maria, H.J.; Kalarikkal, N.; Thomas, S. Synthesis of highly sensitive rGO@ CNT@Fe₂O₃/polypyrrole nanocomposite for the electrochemical detection of Pb²⁺. *Materials Today Commun.* **2021**, 26, 102005. <https://doi.org/10.1016/j.mtcomm.2020.102005>.
109. Oularbi, L.; Turmine, M.; El Rhazi, M. Electrochemical determination of traces lead ions using a new nanocomposite of polypyrrole/carbon nanofibers. *J. Solid State Electrochem.* **2017**, 21, 3289-3300. <https://doi.org/10.1007/s10008-017-3676-2>.
110. Seenivasan, R.; Chang, W.-J.; Gunasekaran, S. Highly sensitive detection and removal of lead ions in water using cysteine-functionalized graphene oxide/polypyrrole nanocomposite film electrode. *ACS Appl. Mat. Interf.* **2015**, 7, 15935-15943. <https://doi.org/10.1021/acsami.5b03904>.
111. Lo, M.; Seydou, M.; Bensghaier, A.; Pires, R.; Gningue-Sall, D.; Aaron, J.-J.; Mekhalif, Z.; Delhalle, J.; Chehimi, M.M. Polypyrrole-wrapped carbon nanotube composite films coated on diazonium-modified flexible ITO sheets for the electroanalysis of heavy metal ions. *Sensors* **2020**, 20, 580. <https://doi.org/10.3390/s20030580>.
112. Dahaghin, Z.; Kilmartin, P.A.; Mousavi, H.Z. Simultaneous determination of lead (II) and cadmium (II) at a glassy carbon electrode modified with GO@Fe₃O₄@ benzothiazole-2-carboxaldehyde using square wave anodic stripping voltammetry. *J. Molec. Liquids* **2018**, 249, 1125-1132. <https://doi.org/10.1016/j.molliq.2017.11.114>.
113. Boonkaew, S.; Chaio, S.; Jampasa, S.; Rengpipat, S.; Siangproh, W.; Chailapakul, O. An origami paper-based electrochemical immunoassay for the C-reactive protein using a screen-printed carbon electrode modified with graphene and gold nanoparticles. *Microchim. Acta* **2019**, 186, 1-10. <https://doi.org/10.1007/s00604-019-3245-8>.
114. Lo, M.; Diaw, A.K.; Gningue-Sall, D.; Aaron, J.-J.; Oturan, M.A.; Chehimi, M.M. Tracking metal ions with polypyrrole thin films adhesively bonded to diazonium-modified flexible ITO electrodes. *Environment. Sci. Pollut. Res.* **2018**, 25, 20012-20022. <https://doi.org/10.1007/s11356-018-2140-x>.
115. Deshmukh, M.A.; Bodkhe, G.A.; Shirsat, S.; Ramanavicius, A.; Shirsat, M.D. Nanocomposite platform based on EDTA modified Ppy/SWNTs for the sensing of Pb (II) ions by electrochemical method. *Frontiers in chemistry* **2018**, 6, 451. <https://doi.org/10.3389/fchem.2018.00451>.
116. Wu, W.; Jia, M.; Zhang, Z.; Chen, X.; Zhang, Q.; Zhang, W.; Li, P.; Chen, L. Sensitive, selective and simultaneous electrochemical detection of multiple heavy metals in environment and food using a lowcost Fe₃O₄ nanoparticles/fluorinated multi-walled carbon nanotubes sensor. *Ecotoxicol. Environmental Safety* **2019**, 175, 243-250. <https://doi.org/10.1016/j.ecoenv.2019.03.037>.
117. Xu, Z.; Fan, X.; Ma, Q.; Tang, B.; Lu, Z.; Zhang, J.; Mo, G.; Ye, J.; Ye, J. A sensitive electrochemical sensor for simultaneous voltammetric sensing of cadmium and lead based on Fe₃O₄/multiwalled carbon nanotube/laser scribed graphene composites functionalized with chitosan modified electrode. *Mat. Chem. Phys.* **2019**, 238, 121877. <https://doi.org/10.1016/j.matchemphys.2019.121877>.
118. Le Hai, T.; Hung, L.C.; Phuong, T.T.B.; Ha, B.T.T.; Nguyen, B.-S.; Hai, T.D.; Nguyen, V.-H. Multiwall carbon nanotube modified by antimony oxide (Sb₂O₃/MWCNTs) paste electrode for the simultaneous electrochemical detection of cadmium and lead ions. *Microchem. J.* **2020**, 153, 104456. <https://doi.org/10.1016/j.microc.2019.104456>.
119. Mariyappan, V.; Manavalan, S.; Chen, S.-M.; Jaysiva, G.; Veerakumar, P.; Keerthi, M. Sr@FeNi-S nanoparticle/carbon nanotube nanocomposite with superior electrocatalytic activity for electrochemical detection of toxic mercury (II). *ACS Appl. Electronic Mat.* **2020**, 2, 1943-1952. <https://doi.org/10.1021/acsaelm.0c00248>.
120. Katowah, D.F.; Hussein, M.A.; Alam, M.; Ismail, S.H.; Osman, O.; Sobahi, T.; Asiri, A.M.; Ahmed, J.; Rahman, M.M. Designed network of ternary core-shell PPCOT/NiFe₂O₄/C-SWCNTs nanocomposites. A Selective Fe³⁺ ionic sensor. *J. Alloys and Compounds* **2020**, 834, 155020. <https://doi.org/10.1016/j.jallcom.2020.155020>.
121. Yıldız, C.; Bayraktepe, D.E.; Yazan, Z.; Önal, M. Bismuth nanoparticles decorated on Na-montmorillonite-multiwall carbon nanotube for simultaneous determination of heavy metal ions-electrochemical methods. *J. Electroanalyt. Chem.* **2022**, 910, 116205. <https://doi.org/10.1016/j.jelechem.2022.116205>.
122. Yu, L.; Wan, J.-W.; Meng, X.-Z.; Gu, H.-W.; Chen, Y.; Yi, H.-C. A simple electrochemical method for Cd (II) determination in real samples based on carbon nanotubes and metal-organic frameworks. *Int. J. Environ. Anal. Chem.* **2022**, 102, 4757-4767. <https://doi.org/10.1080/03067319.2020.1789611>.
123. Tan, R.; Jiang, P.; Pan, C.; Pan, J.; Gao, N.; Cai, Z.; Wu, F.; Chang, G.; Xie, A.; He, Y. Core-shell architected NH₂-UiO-66@ ZIF-8/multi-walled carbon nanotubes nanocomposite-based sensitive electrochemical sensor towards simultaneous determination of Pb²⁺ and Cu²⁺. *Microchim. Acta* **2023**, 190, 30. <https://doi.org/10.1007/s00604-022-05599-6>.

124. Fan, C.; Chen, L.; Jiang, R.; Ye, J.; Li, H.; Shi, Y.; Luo, Y.; Wang, G.; Hou, J.; Guo, X. ZnFe₂O₄ nanoparticles for electrochemical determination of trace Hg (II), Pb (II), Cu (II), and glucose. *ACS Appl. Nano Mat.* **2021**, *4*, 4026-4036. <https://doi.org/10.1021/acsanm.1c00379>.
125. Wang, Y.; Zhao, G.; Zhang, Q.; Wang, H.; Zhang, Y.; Cao, W.; Zhang, N.; Du, B.; Wei, Q. Electrochemical aptasensor based on gold modified graphene nanocomposite with different morphologies for ultrasensitive detection of Pb²⁺. *Sens. Actuat. B: Chemical* **2019**, *288*, 325-331. <https://doi.org/10.1016/j.snb.2019.03.010>.
126. Baghayeri, M.; Alinezhad, H.; Fayazi, M.; Tarahomi, M.; Ghanei-Motlagh, R.; Maleki, B. A novel electrochemical sensor based on a glassy carbon electrode modified with dendrimer functionalized magnetic graphene oxide for simultaneous determination of trace Pb (II) and Cd (II). *Electrochim. Acta* **2019**, *312*, 80-88. <https://doi.org/10.1016/j.electacta.2019.04.180>.
127. Priya, T.; Dhanalakshmi, N.; Karthikeyan, V.; Thinakaran, N. Highly selective simultaneous trace determination of Cd²⁺ and Pb²⁺ using porous graphene/carboxymethyl cellulose/fondaparinux nanocomposite modified electrode. *J. Electroanal. Chem.* **2019**, *833*, 543-551. <https://doi.org/10.1016/j.jelechem.2018.12.039>.
128. Cheng, Y.; Li, H.; Fang, C.; Ai, L.; Chen, J.; Su, J.; Zhang, Q.; Fu, Q. Facile synthesis of reduced graphene oxide/silver nanoparticles composites and their application for detecting heavy metal ions. *J. Alloys Comp.* **2019**, *787*, 683-693. <https://doi.org/10.1016/j.jallcom.2019.01.320>.
129. El-Shafai, N.M.; Abdelfatah, M.M.; El-Khouly, M.E.; El-Mehasseb, I.M.; El-Shaer, A.; Ramadan, M.S.; Masoud, M.S.; El-Kemary, M.A. Magnetite nano-spherical quantum dots decorated graphene oxide nano sheet (GO@ Fe₃O₄): Electrochemical properties and applications for removal heavy metals, pesticide and solar cell. *Appl. Surf. Sci.* **2020**, *506*, 144896. <https://doi.org/10.1016/j.apsusc.2019.144896>.
130. Tan, Z.; Wu, W.; Feng, C.; Wu, H.; Zhang, Z. Simultaneous determination of heavy metals by an electrochemical method based on a nanocomposite consisting of fluorinated graphene and gold nanocage. *Microchim. Acta* **2020**, *187*, 1-9. <https://doi.org/10.1007/s00604-020-04393-6>.
131. Das, T.R.; Sharma, P.K. Hydrothermal-assisted green synthesis of Ni/Ag@rGO nanocomposite using Punica granatum juice and electrochemical detection of ascorbic acid. *Microchem. J.* **2020**, *156*, 104850. <https://doi.org/10.1016/j.microc.2020.104850>.
132. Hwa, K.-Y.; Sharma, T.S.K.; Ganguly, A. Design strategy of rGO-HNT-AgNPs based hybrid nanocomposite with enhanced performance for electrochemical detection of 4-nitrophenol. *Inorganic Chem. Frontiers* **2020**, *7*, 1981-1994. <https://doi.org/10.1039/D0QI00006J>.
133. Bi, C.-C.; Ke, X.-X.; Chen, X.; Weerasooriya, R.; Hong, Z.-Y.; Wang, L.-C.; Wu, Y.-C. Assembling reduced graphene oxide with sulfur/nitrogen-“hooks” for electrochemical determination of Hg (II). *Anal. Chim. Acta* **2020**, *1100*, 31-39. <https://doi.org/10.1016/j.aca.2019.11.062>.
134. Pang, J.; Fu, H.; Kong, W.; Jiang, R.; Ye, J.; Zhao, Z.; Hou, J.; Sun, K.; Zheng, Y.; Chen, L. Design of NiCo₂O₄ nanoparticles decorated N, S co-doped reduced graphene oxide composites for electrochemical simultaneous detection of trace multiple heavy metal ions and hydrogen evolution reaction. *Chem. Engin. J.* **2022**, *433*, 133854. <https://doi.org/10.1016/j.cej.2021.133854>.
135. Erçarıncı, E.; Alanyalıoğlu, M. Dual-functional graphene-based flexible material for membrane filtration and electrochemical sensing of heavy metal ions. *IEEE Sens. J.* **2020**, *21*, 2468-2475. <https://doi.org/10.1109/JSEN.2020.3021988>.
136. Guo, C.; Wang, C.; Sun, H.; Dai, D.; Gao, H. A simple electrochemical sensor based on rGO/MoS₂/CS modified GCE for highly sensitive detection of Pb (II) in tobacco leaves. *Rsc Advances* **2021**, *11*, 29590-29597. <https://doi.org/10.1039/D1RA05350G>.
137. Bhardiya, S.R.; Asati, A.; Sheshma, H.; Rai, A.; Rai, V.K.; Singh, M. A novel bioconjugated reduced graphene oxide-based nanocomposite for sensitive electrochemical detection of cadmium in water. *Sens. Actuat. B: Chemical* **2021**, *328*, 129019. <https://doi.org/10.1016/j.snb.2020.129019>.
138. Wang, L.; Peng, X.; Fu, H. An electrochemical aptasensor for the sensitive detection of Pb²⁺ based on a chitosan/reduced graphene oxide/titanium dioxide. *Microchem. J.* **2022**, *174*, 106977. <https://doi.org/10.1016/j.microc.2021.106977>.
139. Kushwah, M.; Yadav, R.; Berlina, A.N.; Gaur, K.; Gaur, M. Development of an ultrasensitive rGO/AuNPs/ssDNA-based electrochemical aptasensor for detection of Pb²⁺. *J. Solid State Electrochem.* **2023**, *27*, 559-574. <https://doi.org/10.1016/j.chemosphere.2022.137154>.
140. Zheng, H.; Ntuli, L.; Mbanjwa, M.; Palaniyandy, N.; Smith, S.; Modibedi, M.; Land, K.; Mathe, M. The effect of gC₃N₄ materials on Pb (II) and Cd (II) detection using disposable screen-printed sensors. *Electrocatalysis* **2019**, *10*, 149-155. <https://doi.org/10.1007/s12678-018-0504-0>.
141. Xiao, X.-Y.; Chen, S.-H.; Li, S.-S.; Wang, J.; Zhou, W.-Y.; Huang, X.-J. Synergistic catalysis of N vacancies and ~ 5 nm Au nanoparticles promoted the highly sensitive electrochemical determination of lead (ii) using an Au/N-deficient-C₃N₄ nanocomposite. *Environment. Sci.: Nano* **2019**, *6*, 1895-1908. <https://doi.org/10.1039/C9EN00114J>.
142. Ramalingam, M.; Ponnusamy, V.K.; Sangilimuthu, S.N. A nanocomposite consisting of porous graphitic carbon nitride nanosheets and oxidized multiwalled carbon nanotubes for simultaneous stripping

- voltammetric determination of cadmium (II), mercury (II), lead (II) and zinc (II). *Microchim. Acta* **2019**, *186*, 1-10. <https://doi.org/10.1007/s00604-018-3178-7>.
143. Radhakrishnan, K.; Sivanesan, S.; Panneerselvam, P. Turn-On fluorescence sensor based detection of heavy metal ion using carbon dots@ graphitic-carbon nitride nanocomposite probe. *J. Photochem. Photobiol. A: Chemistry* **2020**, *389*, 112204. <https://doi.org/10.1016/j.jphotochem.2019.112204>.
 144. Karthika, A.; Nikhil, S.; Suganthi, A.; Rajarajan, M. A facile sonochemical approach based on graphene carbon nitride doped silver molybdate immobilized nafion for selective and sensitive electrochemical detection of chromium (VI) in real sample. *Adv. Powder Technol.* **2020**, *31*, 1879-1890. <https://doi.org/10.1016/j.apt.2020.02.021>.
 145. Hu, J.-Y.; Li, Z.; Zhai, C.-Y.; Wang, J.-F.; Zeng, L.-X.; Zhu, M.-S. Plasmonic photo-assisted electrochemical sensor for detection of trace lead ions based on Au anchored on two-dimensional gC₃N₄/graphene nanosheets. *Rare Metals* **2021**, *40*, 1727-1737. <https://doi.org/10.1007/s12598-020-01659-z>.
 146. Hu, J.; Li, Z.; Zhai, C.; Zeng, L.; Zhu, M. Photo-assisted simultaneous electrochemical detection of multiple heavy metal ions with a metal-free carbon black anchored graphitic carbon nitride sensor. *Anal. Chim. Acta* **2021**, *1183*, 338951. <https://doi.org/10.1016/j.aca.2021.338951>.
 147. Pu, Y.; Wu, Y.; Yu, Z.; Lu, L.; Wang, X. Simultaneous determination of Cd²⁺ and Pb²⁺ by an electrochemical sensor based on Fe₃O₄/Bi₂O₃/C₃N₄ nanocomposites. *Talanta* **2021**, *3*, 100024. <https://doi.org/10.1016/j.talo.2020.100024>.
 148. Eswaran, M.; Tsai, P.-C.; Wu, M.-T.; Ponnusamy, V.K. Novel nano-engineered environmental sensor based on polymelamine/graphitic-carbon nitride nanohybrid material for sensitive and simultaneous monitoring of toxic heavy metals. *J. Hazardous Mat.* **2021**, *418*, 126267. <https://doi.org/10.1016/j.jhazmat.2021.126267>.
 149. Wang, Y.; Nie, Z.; Li, X.; Zhao, Y.; Wang, H. Highly sensitive and selective electrochemical sensor based on porous graphitic carbon nitride/CoMn₂O₄ nanocomposite toward heavy metal ions. *Sens. Actuat. B: Chemical* **2021**, *346*, 130539. <https://doi.org/10.1016/j.snb.2021.130539>.
 150. Hassanpoor, S.; Rouhi, N. Electrochemical sensor for determination of trace amounts of cadmium (II) in environmental water samples based on MnO₂/RGO nanocomposite. *Int. J. Environmental Anal. Chem.* **2021**, *101*, 513-532. <https://doi.org/10.1080/03067319.2019.1669582>.
 151. Sun, Y.-F.; Li, P.-H.; Yang, M.; Huang, X.-J. Highly sensitive electrochemical detection of Pb (II) based on excellent adsorption and surface Ni (II)/Ni (III) cycle of porous flower-like NiO/rGO nanocomposite. *Sens. Actuat. B: Chemical* **2019**, *292*, 136-147. <https://doi.org/10.1016/j.snb.2019.04.131>.
 152. Vajedi, F.; Dehghani, H. The characterization of TiO₂-reduced graphene oxide nanocomposites and their performance in electrochemical determination for removing heavy metals ions of cadmium (II), lead (II) and copper (II). *Mat. Sci. Engineering: B* **2019**, *243*, 189-198. <https://doi.org/10.1016/j.mseb.2019.04.009>.
 153. Huang, W.; Zhang, Y.; Li, Y.; Zeng, T.; Wan, Q.; Yang, N. Morphology-controlled electrochemical sensing of environmental Cd²⁺ and Pb²⁺ ions on expanded graphite supported CeO₂ nanomaterials. *Anal. Chim. Acta* **2020**, *1126*, 63-71. <https://doi.org/10.1016/j.aca.2020.06.010>.
 154. Koshki, M.-S.; Baghayeri, M.; Fayazi, M. Application of sepiolite/FeS₂ nanocomposite for highly selective detection of mercury (II) based on stripping voltammetric analysis. *J. Food Measurement and Characterization* **2021**, *15*, 5318-5325. <https://doi.org/10.1007/s11694-021-01097-0>.
 155. Wei, J.; Zhao, J.; Li, C.-Y.; Xie, X.-Y.; Wei, Y.-Y.; Shen, W.; Wang, J.-P.; Yang, M. Highly sensitive and selective electrochemical detection of Pb (II) in serum via an α -Fe₂O₃/NiO heterostructure: Evidence from theoretical calculations and adsorption investigation. *Sens. Actuat. B: Chemical* **2021**, *344*, 130295. <https://doi.org/10.1016/j.snb.2021.130295>.
 156. Cheng, X.-L.; Xu, Q.-Q.; Li, S.-S.; Li, J.; Zhou, Y.; Zhang, Y.; Li, S. Oxygen vacancy enhanced Co₃O₄/ZnO nanocomposite with small sized and loose structure for sensitive electroanalysis of Hg (II) in subsidence area water. *Sens. Actuat. B: Chemical* **2021**, *326*, 128967. <https://doi.org/10.1016/j.snb.2020.128967>.
 157. Buica, G.-O.; Stoian, A.B.; Manole, C.; Demetrescu, I.; Pirvu, C. Zr/ZrO₂ nanotube electrode for detection of heavy metal ions. *Electrochem. Commun.* **2020**, *110*, 106614. <https://doi.org/10.1016/j.elecom.2019.106614>.
 158. Jin, W.; Fu, Y.; Hu, M.; Wang, S.; Liu, Z. Highly efficient SnS-decorated Bi₂O₃ nanosheets for simultaneous electrochemical detection and removal of Cd (II) and Pb (II). *J. Electroanal. Chem.* **2020**, *856*, 113744. <https://doi.org/10.1016/j.jelechem.2019.113744>.
 159. Sun, Y.-F.; Li, J.-J.; Xie, F.; Wei, Y.; Yang, M. Ruthenium-loaded cerium dioxide nanocomposites with rich oxygen vacancies promoted the highly sensitive electrochemical detection of Hg (II). *Sens. Actuat. B: Chemical* **2020**, *320*, 128355. <https://doi.org/10.1016/j.snb.2020.128355>.
 160. Krishnan, S.; Chatterjee, S.; Solanki, A.; Guha, N.; Singh, M.K.; Gupta, A.K.; Rai, D.K. Aminotetrazole-functionalized SiO₂ coated MgO nanoparticle composites for removal of acid fuchsin dye and detection of heavy metal ions. *ACS Appl. Nano Mat.* **2020**, *3*, 11203-11216. <https://doi.org/10.1021/acsanm.0c02351>.
 161. Maleki, B.; Baghayeri, M.; Ghanei-Motlagh, M.; Zonoz, F.M.; Amir, A.; Hajizadeh, F.; Hosseinfar, A.; Esmailnezhad, E. Polyamidoamine dendrimer functionalized iron oxide nanoparticles for simultaneous electrochemical detection of Pb²⁺ and Cd²⁺ ions in environmental waters. *Measurement* **2019**, *140*, 81-88. <https://doi.org/10.1016/j.measurement.2019.03.052>.

162. Karthika, A.; Raja, V.R.; Karuppasamy, P.; Suganthi, A.; Rajarajan, M. Electrochemical behaviour and voltammetric determination of mercury (II) ion in cupric oxide/poly vinyl alcohol nanocomposite modified glassy carbon electrode. *Microchem. J.* **2019**, *145*, 737-744. <https://doi.org/10.1016/j.microc.2018.11.030>.
163. Singh, S.; Pankaj, A.; Mishra, S.; Tewari, K.; Singh, S.P. Cerium oxide-catalyzed chemical vapor deposition grown carbon nanofibers for electrochemical detection of Pb (II) and Cu (II). *J. Environmental Chem. Eng.* **2019**, *7*, 103250. <https://doi.org/10.1016/j.jece.2019.103250>.
164. Wang, L.; Lei, T.; Ren, Z.; Jiang, X.; Yang, X.; Bai, H.; Wang, S. Fe₃O₄@PDA@MnO₂ core-shell nanocomposites for sensitive electrochemical detection of trace Pb (II) in water. *J. Electroanal. Chem.* **2020**, *864*, 114065. <https://doi.org/10.1016/j.jelechem.2020.114065>.
165. Bakhsh, E.M.; Khan, S.B.; Asiri, A.M.; Shah, A. Zn/Fe nanocomposite based efficient electrochemical sensor for the simultaneous detection of metal ions. *Physica E: Low-dimensional Systems and Nanostructures* **2021**, *130*, 114671. <https://doi.org/10.1016/j.physe.2021.114671>.
166. Li, G.; Qi, X.; Zhang, G.; Wang, S.; Li, K.; Wu, J.; Wan, X.; Liu, Y.; Li, Q. Low-cost voltammetric sensors for robust determination of toxic Cd (II) and Pb (II) in environment and food based on shuttle-like α -Fe₂O₃ nanoparticles decorated β -Bi₂O₃ microspheres. *Microchem. J.* **2022**, *179*, 107515. <https://doi.org/10.1016/j.microc.2022.107515>.
167. Padmalaya, G.; Vardhan, K.H.; Kumar, P.S.; Ali, M.A.; Chen, T.-W. A disposable modified screen-printed electrode using egg white/ZnO rice structured composite as practical tool electrochemical sensor for formaldehyde detection and its comparative electrochemical study with Chitosan/ZnO nanocomposite. *Chemosphere* **2022**, *288*, 132560. <https://doi.org/10.1016/j.chemosphere.2021.132560>.
168. Hwang, J.-H.; Pathak, P.; Wang, X.; Rodriguez, K.L.; Cho, H.J.; Lee, W.H. A novel bismuth-chitosan nanocomposite sensor for simultaneous detection of Pb (II), Cd (II) and Zn (II) in wastewater. *Micromachines* **2019**, *10*, 511. <https://doi.org/10.3390/mi10080511>.
169. Wei, P.; Zhu, Z.; Song, R.; Li, Z.; Chen, C. An ion-imprinted sensor based on chitosan-graphene oxide composite polymer modified glassy carbon electrode for environmental sensing application. *Electrochim. Acta* **2019**, *317*, 93-101. <https://doi.org/10.1016/j.electacta.2019.05.136>.
170. Wu, S.; Li, K.; Dai, X.; Zhang, Z.; Ding, F.; Li, S. An ultrasensitive electrochemical platform based on imprinted chitosan/gold nanoparticles/graphene nanocomposite for sensing cadmium (II) ions. *Microchem. J.* **2020**, *155*, 104710. <https://doi.org/10.1016/j.microc.2020.104710>.
171. Nguyen, L.D.; Doan, T.C.D.; Huynh, T.M.; Nguyen, V.N.P.; Dinh, H.H.; Dang, D.M.T.; Dang, C.M. An electrochemical sensor based on polyvinyl alcohol/chitosan-thermally reduced graphene composite modified glassy carbon electrode for sensitive voltammetric detection of lead. *Sens. Actuat. B: Chemical* **2021**, *345*, 130443. <https://doi.org/10.1016/j.snb.2021.130443>.
172. He, Y.; Ma, L.; Zhou, L.; Liu, G.; Jiang, Y.; Gao, J. Preparation and application of bismuth/MXene nanocomposite as electrochemical sensor for heavy metal ions detection. *Nanomaterials* **2020**, *10*, 866. <https://doi.org/10.3390/nano10050866>.
173. Zhu, X.; Liu, B.; Li, L.; Wu, L.; Chen, S.; Huang, L.; Yang, J.; Liang, S.; Xiao, K.; Hu, J. A micromilled microgrid sensor with delaminated MXene-bismuth nanocomposite assembly for simultaneous electrochemical detection of lead (II), cadmium (II) and zinc (II). *Microchim. Acta* **2019**, *186*, 1-7. <https://doi.org/10.1007/s00604-019-3837-3>.
174. Hojjati-Najafabadi, A.; Mansoorianfar, M.; Liang, T.; Shahin, K.; Wen, Y.; Bahrami, A.; Karaman, C.; Zare, N.; Karimi-Maleh, H.; Vasseghian, Y. Magnetic-MXene-based nanocomposites for water and wastewater treatment: A review. *J. Water Process Eng.* **2022**, *47*, 102696. <https://doi.org/10.1016/j.jwpe.2022.102696>.
175. Rhouati, A.; Berkani, M.; Vasseghian, Y.; Golzadeh, N. MXene-based electrochemical sensors for detection of environmental pollutants: A comprehensive review. *Chemosphere* **2022**, *291*, 132921. <https://doi.org/10.1016/j.chemosphere.2021.132921>.
176. Dhillon, A.; Singh, N.; Nair, M.; Kumar, D. Analytical methods to determine and sense heavy metal pollutants using MXene and MXene-based composites: Mechanistic prophecy into sensing properties. *Chemosphere* **2022**, 135166. <https://doi.org/10.1016/j.chemosphere.2022.135166>.
177. Zhang, X.; An, D.; Bi, Z.; Shan, W.; Zhu, B.; Zhou, L.; Yu, L.; Zhang, H.; Xia, S.; Qiu, M. Ti₃C₂-MXene@N-doped carbon heterostructure-based electrochemical sensor for simultaneous detection of heavy metals. *J. Electroanal. Chem.* **2022**, *911*, 116239. <https://doi.org/10.1016/j.jelechem.2022.116239>.
178. Chen, Y.; Zhao, P.; Liang, Y.; Ma, Y.; Liu, Y.; Zhao, J.; Hou, J.; Hou, C.; Huo, D. A sensitive electrochemical sensor based on 3D porous melamine-doped rGO/MXene composite aerogel for the detection of heavy metal ions in the environment. *Talanta* **2023**, 124294. <https://doi.org/10.1016/j.talanta.2023.124294>.
179. Ganesh, P.-S.; Kim, S.-Y. Electrochemical sensing interfaces based on novel 2D-MXenes for monitoring environmental hazardous toxic compounds: A concise review. *J. Industrial and Engineering Chem.* **2022**. <https://doi.org/10.1016/j.jiec.2022.02.006>.
180. Zhu, X.; Liu, B.; Hou, H.; Huang, Z.; Zeinu, K.M.; Huang, L.; Yuan, X.; Guo, D.; Hu, J.; Yang, J. Alkaline intercalation of Ti₃C₂ MXene for simultaneous electrochemical detection of Cd (II), Pb (II), Cu (II) and Hg (II). *Electrochim. Acta* **2017**, *248*, 46-57. <https://doi.org/10.1016/j.electacta.2017.07.084>.

181. Feng, X.; Yu, Z.; Long, R.; Li, X.; Shao, L.; Zeng, H.; Zeng, G.; Zuo, Y. Self-assembling 2D/2D (MXene/LDH) materials achieve ultra-high adsorption of heavy metals Ni²⁺ through terminal group modification. *Separ. Purific. Technol.* **2020**, *253*, 117525. <https://doi.org/10.1016/j.seppur.2020.117525>.
182. Rasheed, P.A.; Pandey, R.P.; Jabbar, K.A.; Ponraj, J.; Mahmoud, K.A. Sensitive electrochemical detection of l-cysteine based on a highly stable Pd@ Ti₃C₂Tx(MXene) nanocomposite modified glassy carbon electrode. *Anal. Meth.* **2019**, *11*, 3851-3856. <https://doi.org/10.1039/C9AY00912D>.
183. Desai, M.L.; Basu, H.; Singhal, R.K.; Saha, S.; Kailasa, S.K. Ultra-small two dimensional MXene nanosheets for selective and sensitive fluorescence detection of Ag⁺ and Mn²⁺ ions. *Coll. Surf. A: Physicochemical and Engineering Aspects* **2019**, *565*, 70-77. <https://doi.org/10.1016/j.colsurfa.2018.12.051>.
184. Naseri, M.; Mohammadniaei, M.; Ghosh, K.; Sarkar, S.; Sankar, R.; Mukherjee, S.; Pal, S.; Ansari Dezfouli, E.; Halder, A.; Qiao, J. A Robust electrochemical sensor based on butterfly-shaped silver nanostructure for concurrent quantification of heavy metals in water samples. *Electroanalysis* **2023**, *35*, e202200114. <https://doi.org/10.1002/elan.202200114>.
185. Theerthagiri, J.; Lee, S.J.; Karuppasamy, K.; Park, J.; Yu, Y.; Kumari, M.A.; Chandrasekaran, S.; Kim, H.-S.; Choi, M.Y. Fabrication strategies and surface tuning of hierarchical gold nanostructures for electrochemical detection and removal of toxic pollutants. *J. Hazardous Mat.* **2021**, *420*, 126648. <https://doi.org/10.1016/j.jhazmat.2021.126648>.
186. Malakootian, M.; Hamzeh, S.; Mahmoudi-Moghaddam, H. A new electrochemical sensor for simultaneous determination of Cd (II) and Pb (II) using FeNi₃/CuS/BiOCl: RSM optimization. *Microchem. J.* **2020**, *158*, 105194. <https://doi.org/10.1016/j.microc.2020.105194>.
187. Pathak, P.; Hwang, J.-H.; Li, R.H.; Rodriguez, K.L.; Rex, M.M.; Lee, W.H.; Cho, H.J. Flexible copper-biopolymer nanocomposite sensors for trace level lead detection in water. *Sens. Actuat. B: Chemical* **2021**, *344*, 130263. <https://doi.org/10.1016/j.snb.2021.130263>.
188. He, Y.; Wang, Z.; Ma, L.; Zhou, L.; Jiang, Y.; Gao, J. Synthesis of bismuth nanoparticle-loaded cobalt ferrite for electrochemical detection of heavy metal ions. *RSC Adv.* **2020**, *10*, 27697-27705. <https://doi.org/10.1039/D0RA02522D>.
189. Lei, P.; Zhou, Y.; Zhao, S.; Dong, C.; Shuang, S. Carbon-supported X-manganate (XNi, Zn, and Cu) nanocomposites for sensitive electrochemical detection of trace heavy metal ions. *J. Hazardous Mat.* **2022**, *435*, 129036. <https://doi.org/10.1016/j.jhazmat.2022.129036>.
190. Qureashi, A.; Pandith, A.H.; Bashir, A.; Manzoor, T.; Malik, L.A.; Sheikh, F.A. Citrate coated magnetite: A complete magneto dielectric, electrochemical and DFT study for detection and removal of heavy metal ions. *Surf. Interf.* **2021**, *23*, 101004. <https://doi.org/10.1016/j.surf.2021.101004>.
191. Teodoro, K.B.; Shimizu, F.M.; Scagion, V.P.; Correa, D.S. Ternary nanocomposites based on cellulose nanowhiskers, silver nanoparticles and electrospun nanofibers: Use in an electronic tongue for heavy metal detection. *Sens. Actuat. B: Chemical* **2019**, *290*, 387-395. <https://doi.org/10.1016/j.snb.2019.03.125>.
192. Zhou, J.; Sun, G.; Pan, J.; Pan, Y.; Wang, S.; Zhai, H. A nanocomposite consisting of ionic liquid-functionalized layered Mg (II)/Al (III) double hydroxides for simultaneous electrochemical determination of cadmium (II), copper (II), mercury (II) and lead (II). *Microchim. Acta* **2019**, *186*, 1-7. DOI: 10.1007/s00604-010-0488-9.
193. Padmalaya, G.; Sreeja, B.; Dinesh Kumar, P.; Radha, S.; Poornima, V.; Arivanandan, M.; Shrestha, S.; Uma, T. A facile synthesis of cellulose acetate functionalized zinc oxide nanocomposite for electrochemical sensing of cadmium ions. *J. Inorganic and Organometallic Polymers and Materials* **2019**, *29*, 989-999. <https://doi.org/10.1007/s10904-018-0989-2>.
194. Mourya, A.; Sinha, S.K.; Mazumdar, B. Glassy carbon electrode modified with blast furnace slag for electrochemical investigation of Cu²⁺ and Pb²⁺ metal ions. *Microchem. J.* **2019**, *147*, 707-716. <https://doi.org/10.1016/j.microc.2019.03.082>.
195. Shang, J.; Zhao, M.; Qu, H.; Li, H.; Gao, R.; Chen, S. New application of pn junction in electrochemical detection: The detection of heavy metal ions. *J. Electroanal. Chem.* **2019**, *855*, 113624. <https://doi.org/10.1016/j.jelechem.2019.113624>.
196. Wang, W.; Xu, Y.; Cheng, N.; Xie, Y.; Huang, K.; Xu, W. Dual-recognition aptazyme-driven DNA nanomachine for two-in-one electrochemical detection of pesticides and heavy metal ions. *Sens. Actuat. B: Chemical* **2020**, *321*, 128598. <https://doi.org/10.1016/j.snb.2020.128598>.
197. Xin, X.; Hu, N.; Ma, Y.; Wang, Y.; Hou, L.; Zhang, H.; Han, Z. Polyoxometalate-based crystalline materials as a highly sensitive electrochemical sensor for detecting trace Cr (VI). *Dalton Transactions* **2020**, *49*, 4570-4577. <https://doi.org/10.1039/D0DT00446D>.
198. Cao, L.; Kang, Z.-W.; Ding, Q.; Zhang, X.; Lin, H.; Lin, M.; Yang, D.-P. Rapid pyrolysis of Cu²⁺-polluted eggshell membrane into a functional Cu²⁺-Cu+/biochar for ultrasensitive electrochemical detection of nitrite in water. *Sci. Total Environment* **2020**, *723*, 138008. <https://doi.org/10.1016/j.scitotenv.2020.138008>.
199. Li, Y.; Shi, Z.; Zhang, C.; Wu, X.; Liu, L.; Guo, C.; Li, C.M. Highly stable branched cationic polymer-functionalized black phosphorus electrochemical sensor for fast and direct ultratrace detection of copper ion. *J. Coll. Interface Sci.* **2021**, *603*, 131-140. <https://doi.org/10.1016/j.jcis.2021.06.002>.

200. Xiong, W.; Zhang, P.; Liu, S.; Lv, Y.; Zhang, D. Catalyst-free synthesis of phenolic-resin-based carbon nanospheres for simultaneous electrochemical detection of Cu (II) and Hg (II). *Diamond and Related Materials* **2021**, *111*, 108170. <https://doi.org/10.1016/j.diamond.2020.108170>.
201. Hajjaoui, H.; Soufi, A.; Boumya, W.; Abdennouri, M.; Barka, N. Polyaniline/nanomaterial composites for the removal of heavy metals by adsorption: A Review. *J. Compos. Sci.* **2021**, *5*, 233. <https://doi.org/10.3390/jcs5090233>.
202. Yadav, R.; Kushwah, V.; Gaur, M.; Bhadauria, S.; Berlina, A.N.; Zherdev, A.V.; Dzantiev, B. Electrochemical aptamer biosensor for As³⁺ based on apta deep trapped Ag-Au alloy nanoparticles-impregnated glassy carbon electrode. *Int. J. Environment. Anal. Chem.* **2020**, *100*, 623-634. <https://doi.org/10.1080/03067319.2019.1638371>.
203. Gao, Z.; Wang, Y.; Wang, H.; Li, X.; Xu, Y.; Qiu, J. Recent aptamer-based biosensor for Cd²⁺ detection. *Biosensors* **2023**, *13*, 612. <https://doi.org/10.3390/bios13060612>.